FACULTY OF MATHEMATICS, PHYSICS AND INFORMATICS
COMENIUS UNIVERSITY BRATISLAVA

Department of Nuclear Physics and Biophysics

Radioactivity of Atmospheric Aerosol Particles and their Elemental Contents

PhD. Thesis

Jana Merešová

Supervisor:
Doc. Ivan Sýkora, PhD.

Bratislava 2008

Abstract

Since March 2001 the periodic checking of atmospheric aerosols radioactivity in Bratislava, locality Líščie údolie, has been carried out. Time variations of ^{7}Be, ^{210}Pb, ^{137}Cs, and ^{40}K activity concentrations are periodically investigated using standard gammaspectrometry. The average value of cosmogenic ^{7}Be concentration within the observed period was 2.5 mBq m^{-3}. ^{210}Pb is a long-lived daughter product of ^{222}Rn and its average value was 0.77 mBq m^{-3}. Activity concentrations of ^{7}Be and ^{210}Pb show typical seasonal variations with mutually inverse trends. The concentrations were observed to be higher in spring and early summer for ^{7}Be and opposite to that in winter months there were higher for ^{210}Pb. The ^{7}Be/^{210}Pb activity ratios are presented and correlation study has been carried out between the meteorological parameters and concentrations of radionuclides. The activity concentrations of anthropogenic ^{137}Cs and primordial ^{40}K were determined based on measurements of cumulated monthly samples. Values of ^{137}Cs and ^{40}K reached the averages of 0.52 and 5.2 μ Bq m^{-3}, respectively. The observed average values may be considered as representative at the ground level air in our geographical region.

Also the results of precipitation measurements since July 2005 are presented. Average monthly depositions of ^{7}Be and ^{210}Pb were 79.4 and 8.47 Bq m^{-2}, respectively. ^{137}Cs and ^{40}K depositions were 38.1 and 794 mBq m^{-2}, respectively. Monthly depositions of ^{7}Be and ^{210}Pb radionuclides are relatively highly correlated with the total monthly precipitation, meanwhile the depositions of ^{137}Cs and ^{40}K have a lower dependency on the rainwater amount.

A diffusion model for vertical profile of ^{7}Be activity concentration up to 30 km in the atmosphere was developed. The atmospheric activity concentrations and monthly depositions of ^{7}Be were used for evaluation of turbulent diffusion coefficient and scavenging coefficient.

Sixteen filter samples from the year 2004 were designated for elemental analysis. As a result of two irradiations and four gamma-spectrometric measurements the concentrations of 30 chemical elements (Na, Al, Cl, K, Ca, Sc, Ti, V, Cr, Mn, Fe, Ga, As, Se, Br, Rb, In, Sb, I, Cs, Ba, La, Sm, Dy, Tm, W, Au, Hg, Th, U) were determined using instrumental neutron activation analysis (INAA). Additionally the concentrations of other 6 elements (Cr, Ni, Cu, Zn, Cd, Pb) were measured by atomic absorption spectrometry (AAS). For some elements, mainly of soil origin, elevated concentrations in the summer season were observed. In comparison to other European cities elemental contents in air are lower for Bratislava.

Acknowledgements

First of all I would like to thank to my supervisor, Doc. RNDr. Ivan Sýkora, PhD. for his continuous help, useful advices, and support during last few years.

The special gratitude goes to Doc. RNDr. Matej Florek, CSc. for all his valuable suggestions and patient guidance in the field of neutron activation analysis.

I am deeply grateful to Marina Vladimirovna Frontasyeva for her help, inspirational consultations and for giving me the chance to visit Dubna and to work at Joint Institute for Nuclear Research.

I am very indebted to the Mr. Miroslav Šulc for his continuous effort in maintenance of the sampling devices.

And many thanks go to my colleagues at the department, especially to Miroslav Ješkovský and Ján Šimon for many enthusiastic discussions and for helping me to solve incoming problems.

Finally, I want to thank my beloved family and my friends for their continuous encouragement and support during past years and especially to my boyfriend Nino for his love.

Contents

Chapter 1

Introduction

Sustainable civilization progress requires the maximal limitations of pollution loads to the environment. Therefore, the environment and its protection is getting nowadays more and more attention of the public and even of industry companies. To solve these complex environmental issues the detailed knowledge of processes taking place in the nature is essential.

Physics, along with the biology and chemistry, is the tool for studying and solving numerous phenomena in question on local and global scale, too. The particular example can be found in radionuclides, both natural and anthropogenic, serving as tracers or indicators of several environmental processes. They can reveal new features or dynamics of individual systems of the Earth: the atmosphere, the hydrosphere, the biosphere, or the lithosphere. A good example is the global warming, at present the most discussed environmental problem worldwide. Greenhouse gas CO_2 plays a crucial role in the changes of climate and it may be traced by using the radionuclide ^{14}C.

This work is focused on the atmosphere, one of important parts of our environment. The atmosphere is very dynamic and usually all present pollutants are very quickly diffused to long distances. Therefore, the constant monitoring of air quality is necessary for immediate action on the source. Environmental monitoring of radioactivity of atmospheric aerosol particles in surface air is the scope of our study. Naturally occurring radionuclides such as ^{7}Be, ^{210}Pb and ^{214}Bi are commonly detected in the air filter. However, fission products, such as ^{59}Fe, ^{95}Nb and ^{131}I would be found in the air filter in the case of nuclear accidents in nuclear power plants or nuclear weapon testing.

At the Department of Nuclear Physics and Biophysics at the Faculty of Mathematics, Physics and Informatics there is a long tradition in measuring the radioactivity of the low-level atmosphere. This study follows the preceding work [Povinec88], [Ďurana96]. In Figure 1.1 there are presented temporal variations of ^{7}Be activity concentrations determined in years 1981 - 1994.

Cosmogenic radionuclides are produced in higher altitudes in the interaction of galactic cosmic rays with atoms constituting the atmosphere. Particularly, radionuclide ^{7}Be is the most important cosmogenic radionuclide in studying atmo-

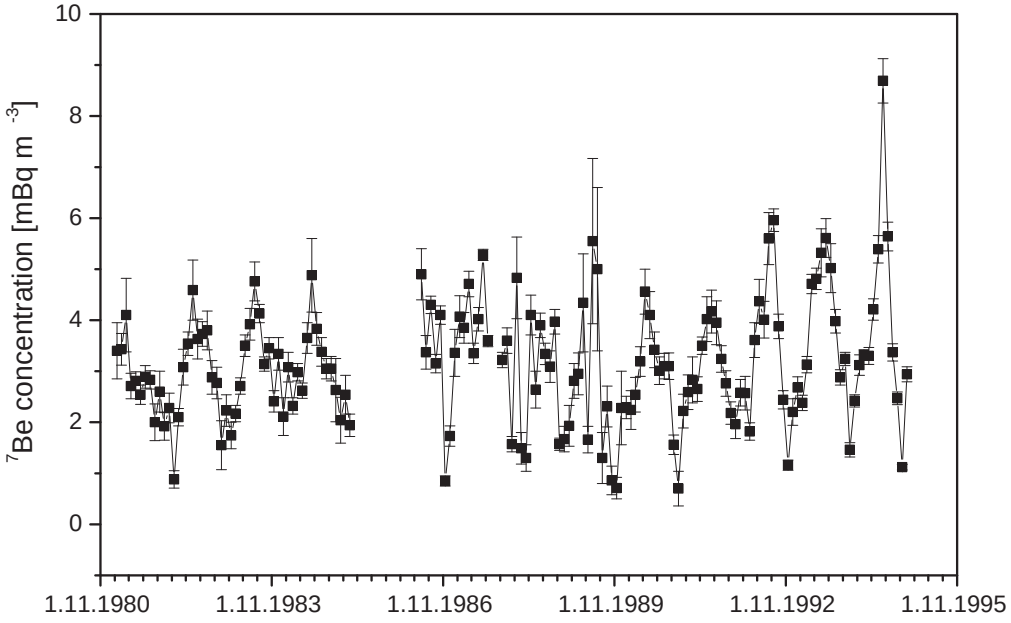

Figure 1.1: Temporal variations of ^{7}Be concentration in ground level air in Bratislava in period 1981 - 1994 [Ďurana96].

spheric processes because of its convenient half-life, sufficiently detectable gamma-radiation and known source. Also its content has not been altered by anthropogenic inputs, such as nuclear weapons testing and accidents at nuclear facilities. It serves for investigations of vertical and horizontal transfer of air masses, transport of aerosol particles within the troposphere, and exchange processes between the stratosphere and the troposphere. ^{7}Be together with ^{10}Be were applied in studies of atmospheric circulation [Bhandari66], [Raisbeck81], [Koch98]. ^{7}Be and ^{35}S were utilized as tracers for studies of the kinetics of SO_2 oxidation and dry deposition [Tanaka95]. Today, these measurements may be very useful for evaluation of the range and tendencies of potential changes in global circulation pattern.

^{7}Be is applied not only in atmospheric research but also in other environmental studies. It was used to estimate soil erosion rates associated with individual events or short periods [Blake99], [Wilson03], or to evaluate the half life of suspended particles in the river estuarine turbidity maximum [Ciffroy03]. Since ^{7}Be has its origin in the outdoor atmosphere it is used in experiments examining the entrance of aerosol particles to indoor air [Roed87].

The long-lived progeny of inert gas ^{222}Rn, ^{210}Pb, is used as a surrogate for other atmospheric components in the atmospheric research. Of the various components for which ^{210}Pb can be considered a surrogate, the most applicable appears to be sulfate. The reason for this is that sulfate, like ^{210}Pb, is derived from

gaseous precursor (SO_2). The conversion to an aerosol-carried species takes place at an approximately similar rate and ^{210}Pb and SO_4^{2-} attach to the same class of submicrometer aerosol [Turekian89], [Graustein83]. Since the primary source of mercury in the atmosphere is a gaseous element, its precipitation can be tracked by ^{210}Pb [Lamborg00]. The concentration ratio of ^{210}Pb to other ^{222}Rn decay products can be used to obtain information on the residence time of aerosols [Papastefanou06], [Baskaran01]. Moreover, ^{210}Pb is often used in geophysical applications, like in modeling various bio-geochemical cycles of lacustrine, estuarine and coastal marine environments as well as soils, peatlands, polar and glacial ices [El-Daoushy88].

The aerosol tracers ^{7}Be and ^{210}Pb, taken together, offer an excellent test for the simulation of vertical transport and aerosol scavenging in global models. The two radionuclides are widely used in three-dimensional chemical tracer models [Koch96a], [Rehfeld95]. The transport model of Heinrich *et al.* succeeded in reproducing daily variations of ^{7}Be and ^{210}Pb concentrations. Calculated daily concentrations were compared to measured ones. The three selected stations belong to the network of the International Monitoring System developed in the framework of the Comprehensive Test Ban Treaty (CTBT) [Heinrich07].

A simpler approach was used in studies of the one-dimensional steady state diffusion model [Talpos97], [Jasiulionis05]. The mean vertical concentration profile of ^{7}Be can give information about the vertical transport in the atmosphere and microphysical processes of incorporation of aerosol particles by cloud droplets.

The two radionuclides have been found to be useful since they are associated with the same class of submicrometer aerosol particles as that which carries pollutant species such as SO_4^{2-} [Graustein83]. As ^{210}Pb has its source in the ground air and ^{7}Be has its major source in the stratosphere and higher troposphere, the sources of chemical species in the lower free troposphere can be determined by using the ^{7}Be/^{210}Pb ratio. Such a study showed that the primary source of ozone in the lower free troposphere of the eastern Atlantic was the upper troposphere [Graustein96].

Even after 45 and 22 years after the nuclear-test-ban treaty and Chernobyl accident, respectively, the atmospheric concentration of ^{137}Cs is on detectable levels. Several works, presenting results of gamma spectrometric measurements of ^{137}Cs concentrations in air [Papastefanou96], [Kozak97], [Kulan06], reveal a certain interest of this fission derived radionuclide. But nowadays the focus from the radiation protection intentions changed to the utilization of ^{137}Cs as a tracer of several natural processes. For example, it has been used to study soil erosion and resuspension processes [Igarashi96].

Air pollution ranks among important environmental problems occurring worldwide. Elemental content of airborne particulate matter can provide important information on the degree of atmospheric pollution and further evaluation of the potential health risk to the population. Increased concentrations of air pollutants cause health damages, diminish forests, reduce biodiversity, *etc.* Several epidemiological studies have shown positive correlation between different aerosol character-

istics and increased human morbidity and mortality [Dockery93], [Pope95]. Moreover, the airborne particles significantly influence several atmospheric processes, for example creation of clouds, or may change the transfer of solar radiation. For this reasons it is necessary to know their chemical composition and physical characteristics in order to understand their behavior and impact.

A balance between sources, chemical transformations in the atmosphere, long-range transport effects and removal processes influences the composition of atmospheric particles. Measurements of the spatiotemporal variations in the concentration of aerosol particles, their physical properties and chemical composition are essential to establish a fundamental, quantitative understanding of their direct sources, their formation from chemical reactions in the atmosphere and to find out how their properties determine their impacts on the global climate and human health.

Several studies around the world are utilizing numerous analytical methods in the evaluation of air quality [Bem03], [Utsunomiya04], [Eleftheriadis01], [Wróbel00], [Salma02], [Rizzio01], [Cao02]. In spite of the competing non-nuclear analytical techniques (AAS, ICP-ES, ICP-MS, *etc.*), neutron activation analysis continues to be the most powerful multi-element analytical technique used in geosciences and material sciences [Frontasyeva06].

1.1 Objectives of the thesis

In general the objectives of the presented PhD. thesis can be summarized in the following points:

- Basis of this work consists in the experimental data of activity concentrations of radionuclides ^{7}Be, ^{210}Pb, ^{137}Cs, and ^{40}K in the ground level atmosphere and in the precipitations. To obtain such data particular sampling and measuring equipment is required. Securing the stability and optimization of the sampling conditions are necessary requirements for the reliability of the experimental data. The detailed analysis of all possible influencing factors is needed. The additional corrections for radioactive decay, calibration, *etc.* have to be applied. Since the levels of determined radioactivity are very low, especially of ^{137}Cs and ^{40}K, the influence of the background radiation to the gammaspectrometric measurement has to be considered and evaluated.

- Different statistical analytical tools will be applied on the data of activity concentrations in air and precipitation, or depositional fluxes of the radionuclides. The correlation analysis with the meteorological parameters like air temperature, atmospheric pressure, amount of precipitation, *etc.*, should reveal the processes and significance of their impact on the variations of radioactivity level in the atmosphere.

- Furthermore, the results of ^{7}Be activity concentration in air and its depositional fluxes should be used in the model of vertical distribution of this

radionuclide in the atmosphere in order to evaluate the diffusion of aerosol particles and their scavenging by precipitation. Vertical mixing in the troposphere and stratosphere, the radioactive decay, wet deposition as well as gravitational sedimentation are physical processes considered in the model.

- By utilizing the neutron activation analysis on aerosol filter samples we attempt to asses the level of air pollution in Bratislava in respect of heavy metals and other trace elements. Determination of the elemental composition of the atmospheric aerosol particles can provide important information about their sources and impacts on the human health or climate.

Chapter 2

Atmosphere

The atmosphere is gaseous envelope surrounding the Earth separating it from outer space. The name comes from Greek atmos (steam, gas) and sphaira (sphere). Although it contains many gases, more than 99.9% of its weight is contributed to nitrogen, oxygen, and argon. The total mass of the dry atmosphere is estimated to be about 50×10^{17} kg, to which may be added 1.5×10^{17} kg of water vapor, the most variable constituent and the one that governs many of its thermodynamic characteristics. The atmosphere protects life on Earth by absorbing ultraviolet solar radiation and reducing temperature extremes between day and night. Compared with the other Earth's spheres it is distinguished by its low weight, high movability and unstableness. Its properties are significantly changing with the altitude; mass density and atmospheric pressure are exponentially decreasing with the increase of height (Figure 2.1). The most often used model is the U.S. Standard Atmosphere which depicts idealized year-round mean conditions for middle latitudes such as 45N, for a range of solar activity that falls between sunspot minimum and sunspot maximum [USSA62]. The Earth's atmosphere is usually divided according to the temperature behavior into layers called: troposphere, stratosphere, mesosphere, ionosphere (or thermosphere), exosphere and magnetosphere.

The effects of inhaling particulate matter have been widely studied in humans and animals. The size of the particle is a main determinant of where in the respiratory tract the particle will come to rest when inhaled. Larger particles are generally filtered in the nose and throat and do not cause problems, but particulate matter smaller than about 10 μm can settle in the bronchi and lungs and cause health problems. The health effect depends on breathing rate, the volume of lungs and others. The rough estimate states that about 50% of inhaled aerosols enter the respiratory tract [ICRP66].

2.1 Structure and composition of atmosphere

Troposphere is the lowest layer starting at the surface going up to between 7 km at the poles and 17 km at the equator with some variation due to weather factors. The troposphere has a great deal of vertical mixing due to solar heating at the

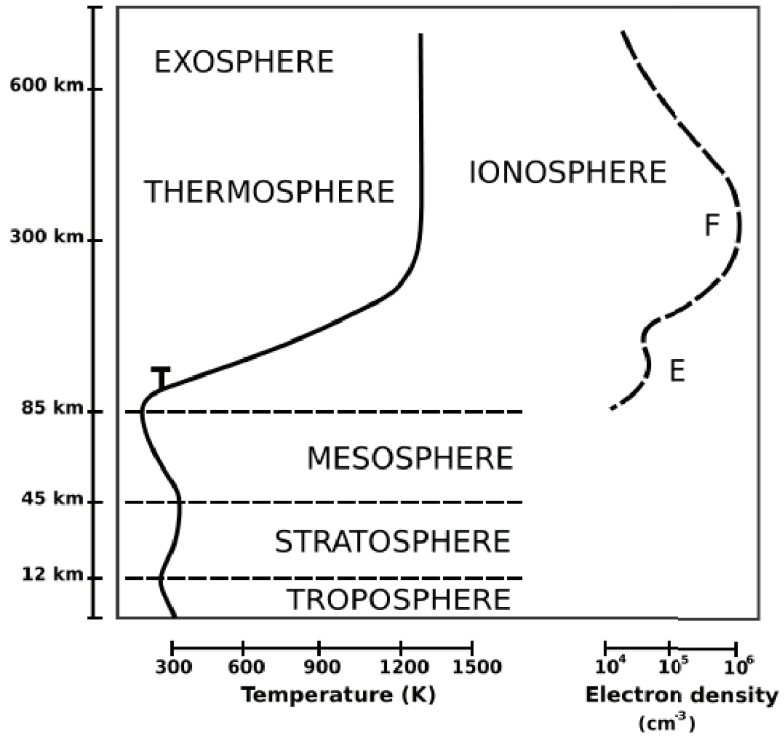

Figure 2.1: The trend of air temperature and electron density versus altitude and the corresponding layers of atmosphere.

earth's surface. This heating warms air masses, which then rise to release heat that further elevates the air masses. This process continues until all water vapor is removed. In the troposphere, on average, temperature decreases of 6.5°C for 1 km of height due to expansive cooling. The boundary between the troposphere and the stratosphere is called tropopause. Here is the temperature of the air about -50°C, and the air is almost completely dry.

Stratosphere is the second layer of Earth's atmosphere, just above the troposphere, and below the mesosphere. The stratosphere starts from 7-17 km range to about 50 km altitude above the surface. It has temperature increasing with height. This is in contrast to the troposphere, which is cooler higher up and warmer down. Stratosphere is heated from above by absorption of ultraviolet radiation from the Sun by an ozone layer. The top of the stratosphere has a temperature of about -3°C, just slightly below the freezing point of water. This top is called the stratopause, above which temperature again decreases with height. The vertical stratification, with warmer layers above and cooler layers below, makes the stratosphere dynamically stable: there is no regular convection and associated turbulence in this part of the atmosphere.

Ozone in the earth's stratosphere is created by ultraviolet light striking oxygen molecules containing two oxygen atoms O_2, splitting them into atomic oxygen; the atomic oxygen then combines with unbroken O_2 to create ozone, O_3. The region

Table 2.1: Chemical composition of particulate-free dry atmosphere

Component	Concentration [mg m^{-3}] (15°C, 101.3 kPa) [Závodský01]	Volume [%] [Bailey02]	Mean residence lifetime τ [Závodský01]
N_2	9.2×10^8	78.084	$2. \times 10^7$ years
O_2	2.8×10^8	20.948	10^4 years
Ar	1.6×10^7	0.934	?
CO_2	6.5×10^5	0.035	50 - 200 years
Ne	1.6×10^4	0.00182	10^9 years
CH_4	1.2×10^3	0.00017	10 years
Kr	4.1×10^3	0.00011	?
H_2	50	0.00005	1.8 years
N_2O	500	0.00003	120 years
CO	200	0.00001	3 months
Xe	500	9×10^{-6}	?
O_3	60	1-10 $\times 10^{-6}$	2 months
NO_2	2	2×10^{-6}	6 days
NH_3	2	6×10^{-7}	5 days
SO_2	2	2×10^{-7}	2 days
H_2S	0.2	1×10^{-8}	2 days

from about 10 to 50 km rich in ozone is called ozonosphere or ozone layer. The mesosphere is layer from about 50 km to the range of 80 to 85 km, temperature decreasing with increasing height. Temperatures in the upper mesosphere fall as low as -100°C, varying according to latitude and season. The thermosphere is the layer from 80-85 km to 640 km. Thermospheric temperatures increase with altitude due to absorption of highly energetic solar radiation by the small amount of residual oxygen still present. Temperatures are highly dependent on solar activity, and can rise to 2000°C. The exosphere is the uppermost layer of the atmosphere. It is only from the exosphere that atmospheric gases, atoms, and molecules can escape into space.

The upper mesosphere and lower thermosphere is the area with elevated concentrations of electrically charged particles (Figure 2.1). They are ionized by solar radiation, therefore it is called ionosphere. It plays an important part in atmospheric electricity and forms the inner edge of the magnetosphere. The Earth's magnetosphere is a region in space whose shape is determined by the Earth's internal magnetic field, the solar wind plasma, and the interplanetary magnetic field. It is a mix of free ions and electrons from both the solar wind and the Earth's ionosphere. The magnetosphere is distinctly non-spherical. On the side facing the Sun, the distance to its boundary (which varies with solar wind intensity) is about

70 000 km and on the night side it is stretching to long distances of about 130-160 thousand km.

At an altitude of about 100 km is the turbopause. Below these line has the Earth's atmosphere a more-or-less uniform composition (the ratio of main components like N_2, O_2, Ar is stable); this constitutes the homosphere. The main mechanism of vertical mixing is turbulent diffusion (vertical fluxes of momentum, mass and energy). Above the turbopause is the composition of atmosphere varying with altitude, thus this layer is called the heterosphere. The length of the mean free path between molecules is about 2.5 cm at 100 km and about 25 m at 300 km [Petterssen68] so there is no formation of turbulent diffusion and in vertical transfer is only molecular diffusion applied. Above an altitude of about 600 km, the molecules are thought to behave as satellites in free elliptical orbits about the Earth [Mason82].

In Table 2.1 is the list of main chemical components of atmosphere, their concentration, % by volume and mean residence lifetime. The shorter is lifetime τ of the component the larger are spatial and temporal variations of its concentration. At the $\tau > 100$ years is the concentration homogeneous in whole troposphere and stratosphere. Usually, the atmosphere also contains water wapor and aerosol, but these occur in amounts that vary widely from place to place and from time to time.

2.2 Atmospheric circulation

Atmospheric circulation is the large-scale movement of air in zonal (along latitude), meridional (along meridian) and vertical directions. It is the means by which energy, momentum and vapor is distributed on the surface of the Earth. The large-scale structure of the atmospheric circulation varies from year to year, but the basic structure remains fairly constant. It is integral result of solar radiation balance in different latitudes, rotation of the Earth, gravitational forces, uneven distribution of lands and oceans and surface friction of floating air. The atmosphere is rotating in the same direction as the Earth but westerly winds move faster and easterly winds move slower than the Earth's surface.

The general circulation of atmosphere results mainly because of the vertical temperature gradient. This gradient is influenced by the distribution of total solar radiation over land and oceans. Horizontal advection, water vapor from oceans, heating of air and upper levels of soil are the means of the solar radiation transfer. Daily sums of global solar radiation are different on northern and southern hemisphere due to the eccentricity of Earth's orbit. The solar heating, on average is largest near the equator and smallest at the poles. Poleward is the balance of energy transfer rapidly decreasing and the difference between land and water surface vanishes on polar zones almost completely.

Warm air rises to 10-15 km, creating a low pressure center. Surrounding air is moving into the equatorial region, into the low pressure area and the air is heated

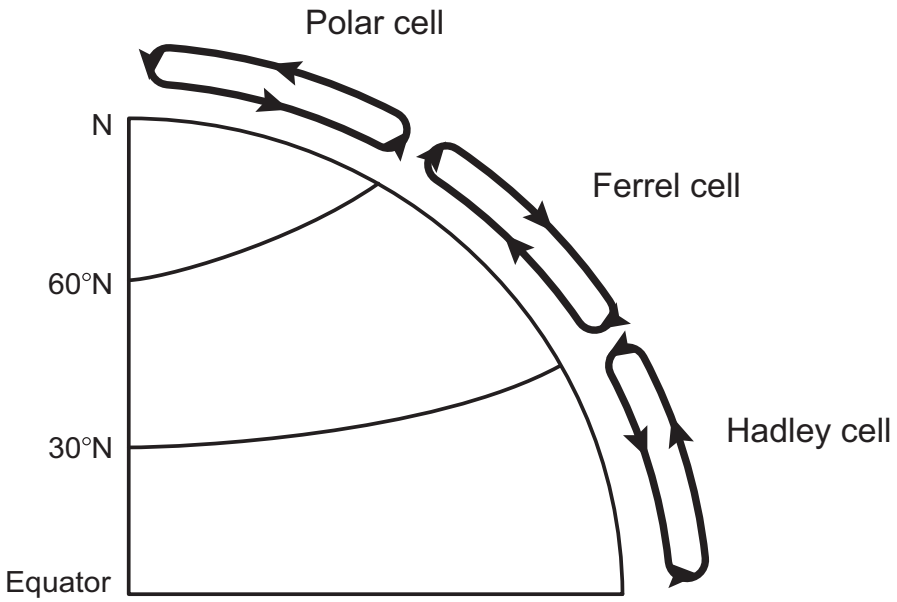

Figure 2.2: Three-cell model of general atmospheric circulation in the Northern Hemisphere [Bailey02].

by insolation and rises. Warm air then moves poleward where it is cooled and descends at $\sim 30^\circ$ of latitude, creating a high pressure area. Air moves out of the high pressure centers towards the equatorial low pressure centers completing a circulation cell known as a Hadley cell. The Hadley cell is a circulation pattern that dominates the tropical atmosphere.

The intertropical convergence zone, also known as the Monsoon trough, is a belt of low pressure girdling Earth at the equator. It is formed by the vertical rise of warm, moist air from the latitudes above and below the equator. The location of the intertropical convergence zone varies over time. Over land, it moves back and forth across the equator following the Sun's zenith point. Over the oceans the seasonal cycle is more subtle, as the convection is constrained by the distribution of ocean temperatures.

In subtropical latitudes between 30 and 35 degrees both north and south is the subtropical high pressure belt (horse latitude). This region is an area of variable winds mixed with calm. Polar regions, with very cold air, tend to be high pressure center. Air movement will be away from the poles towards the mid-latitudes. Air in the subtropical high pressure belt is hot and moving away from the tropics towards the mid-latitudes. These two conflicting air masses, one hot, one cold, meet at the polar front. Along the polar front, the warm air, being less dense, will rise over the cold air. Some of this air returns at high altitude to the region above the subtropical belt completing what is known as the Ferrel cell. Some of this air continues poleward completing the polar cell circulation.

Tropospheric and stratospheric behavior results from the circulation described above. Warm air enters the stratosphere in the tropical regions and rises to an

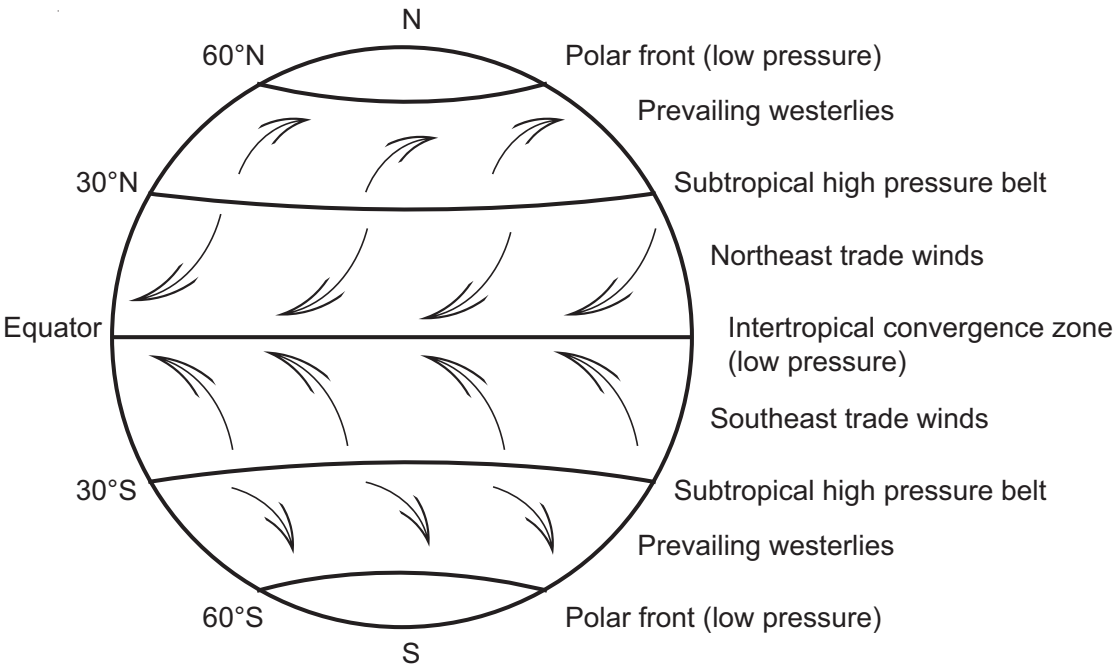

Figure 2.3: Scheme of prevailing wind patterns on the Earth's surface [Bailey02]

altitude of about 30 km, at which level it begins to move toward the poles. Discontinuities in the tropopause in the temperate regions facilitate transfer from the stratosphere to the troposphere. Here the westerly jet streams occur with transport velocities of 100 to 300 km h^{-1} and are accompanied by strong vertical mixing. The transfer rate from the lower stratosphere is most intensive in the winter and early spring.

Chapter 3

Atmospheric aerosol

Aerosols alternatively referred to as particulate matter (PM), or fine particles, are tiny particles of solid or liquid suspended in a gas. It includes a wide range of phenomena such as dust, fume, smoke, mist, fog, haze, and smog. They range in size from a few nanometers (nm) to tens of micrometers (μm) in diameter, from freshly nucleated clusters containing few molecules to cloud droplets and crustal dust particles. Atmospheric aerosol particles in general follow a trimodal distribution including:

1. the Aitken nuclei mode (from 0.003 to 0.07 μm, average 0.015 μm),

2. the accumulation mode (from 0.07 to 2 μm, average 0.3 μm), and

3. the coarse mode (from 2 to 36 μm, average $>$ 10 μm) [NRC79].

These modes originate separately, are transformed separately, are removed from the atmosphere by different mechanisms, have different lifetimes, have different chemical composition, have different optical properties, and differ significantly in their deposition patterns in the respiratory tract.

The notation PM10 is used to describe particles of 10 μm or less and PM2.5 represents particles less than 2.5 μm in aerodynamic diameter; other numeric values may also be used. This range of sizes represents scales from a gathering of a few molecules to the size where the particles no longer can be carried by the gas.

The radionuclides produced in the atmosphere, with the exception of gaseous elements, are attached to aerosol particles. Hence the transportation and deposition characteristics of radionuclide become those of aerosol particles. The most abundant aerosols in terms of surface area are the accumulation mode particles. This size class carries many of the chemical species in the atmosphere that have low volatility and also have gaseous precursors. Accumulation mode aerosols are most subject to long-distance transport and scavenging by precipitation is the principal mechanism of their removal from the atmosphere. Therefore the airborne radionuclides like ^{7}Be or ^{210}Pb are becoming good tracers for the aerosols and related studies of atmospheric mixing.

3.1 Relevance of aerosols

Atmospheric aerosols have significant local, regional and global impacts. Local impacts include vehicular and industrial processes and forest fires that can lead to urban air pollution and possible adverse health effects. Regionally can be aerosols transported from areas of high emissions to relatively clean remote regions. Trough their role in heterogeneous chemistry have aerosols the potential to significantly influence the entire globe.

Also their effect on the Earth's climate as they scatter incoming shortwave radiation back to space and serve as condensation nuclei for cloud droplet formation is of high importance. At present, the radiative effects of aerosols have the dominant uncertainties in global climate predictions to quantify changes due to man-made changes in composition of the atmosphere [IPCC07]. A better understanding of the formation, composition and transformation of atmospheric aerosols is of critical importance in order to better quantify these effects.

Environmental aspects

Aerosol particles in the size range of 0.1 - 1.0 μm scatter light with high efficiency [Cheng00]. Therefore, the degradation of visibility is one of the most perceptible aspect of urban air pollution. Aerosols also act as sites for heterogeneous chemical reactions to take place. The most significant of these reactions are those that lead to the destruction of the stratospheric ozone.

In the recent report of the Intergovernmental Panel on Climate Change (IPCC) concluded that changes in the atmospheric abundance of greenhouse gases and aerosols, in solar radiation and in land surface properties alter the energy balance of the climate system [IPCC07]. These changes are expressed in terms of radiative forcing, which is used to compare how a range of human and natural factors drive warming or cooling influences on global climate (Figure 3.1). It is an index of the importance of the factor as a potential climate change mechanism. Because aerosol particles in the atmosphere scatter sunlight back into space, they reduce the amount of energy absorbed by the Earth.

Aerosols have, so called, indirect effect on climate by changing the properties of clouds. Aerosols contribute to determining the reflectivity of clouds - cloud albedo. They also affect precipitation processes. Aerosols influence the initial droplet size distributions, and can subsequently influence the effectiveness of coalescence. Furthermore, aerosols influence freezing processes in mixed-phase clouds. Both these processes (coalescence and freezing) influence precipitation development. Precipitation is a key component in the atmospheric energy balance trough the redistribution of latent heat. Hence we can say that aerosols influence the dynamical processes in the atmosphere that drive cloud formation and development [Noone01].

As can be seen in Figure 3.2 particulate pollution increases cloud albedo. For a dynamic forcing that creates a cloud with a given vertical extent and liquid water

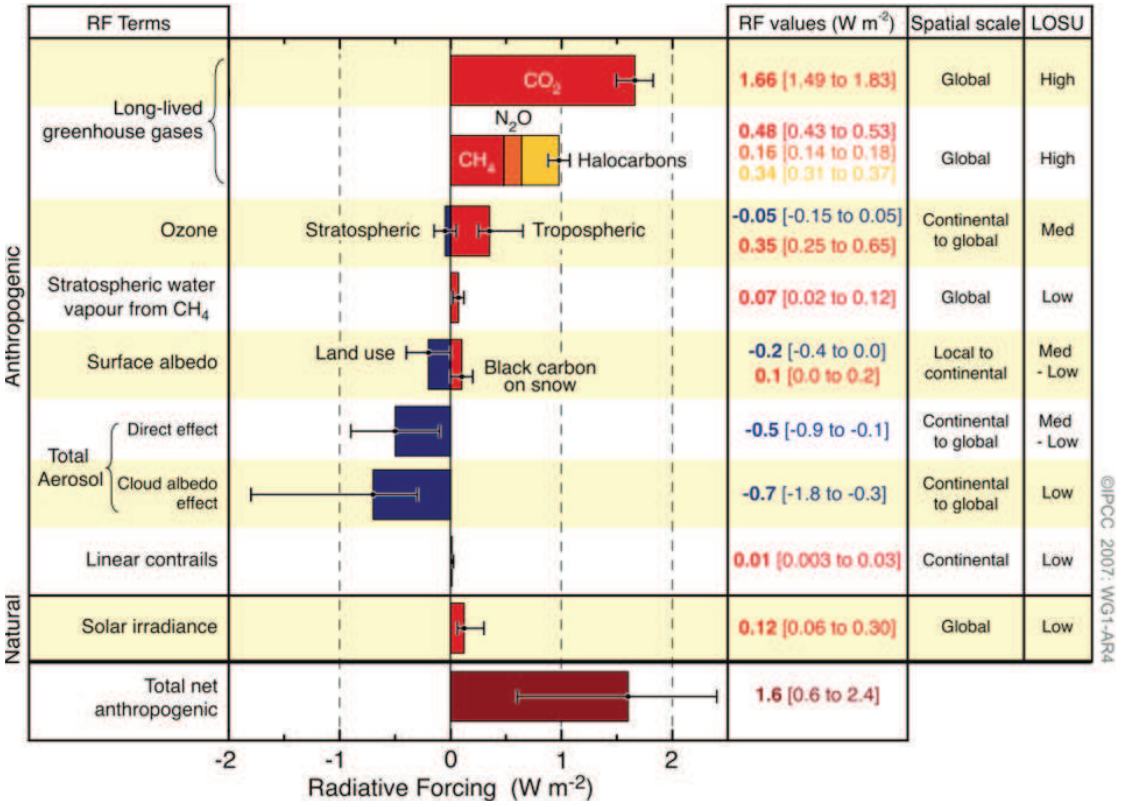

Figure 3.1: Global average radiative forcing estimates and ranges in 2005 for anthropogenic agents and mechanisms, together with the typical geographical extent (spatial scale) of the forcing and the assessed level of scientific understanding (LOSU). Volcanic aerosols contribute an additional natural forcing but are not included due to their episodic nature [IPCC07].

content, an increase in aerosol concentration can result in the formation of a larger number of smaller droplets as compared to unperturbed cloud [Twomey74].

The same processes that tend to increase cloud albedo tend to decrease precipitation formation. If precipitation is suppressed, water and latent heat that would have been removed from the atmosphere remains aloft and can be transported to other locations before it is deposited to the surface. This redistribution may have the potential to influence circulation patterns.

Health effects

Many epidemiological studies have observed connections between particulate air pollution and human health [Dockery93], [Pope95]. Elevated particulate air pollution has been associated with declines in lung function and increases risk of cardiopulmonary and lung cancer mortality.

Trace metals influence the toxicity of airborne particulate matter. Metals are redoxactive and can, therefore, induce or catalyse chemical change leading to pro-

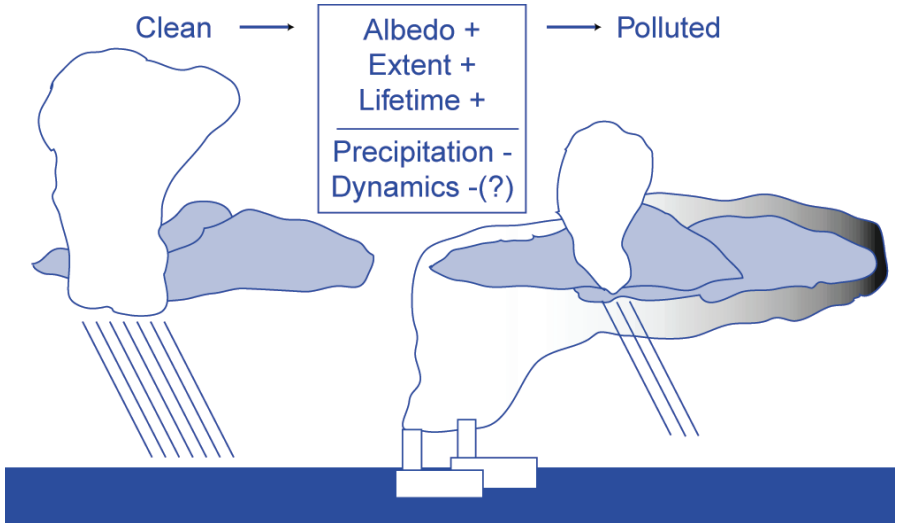

Figure 3.2: Indirect effects of aerosols on cloud properties. The rectangle indicates the expected sign of the effect (increase or decrease) going from clean to polluted conditions [Noone01].

duction of free radicals, which have known ability to cause tissue inflammation. Toxicological studies showed that ultrafine particles of less than 100 nm appear to have considerably enhanced toxicity per unit mass and that their toxicity increases as particle size decreased. The large surface area provided by ultrafine particles in contact with the lung provides the opportunity for surface chemistry of the particles to have a profound effect [Donaldson98].

3.2 Aerosol sources

Atmospheric aerosol can be formed due to dispersion from the surface or condensation (chemical reactions) [Závodský01]. Sources of particulate matter can be anthropogenic or natural. Table 3.1 indicates that particles of anthropogenic origin constitute between 5 and 45% of the total in atmosphere. The natural aerosols originate from volcanic activity, meteorites, dust storms, forest fires, and sea spray. Human activities, such as the burning of fossil fuels, industrial processes, nonindustrial fugitive processes (e.g. construction work), and transportation sources also generate aerosols. Averaged over the globe, anthropogenic aerosols currently account for about 10% of the total amount of aerosols in our atmosphere.

Mineral sources

Coarse aerosol with the diameter larger than 2.5 μm is created by the weathering of the terrestrial material (bulk to particle conversion). Soil are formed by the weathering of crustal material of the Earth. Rock slowly disintegrate trough the action of water, chemically by the leaching of soluble components, and mechani-

Table 3.1: Estimate of particles emitted into or formed in the atmosphere each year [Bailey02]

Particle sources	Quantity [megatons/year]
Natural	
Soil and rock debris	100-500
Forest fires	3-150
Sea salt	300
Volcanic action	25-150
Gaseous emissions	
Sulfate from H_2S	130-200
NH_4^+ salts from NH_3	80-270
Nitrate from NO_x	60-430
Hydrocarbons from vegeration	75-200
Natural particle subtotal	773-2200
Antropogenic	
Direct emissions, smoke, *etc.*	10-90
Gaseous emissions	
Sulfate from SO_2	130-200
Nitrate from NO_x	30-35
Hydrocarbons	15-90
Anthropogenic particle subtotal	185-415
Total	958-2615

cally by the freeze-thaw cycle of water. In this way is crustal material transformed into clay minerals, carbonates, and quartz grains (sand). Once the material has been broken to grain sizes less than 1 mm it can be moved by wind force into air. Most of these particles return quickly to the ground, only particles with radii smaller than about 100 μm can remain airborne for a longer period of time.

Sea spray

The production of sea-salt aerosols is due to the agitation of the sea surface by wind force, and in this regard its formation is similar to that of dust aerosol. Seawater contains sea salt to about 3.5% by weight, of which 85% is sodium chloride. As the drops enter the atmosphere they experience lower relative humidities and dry up until their water content is in equilibrium with the environment.

Gas to particle conversion

Fine particles with the diameter smaller than 2.5 μm are produced mainly via condensation, called gas to particle conversion. In the case, the new particle is

created it is called homogenous nucleation (Aitkinen mode). Molecular clusters are formed due to weakly attractive forces between molecules, the Van der Waals forces. The best-known reaction of this kind is the oxidation of SO_2 to H_2SO_4 and its neutralization by ammonia to form sulfate salts. The heterogeneous nucleation is process where the existing particles are interacting.

Miscellaneous sources

Biogenic particles are released from plants in the form of seeds, pollen, spores, *etc.* The concentrations and populations of pollen and spores change rapidly with locality, season, time of the day, and meteorological concentrations. In contrast to plant derived particles, bacteria usually occur attached to other aerosol particles because they are mobilized together with dust.

Volcanism constitutes another source of particulate matter in the atmosphere. Sulfur is emitted from volcanoes largely in the form of SO_2, which is subsequently oxidized to H_2SO_4.

Forest fires are the next source of atmospheric aerosol particles. They emit particles into a plume reaching far into troposphere, but not into the stratosphere like during volcanic activities.

3.3 Aerosol properties

3.3.1 Aerosol chemical composition

The chemical composition of individual aerosol particles varies widely and depends on their source. The main constituents are sulphates, ammonium, nitrate, sodium, organic, crustal elements, trace metals, sea salt, hydrogen ions, carbonaceous material and water.

We distinguish three types of atmospheric aerosol: the continental, the maritime, and the tropospheric background aerosol. By chemical composition, the first type contains mainly materials from the surface sources, mineral oxides and other substances blown from the Earth's crust. Sea salt consists mainly of sodium chloride originated from sea spray and other constituents of atmospheric sea salt reflect the composition of sea water, and thus include magnesium, sulfate, calcium, potassium, *etc.* The third type represents an aged and much diluted continental aerosol. Also the fourth category of aerosol exists, the properties of urban aerosol particles are changed by anthropogenic influences.

Secondary particles derive from the oxidation of primary gases such as sulfur and nitrogen oxides into sulfuric acid (liquid) and nitric acid (gaseous). The precursors for these aerosols, i.e. the gases from which they originate, may have an anthropogenic origin (from fossil fuel combustion) and a natural biogenic origin. In the presence of ammonia, secondary aerosols often take the form of ammonium salts, i.e. ammonium sulfate and ammonium nitrate.

Toxic metals in atmospheric aerosol

In this section are properties, sources and relevance of eight toxic metals discussed. Elements are emitted into the atmosphere from several anthropogenic and natural sources. They attach to aerosol particles and hence represent a potential threat to human health. Therefore, are the atmospheric concentrations of these pollutants of a great interest of several national and international organizations. For example, the European Commission Regulation no. 166/2006 established the European Pollution Release and Transfer Register, which deals with about 50 pollutants including some heavy metals (As, Cd, Cr, Cu, Hg, Ni, Pb, and Zn) [EC166/2000].

Vanadium (V) is relatively mobile in the environment. Natural sources (65 000 tons per year) are the weathering of V-minerals, volcanic activities, fires, or showers of meteorites. Anthropogenic sources (210 000 tons per year) are V steel and alloys producers, jet engines, electronic, ceramic and glass works, *etc.* However, the most important source of V is the burning of crude oils, coal, bitumen, *etc.* The rural atmosphere contains 0.001-3 ng of V per m^3, the urban industrial atmosphere 7-200 ng m^3. V is essential in the control of some enzymes in many animal species. Although the necessity of V was not confirmed for humans, sometimes a dose of about 0.1 mg pre day is recommended for an adult human. Exposure to large amounts of v mainly trough inhalation is toxic. Inhalation exposures to 35 mg m^3 are considered immediately dangerous to life and health. The maximum safe concentration of V in the atmosphere is recommended to be 1 μ m^3.

Chromium (Cr) is relatively abundant crustal element presented in the average concentration of about 120 mg kg^{-1} in the Earth crust. Natural sources producing approximately 358 000 tons of Cr per year are the weathering of ultrabasic and basic rocks (200-2000 mg kg^{-1}). Brown coal contains on average 550 mg of Cr per one kg, while in coal ash the Cr content may increase up to 155 kg^{-1}. Anthropogenic sources of Cr are the combustion of fossil fuels, the processing of Cr based ores, metallurgical, chemical and leather industries. The species Cr^{3+} is essential for animals and humans for sugar metabolism and its deficiency causes diabetes. Cr is toxic and carcinogenic element. It is blamed for inducing allergies, chromosome damages, lung cancer.

Iron (Fe) is relatively abundant, typical crustal element. Natural emission source of Fe (27 775 300 tons per year) is weathering of Fe-based minerals. Anthropogenic sources of Fe (10 700 000 tons per year) are melting and steel works, ferrous metallurgy, industrial furnaces, *etc.* It is essential element for plants and animals, but in excess can be toxic. Fe intake of 20-30 mg kg^{-1} day^{-1} can cause intoxication and dose above 60 mg kg^{-1} day^{-1} is usually lethal. Iron is considerably higher in Slovakia than in neighboring countries (Austria, Czech Republic and Poland). Besides emissions from the metallurgical and engineering industries, iron species are naturally abundant in compounds of rock and soil material [Suchara07].

Nickel (Ni) is relatively abundant element on the Earth. The main natural source of Ni (28 300 tons pre year) is the weathering of parent rocks. Anthropogenic emission (98 000 tons pre year) include works producing and processing

Ni alloys. Burning of fossil fuels releases also significant amounts of Ni into the atmosphere (about 60% [Suchara07]). Urban air may contain about 10-20 ng of Ni per m^3 compared with about 0.5-5.0 ng m^3 in the rural air. Ni is biogenous essential element. Its inefficiency decreases animal growth, causes anaemia and some enzyme disfunctions. But it is also carcinogenic, long exposure of Ni may cause for example lung cancer. Also some allergies, renal tubular disfunctions, and dermatitis in humans were observed. About 10% of women and 2% of men in the population are highly sensitive to Ni (coins, jewelery, *etc.*).

Natural production of copper (Cu) is about 20 000 tons per year. The source is weathering of usually Cu-sulphide microglobules being present in parent rocks. Anthropogenic Cu sources producing about 265 000 tons per year are Cu smelting and electroplating works, Cu alloy foundries, coal combustion, *etc.* Cu is essential element for bacteria, algae, fungi, plants and animals. However, a high input of Cu into biota may act toxically. Minimal hazardous limit for oral Cu uptake is 0.01 mg kg^{-1} day^{-1}. Carcinogenicity of Cu was not confirmed reliably. Metallurgical industry including processing of non-ferrous metals (75%), and smelters belong to the main pollution sources of Cu. Distribution of deposition loads of some other metals (Zn, Ag, Sb, Pb) shows very similar pattern in Slovakia [Suchara07].

Natural sources of zinc (Zn) (35 800 tons per year) include the weathering of minerals, volcanic activities and large vegetation fires. Anthropogenic sources are melting of Zn ores, recycling of Zn wastes, electroplating works, some chemical plants, *etc.* Zn is emitted in to the atmosphere by burning of coal in power plants and industrial furnaces and waste incinerators. Zn is essential element. It is needed for synthesis of DNA, transcription of RNA, operation of immune system, for bone and teeth mineralization, *etc.* The recommended daily allowance of Zn is 12 and 15 mg per day for woman and man, respectively. Zn toxicity for humans appears after the inhalation of Zn dust causing a fever for several days or lung oedema. Zn may support the growth of cancerous tumors. Chronic toxicity may cause a copper deficiency.

Cadmium (Cd) is not much abundant element in the Earth crust. Natural sources of Cd such as volcanic emissions, transport of eroded materials, vegetation fires, and sea spray may release annually about 300 tons of Cd. Annual anthropogenic sources may be about 5500 tons. Important Cd sources are non-ferrous smelters, coal power plants, incinerators of municipal wastes, car exhausting fumes, *etc.* The typical Cd content in street dust is 1-7 mg kg^{-1}. Cd is very toxic metal, the lethal dose is 250-500 mg. Cigarette smoking and consumption of food in contaminated food chains can increase the intake of Cd dramatically. Acute or chronic exposure to Cd may cause bronchitis, renal damage, malfunctioning of the kidneys, hypertension and bone softening. Cd causes lung and prostate cancer and it is suspicious for initiating cancer of other organs. A half-life time for Cd in human body is 10-30 years. Cd emissions in Slovakia are associated mainly with the operation of ferrous metal industry in the town Košice [Suchara07].

Mercury (Hg) is an element that occurs naturally in the environment. However, human activity has significantly changed its cycling in recent centuries. The main

natural sources of Hg are diffusion from the Earth's mantle, evaporation from the sea surface, and geothermal activity. The largest anthropogenic source on a global scale is the combustion of coal and other fossil fuels. Others sources include metal production, cement production, waste disposal. A significant contribution comes from gold production. On a global scale, the estimated anthropogenic emissions represent about two-thirds of the total [Lamborg02]. According to official emission data, supplemented with the expert estimates, the total for anthropogenic emissions in Europe was 413 tons in 1990 [Berdowski97]. Hg and its compounds are highly toxic substances. Acute poisoning following exposure to Hg vapor at high levels (more than 1000 μg m^{-3}) for a short period can cause severe irritation of the airways, pneumonitis, pulmonary oedema and other symptoms of lung damage. It can damage the brain, nerves, kidneys and lungs and, in extreme cases, can cause coma and/or death.

Lead (Pb) is counted among the least mobile metals in the environment. The natural source (4 000-6 000 tons per year) is the weathering of Pb-based minerals from parent rocks. It is believed that the atmosphere, which is not influenced by human activities, may contain less than 0.04 ng of Pb in m^3. Pb may be also released into the atmosphere during large vegetation fires and volcanic activities. Anthropogenic sources of Pb (400 000 tons per year) are works producing, recycling and utilizing Pb, producers of batteries, Pb-based pigments, crystal glass and ceramics, *etc.* Less Pb is released by fossil fuels and waste incineration. Also burning of coal is an important source because about 20 mg of Pb is released trough combustion of one kg of coal. Pb is not necessary element either for plans or animals. Higher income is toxic. Absorbed Pb is accumulated in bones. Pb affects the peripheral and central nervous systems, blood cells, and metabolism of vitamin D, calcium, and iron. May cause reproductive difficulties, carcinogenic effects, renal insufficiency, *etc.*

3.3.2 Particle size

Size distribution of the aerosol particles is the result of a combination of atmospheric processes like coagulation of ultrafine particles, fog and cloud droplet formation, evaporation and condensation, washout, rainout and sedimentation and of contributions of dust storms and combustion products.

^{7}Be as well as ^{210}Pb have been used in studying the description of environmental processes such as aerosol transport and residence times in troposphere [Dutkiewitz85], [Azahra03], [Vecchi05], aerosol deposition velocities [Young80], [Bleichrodt63], [Ueno03], and aerosol trapping above ground vegetation [Bondietti84].

In the years 1994-1996 Winkler *et al.* were investigating the size distribution of ^{7}Be and ^{210}Pb associated with the atmospheric aerosols [Winkler98]. They have determined the activity median aerodynamic diameter (AMAD). The aerodynamic diameter is defined as the diameter of a unit density sphere (1 g cm^{-3}) that has the same settling velocity in air as the particle under consideration [Hinds82]. Settling velocity is determined by a balance between aerodynamic drag and gravitational

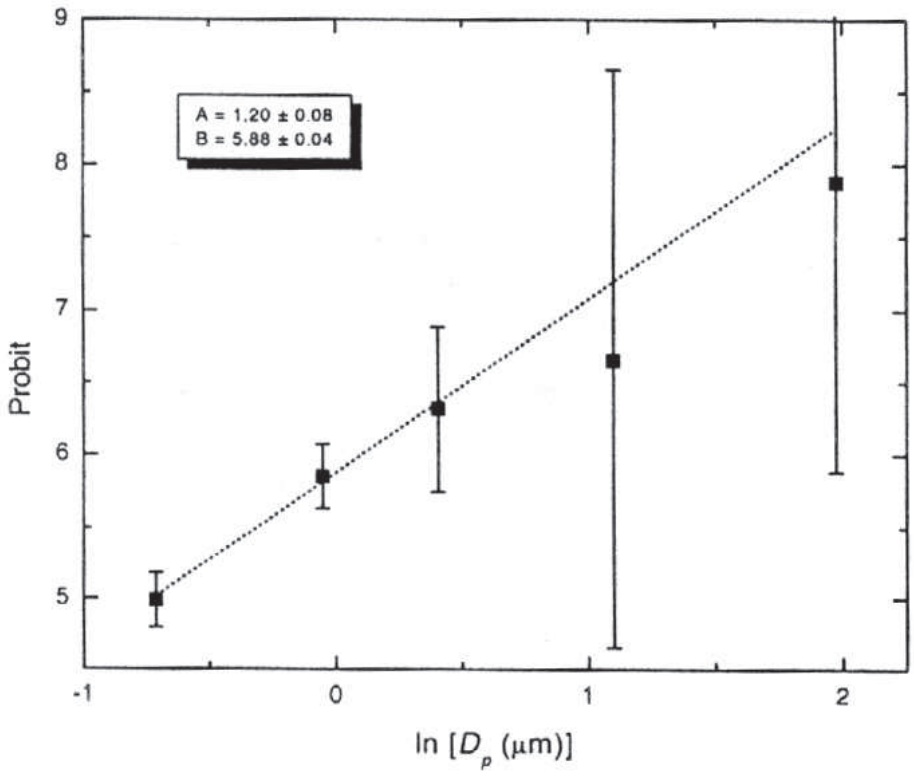

Figure 3.3: An example of a plot of the cumulated percentage of ^{7}Be activity versus the aerodynamic diameter (D_p), in probit and ln scales, respectively. From the best fit line y = Ax + B is the AMAD value determined. In this particular case it is 0.48 μm [Yu02].

force. AMAD is defined such as diameter of aerosol particles that corresponds to median of the distribution of airborne particle radioactivity. AMADs are usually accompanied by the geometric standard deviation which characterizes the variability of the particle size distribution. The value of AMAD is usually determined geometrically as shown on Figure 3.3. The logarithm of the aerodynamic diameter (D_p) is plotted versus the cumulated percentage of activity (out of the total sum of activities on all stages of cascade impactor) less than D_p. The AMAD is obtained by the D_p value corresponding to mean or 50% cumulative probability.

The values of aerodynamic diameter are determined with the limitations of the special sampling device, which allows selection of aerosol particles in cascade according their size. The value of AMAD for ^{7}Be ranged from 0.44 to 0.74 μm, with average 0.57 μm for ^{7}Be [Winkler98]. During the period of high ^{7}Be atmospheric concentrations, for example in the summer, relatively low values of AMAD have been observed. In another study, the AMAD varied from 0.33 to 1.15 μm and also was the negative correlation with air concentrations of ^{7}Be (correlation coefficient

-0.61) observed [Yu02]. Analogous to ^{7}Be, minimum AMADs were observed for ^{210}Pb in summer season. The values ranged from 0.28 to 0.74 μm, with average 0.52 μm [Winkler98]. This suggests a positive correlation between ^{7}Be-AMAD and ^{210}Pb-AMAD.

The activity size distribution for radionuclides of atmospheric origin like ^{7}Be and ^{210}Pb is determined mainly by two different processes: attachment of radionuclides on particles and transformation of the aerosol. The attachment process is controlled by diffusion taking into account electrostatic forces and gas kinetics. For small particles the attachment is proportional to d^2, the particle surface [Baust67], [Lassen60]. For particles with $d > 1$ μm is approximately proportional to d. Calculations of Baust [Baust67] show that about 90% of the natural activity should be initially attached to particles smaller than $d = 0.5\mu$m. Results of measurements of Lassen and Rau [Lassen60] confirm the predicted dependence on d.

The aerosol transformation changes the activity size distribution. Corresponding processes are coagulation and deposition. When particles are present in an aerosol they collide with each other. During that they may undergo coagulation. This process leads to a change in the aerosol size distribution function. Coagulation is very intensive in conditions of high humidity. Fine particles (< 2.5 μm) are mostly hygroscopic and the water mass fraction increases with relative humidity. Water comprises more than 50% of the fine particle mass at relative humidities exceeding 70-80% [Zhang93] and aerosol water content rises sharply above relative humidities of 80%.

Precipitations play important role in these processes [Winkler98]. Wet deposition affects the ^{210}Pb aerosol, formed in ground-level air, to larger extent than the ^{7}Be aerosol which originates from stratosphere and upper troposphere. Lower AMADs were found during the summer season for both radionuclides, but the decrease is much larger for ^{210}Pb and coincides even with the surface median diameter (SMD), which is not the case in the winter period. At this location summer is the season with the highest amount of precipitations. Conclusion of these observations is that the seasonal variation of the AMAD is connected with the seasonal distribution of the rainfall. The same result was observed by Bondietti *et al.* [Bondietti88] for a location Oak Ridge, characterized by higher amounts of rainfall in winter and the lowest AMAD values for ^{210}Pb in the same season. According the observations at the Hong Kong experiment [Yu02], wet precipitation in the middle of the sampling period decreases the ^{7}Be activity in atmospheric aerosol and increases the AMAD. The increase of AMAD is caused by intense coagulation in humid air. Wet precipitation before or at the beginning of sampling period decreases both ^{7}Be activity and AMAD.

3.4 Transport and deposition of aerosols

The level of atmospheric aerosols is governed by actual meteorological conditions. Aerosol particles in the troposphere are deposited on the surface of the Earth

mainly by scavenging action of rain. Dry deposition results from gravitational setting and binding on surfaces exposed to turbulent air flow. When precipitation occurs bellow the rain-forming level, the aerosols are washed by falling raindrops (washout). At higher altitudes the airborne particles serve as condensation nuclei for creation of raindrops (rainout).

Analysis of ^{7}Be and^{137}Cs in precipitation showed that the activity concentration of radionuclides in rainwater depends on whether the rainfall event is of short or long duration and on the amount of precipitation [Ioannidou06]. The raindrops remove the major amount of aerosols in the first part of rainfall event, and any additional increase in the total rainfall amount will not result in an additional increase of aerosol particles in rainwater.

Also when the precipitation rate decreases, the activity concentrations of investigated radionuclides ^{7}Be and ^{137}Cs in rainwater increase [Ioannidou06]. Low precipitation rates during drizzles means that very small raindrops occur, which have a much larger surface area and thus results in higher removal of aerosols. But large drops are not densely concentrated and have smaller cross-sectional area-to-volume ratio, therefore the concentration of aerosol particles in rainwater will be relatively low.

Snowfall events are more effective in scavenging of aerosols in respect of rainfall events of the same precipitation rate [McNeary03]. It is because of the surface area of snow flurries is significantly higher (flurries average density is 0.1 g cm^{-3}). In addition flurries can easily flow around by the wind and hence the volume of air swept will be much higher than that of water drops.

High humidity of air is connected with the low vertical transfer therefore leads to low concentration of aerosols originating from the stratosphere. Also during high relative humidity conditions, condensation becomes more intense, resulting in increased wet scavenging rate of aerosols [Gerasopoulos01].

Low barometric pressure causes turbulent flows in atmosphere and increases windiness and cloudiness. This is related higher concentration of aerosols in air. On the contrary high pressure leads to calm weather and hence lower concentrations of aerosols from stratosphere.

The influence of wind and its intensity to radioactivity of atmospheric aerosol particles has local character. The wind flows which passed trough regions with elevated radioactivity are bringing air masses rich for active aerosols. The air temperature influences the composition of atmospheric aerosols. The convection induced by air heated from Earth's surface pushes the cold air rich for cosmogenic nuclides downwards. During the inversion is the cold air closer to the Earth and opposite conditions typical for winter season occur.

In the case of long-lived radionuclides like ^{10}Be (1.5×10^{6} years) or ^{210}Pb (22 years) is resuspension from the Earth's surface of relatively high relevance for the determination of deposition rate [Brown89]. It can constitute about 25% of total deposition. It is feasible to use the concentrations of Ca and Mg as indicators of soil contamination. Although ^{7}Be can be also found in soils the short half life of 53 days makes its resuspension from soil negligible.

3.5 Residence time of aerosols

In general, the smaller and lighter a particle is, the longer it will stay in the air. Larger particles (> 10 μm) tend to settle to the ground by gravity in a matter of hours whereas the smallest particles (> 1 μm) can stay in the atmosphere for weeks. The mean residence time in the troposphere is about 30 days on the average, but this can vary from 5 days in the low-level air to 40 days in the higher altitudes. There is also a dependence of the tropospheric aerosol residence time on the latitude [Koch96a]. The residence time of atmospheric aerosol can be estimated by means of radioactive nuclides as tracers, which become attached to aerosol particles and are removed with them by precipitation and dry fallout.

Troposphere

The residence time of aerosols τ in low-level atmosphere can be calculated using the AMAD and mean grow rate (MGR), which varies from 0.004 to 0.005 μm h^{-1} [McMurray82].

$$\tau = \frac{AMAD - AMAD_{Aitken}}{MGR} \tag{3.1}$$

The $AMAD_{Aitken}$ is a diameter of Aitken nuclei and its value is 0.015 μm. Using this formula have Winkler *et al.* calculated the mean residence times of ^{7}Be and ^{210}Pb aerosols for 5-6 days and 4-5 days, respectively [Winkler98]. For ^{210}Pb was observed relatively short residence time of 3-4 days in summer in comparison to winter value of 6-7 days. Yu and Lee determined the mean residence times of ^{7}Be to be 3.2-11.8 days (MGR = 0.004 μm h^{-1}) and 2.6-9.4 days (MGR = 0.005 μm h^{-1}) [Yu02].

Another way for the mean tropospheric residence life time of cosmic ray produced nuclides can be deduced from measurements of the average tropospheric content N, atoms m^{-2}, and the mean deposition rate D, atoms m^{-2} s^{-1}.

$$\tau D = N \tag{3.2}$$

It may be also determined from the known tropospheric production rate P and the measured deposition rate.

$$P = D(1 + \lambda\tau) \tag{3.3}$$

where λ is the disintegration constant of the radionuclide, s^{-1}. At higher latitudes these procedures are not applicable because exchange of air between stratosphere and troposphere is not taken into account [Bleichrodt78]. The stratospheric ^{7}Be may represent about 30% in the troposphere [Bleichrodt63]. That fact leads to overestimation of the tropospheric deposition of ^{7}Be followed by underestimation of the residence time.

Bleichrodt in his work [Bleichrodt78] used for τ determination equation 3.3. For the average tropopause height of 9 km was a minimum for the tropospheric

residence time of 22 days obtained. For the tropopause height of 11 km was τ for 33 days determined. Ďurana *et al.* [Ďurana96] calculated for tropopause height ranged from 8 to 12 km the tropospheric residence time values of 27 and 48 days, respectively.

Stratosphere

The mean stratospheric residence time of aerosols consequently depends on the altitude at which it is introduced, the season of year, and the latitude. Dust injected into the lower polar stratosphere by Russian thermonuclear explosions was found to have a mean residence time of less than 6 months, whereas in tropical latitudes the residence time has been found to be from 2 to 3 years for radionuclides introduced into the middle stratosphere and 5 to 10 years if injected at 100 km [Feely60]. Generally we can say the stratospheric residence time of aerosols is about 1-2 years, because of the thermal structure of the stratosphere and its separation from the troposphere by the tropopause. Investigating the $^{7}Be/^{90}Sr$ ratio have Dutkiewicz and Husain [Dutkiewitz85] determined the stratospheric mean residence time of 16 months.

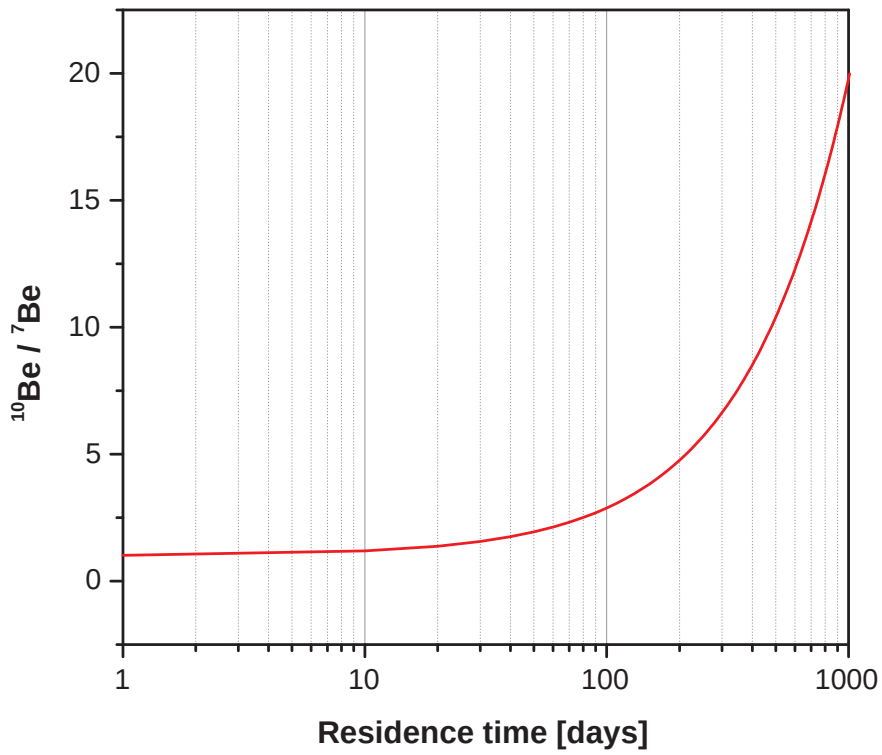

Figure 3.4: Ratio of $^{10}Be/^{7}Be$ as a function of residence time for isolated air mass (Q = 0 in equation 3.4). Adopted from [Raisbeck81].

The next method uses for residence time calculation the ratio of the tropospheric concentrations of two nuclides with different half-lives, the residence times for the two being assumed to be identical. Such an example is the ratio of two cosmogenic radionuclides ^{10}Be/^{7}Be. The half-lives of ^{10}Be and ^{7}Be are 1.5 million years and 53.2 days, respectively. The ^{10}Be/^{7}Be ratio in an actual air mass reflects the source and "age" of any air with which it has been mixed. Therefore it is a very sensitive parameter for studying the origin, residence times, mixing patterns, and in particular for identifying injection of stratospheric air into the troposphere.

$$\frac{^{10}Be}{^{7}Be} = \frac{P_{10} + Q_{10}}{P_7 + Q_7} \cdot \frac{\lambda_r + \lambda_7}{\lambda_r} \cdot \frac{1 - e^{-\lambda_r t}}{1 - e^{-(\lambda_r + \lambda_7)t}} \tag{3.4}$$

where P_i and Q_i are production and injection of ^{i}Be into the air mass, respectively. λ_7 is the decay constant of ^{7}Be, and λ_r is an equivalent constant for removal of aerosol particles. To approximate the total stratosphere at equilibrium, the values of Q_{10} and Q_7 are zero, and $t \to \infty$. As can be seen from Figure 3.4 ^{10}Be/^{7}Be ratio is a slowly varying function for residence times smaller than the ^{7}Be half-life, but rapidly increasing for longer residence times. This is the feature which makes the ratio a sensitive indicator of the origin and age of the air mass in which it is measured. Using equation 3.4 Raisbeck and Yiou [Raisbeck81] determined stratospheric residence time of about 350 days.

Chapter 4

Radioactivity of atmospheric aerosol

Radioactive substances enter the atmosphere from both natural and anthropogenic sources. Natural radionuclides in the atmosphere have two principal sources: radon and its progeny derived from Earth's surface (^{210}Pb) and cosmic-ray-produced nuclides (^{7}Be). Dust from the resuspension of soils can also provide secondary sources (^{40}K). Anthropogenic radioactivity in the atmosphere on global scale originates mainly from nuclear weapons testing or accidents of nuclear power plants (^{137}Cs). The airborne non-volatile radionuclides attach to the first aerosol particles they encounter and their fate will become the fate of their carrier.

4.1 Radionuclide ^{7}Be

As particles of cosmic radiation pass trough the atmosphere, they induce several nuclear reactions with the elements present in air and produce radionuclides, such as ^{7}Be, ^{10}Be, ^{3}H, ^{36}Cl, ^{22}Na or ^{14}C, called cosmogenic radionuclides [Lal67]. In tropospheric aerosol particles is the radioactivity of ^{7}Be most significant from these nuclides. Others are either gaseous, and/or have very low activities.

^{7}Be is short-lived (half-life 53.5 days) radionuclide produced mainly in the stratosphere in spallation reactions of light atmospheric nuclei (C, N, O) with particles of the primary component of cosmic rays (protons and neutrons). Following equations constitute for the reactions of ^{7}Be formation:

$$^{12}_{6}C + ^{1}_{1}p \rightarrow ^{7}_{4}Be + ^{6}_{3}Li \qquad ^{12}_{6}C + ^{1}_{0}n \rightarrow ^{7}_{4}Be + ^{6}_{2}He$$

$$^{14}_{7}N + ^{1}_{1}p \rightarrow ^{7}_{4}Be + 2^{4}_{2}He \qquad ^{14}_{7}N + ^{1}_{0}n \rightarrow ^{7}_{4}Be + ^{8}_{3}Li$$

$$^{16}_{8}O + ^{1}_{1}p \rightarrow ^{7}_{4}Be + ^{10}_{5}Be \qquad ^{16}_{8}O + ^{1}_{0}n \rightarrow ^{7}_{4}Be + ^{10}_{4}Be$$

$$^{16}_{8}O +^{1}_{1} p \rightarrow^{7}_{4} Be +^{7}_{3} Li +^{3}_{2} He \qquad ^{16}_{8}O +^{1}_{0} n \rightarrow^{7}_{4} Be +^{6}_{2} He +^{4}_{2} He$$

The production rate varies from year to year according to variations in flux of primary cosmic radiation caused by the 11-year sun cycle. Newly created ^{7}Be atoms diffuse in the atmosphere until they bind to fine aerosol particles. ^{7}Be decays via electron capture to ^{7}Li and the gamma-lines of 477.5 keV with 10.3% probability are emitted. This line is most often used for its determination via gamma-spectrometric method. The concentrations of ^{7}Be change seasonally at ground-level air. The reasons are discussed below.

4.1.1 Production

The production rate of cosmogenic nuclides depends on the cosmic ray particle flux. This flux is modulated by two processes: variations of the geomagnetic field intensity and the solar activity. From measurements of cosmogenic radionuclides with different half-lives and different irradiation histories in meteorites, the average galactic cosmic ray flux was inferred to be constant within 10% during the last few million years [Vogt90].

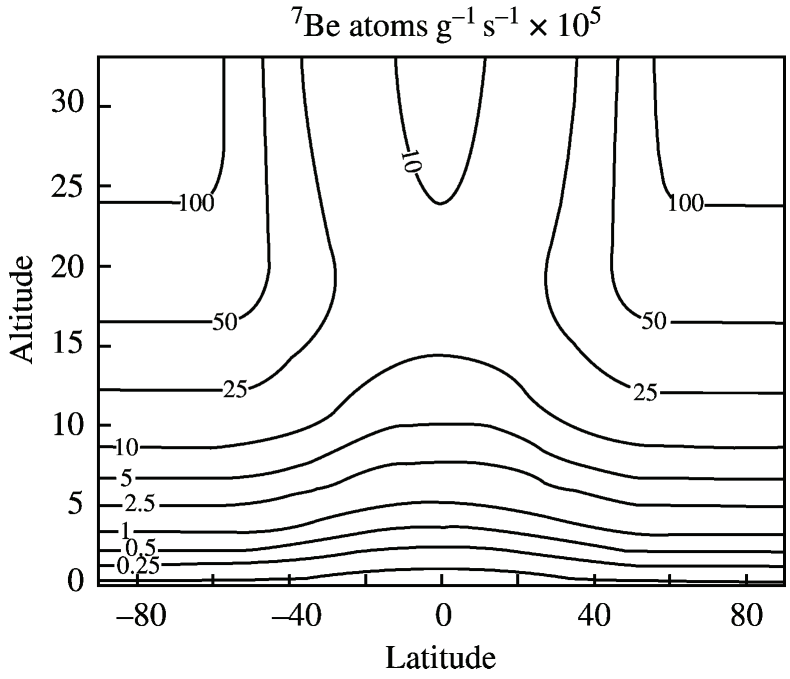

Figure 4.1: Production of ^{7}Be in the atmosphere as a function of latitude and altitude based on data from Lal and Peters [Lal67].

Cosmic rays

The cosmic rays are energetic particles originating from space that enter the Earth's atmosphere. We distinguish primary and secondary cosmic rays to the intent that primary cosmic rays can interact with interstellar matter and matter of the Earth forming secondary cosmic rays. The primary cosmic rays are divided according to their origin: to galactic and solar cosmic rays. Galactic component constitutes in 87% of protons, 12% of alpha particles and the rest is represented by heavier nuclei with atomic number from 3 to 90 [Simpson83]. The sun emits particles with typical energies of about 1 to 100 MeV, 98% protons and the rest 2% are heavier particles. Because of their relatively low energies, they can cause nuclear reactions in the atmosphere only at high latitudes (above 60°), and even there the nuclide production is restricted to the very top of the atmosphere.

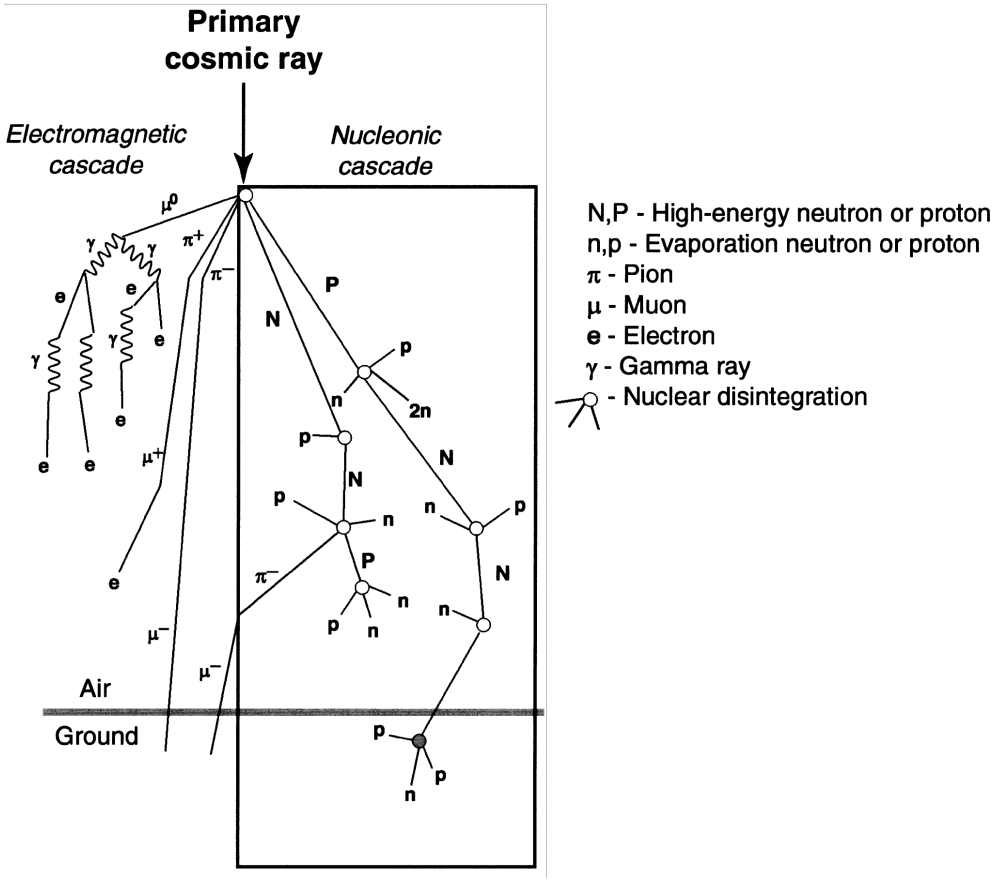

Figure 4.2: Propagation of the secondary cascade through the atmosphere [Simpson00].

The primary cosmic rays entering the Earth's atmosphere consist mainly of protons with the energies around 1 GeV. At that high energies are colliding with the atoms of atmosphere and contribute to the development of a particle cascade. After production of several generations of particles, the cascade process ends when

the energies of the particles become too low for further particle production. These are the secondary cosmic rays, called also hadronic cascade. It is composed of protons, neutrons, pions, and other strongly interacting particles. The hadronic cascade is usually accompanied by an electromagnetic cascade, composed of electrons, positrons, muons, photons, and neutrinos. It becomes important in the production of cosmogenic nuclides mainly by muons only at great depths bellow the Earth's surface [Masarik99].

According to the results of Masarik and Beer [Masarik99], is the neutron flux larger by almost two orders of magnitude. At atmospheric depths exceeding 180 g cm^{-2}, the total flux shows an exponential decrease. This decrease is is smaller in lower latitudes. The relative contribution of neutrons to the total flux of cosmic ray particles increases from 90% near the top of the atmosphere to 98% at sea level. Therefore, the majority of cosmogenic nuclides are produced by neutron reactions. The contribution of muons and pions to the production is insignificant. The muons participate only in the weak and electromagnetic interactions and therefore induce only a few nuclear reactions. Though the pions interact strongly, there are 100 to 1000 times less pions than protons in the atmosphere present.

Geomagnetic field

Incoming particles of cosmic rays are deflected by the geomagnetic field of the Earth. The magnitude of deflection depends on their magnetic rigidity and angle of incidence.The rigidity of a particle is defined as the momentum per unit charge

$$R = \frac{pc}{Ze} \tag{4.1}$$

where p is the momentum, Ze is the charge of the particle, and c is the velocity of light. The value of this cutoff tends to increase with decreasing latitude (Figure 4.3), resulting in lower cosmic-ray intensity towards the equator [Shea83].

Sedimentary paleomagnetic records showed that the intensity of the Earth's geomagnetic field varied in the past from almost zero to twice its present intensity [Guyodo96]. From the analysis of calculated dependencies, Masarik and Beer [Masarik99] concluded that changes in the geomagnetic field intensity lead to changes in the atmospheric production rate pattern for all cosmogenic radionuclides. The ratios for global average production rate for zero geomagnetic field and a doubling of the present intensity are 2.7, 2.7, and 2.9 for ^{10}Be, ^{36}Cl, and ^{14}C, respectively.

Sun modulation

Sun modulation is the dominant cause of the observed galactic cosmic ray variability. Solar activity reduces the flux of galactic cosmic ray particles and during a typical 11-year solar cycle varies the low-energy part of galactic cosmic ray flux (< 1 GeV nucleon^{-1}) by an order of magnitude. That is followed by a decrease

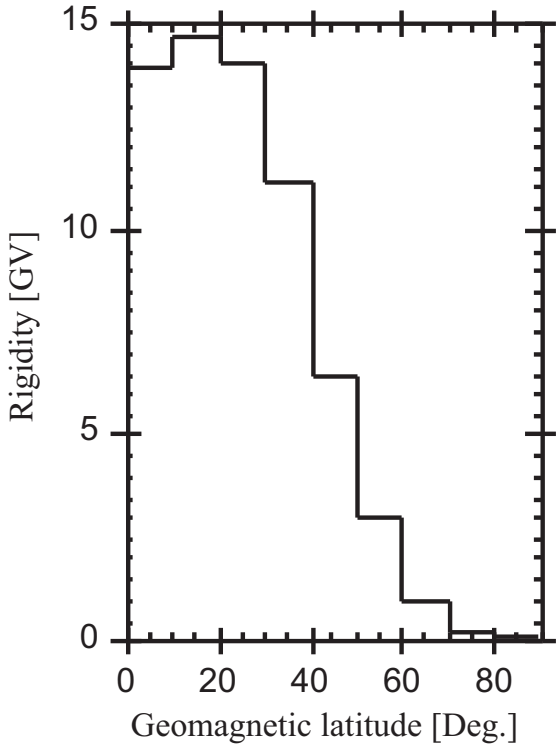

Figure 4.3: Vertical cutoff rigidities as a function of geographical latitude [Shea83].

in the production rate of cosmic ray products, such as ^{7}Be that is therefore expected in a global scale. With increasing energy of cosmic ray particles becomes the modulation effect weaker. The effect of geomagnetic rigidity enhances the sun modulation significantly at high latitudes, but has only a small effect on the flux at low latitudes.

The sun modulation of galactic cosmic rays is expressed trough the modulation parameter Φ. Masarik and Beer [Masarik99] determined values of Φ for the period 1953-1995. As can be seen from Figure 4.4, Φ varied from 400 up to 1200 MeV. There is an inverse relationship between solar activity and cosmic ray flux, but the data does not show a one-to-one correlation.

In 1848 Rudolph Wolf devised a daily method of estimating solar activity by counting the number of individual spots and groups of spots on the face of the sun. Wolf confirmed the existence of a cycle in sunspot numbers. The more accurately was determined the cycle's length to be 11.1 years. The cosmic galactic rays which are responsible of ^{7}Be production showed an inverse correlation to sunspot cycle, because the sun's magnetic field is stronger during a sunspot maximum and shields the Earth from cosmic rays [Azahra03]. Therefore, a negative correlation is expected between the atmospheric concentrations of ^{7}Be and sunspot numbers as can be seen in Figure 4.5.

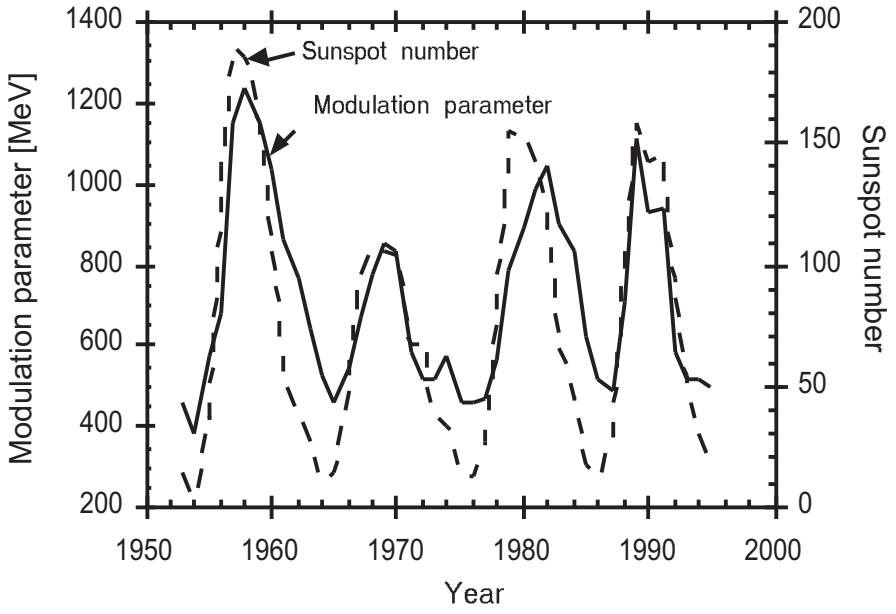

Figure 4.4: Solar modulation parameters Φ for the period 1953-1995 determined from Deep River neutron monitor data and mean annual Wolf sunspot numbers [Masarik99].

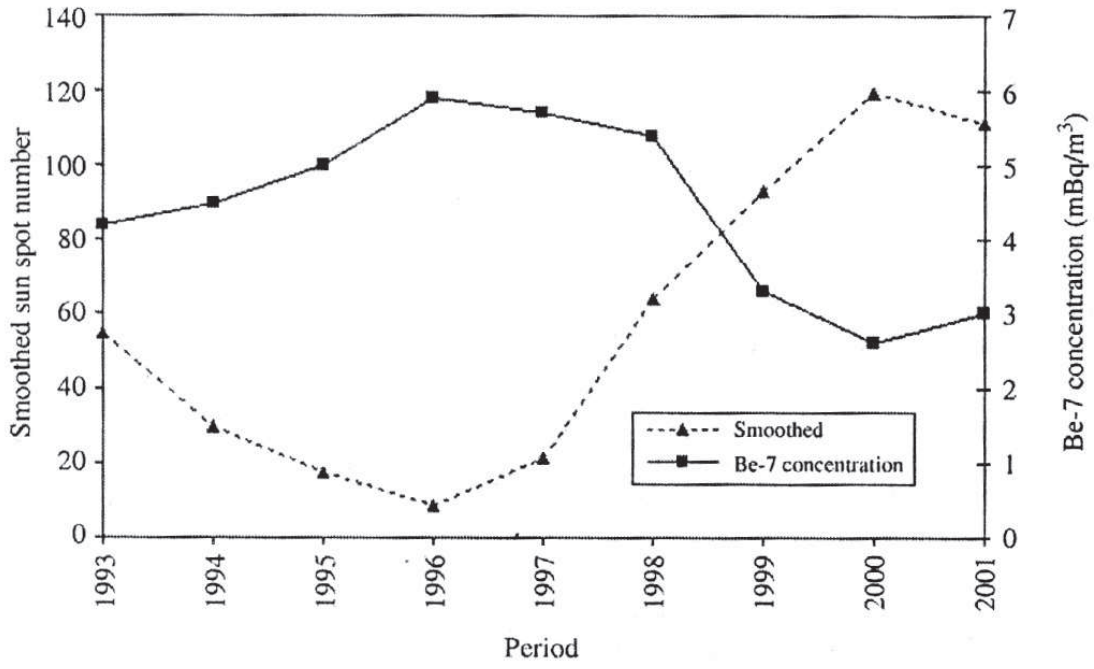

Figure 4.5: Annually smoothed average number and mean annual ^{7}Be concentration in the period 1993-2001 [Azahra03].

Altitude

Production rate of cosmogenic nuclides is decreasing with increased atmospheric depth. It is caused by the decrease of cosmic ray particles intensity with the altitude. According to the model of Masarik and Beer [Masarik99] in the average the stratosphere contributes 55.1% to the total production of ^{7}Be. Nagai *et al.* [Nagai00] calculated the average stratospheric production rate of ^{7}Be to be 60% of total.

4.1.2 Seasonal variations

In many works [Dueñas03], [Azahra03], [Koch96] are seasonal variations in the concentration of ^{7}Be in surface air observed. Often [Todorovic99], [Dueñas04] have been these changes attributed to the influences of variations in the rate of exchange of air masses between the stratosphere and the troposphere. However there are also other influencing factors. Feely *et al.* [Feely89] stated that level of ^{7}Be in lowest layer of atmosphere generally depends on four processes:

1. the exchange of air between the stratosphere and the troposphere,
2. the rate of vertical mixing within the troposphere,
3. the poleward transfer from middle and subtropical latitudes to high latitudes, and
4. the scavenging by precipitation.

Transport processes

The exchange of air masses between the stratosphere and the troposphere is most common at middle latitudes and most rapid during the spring months. The stratospheric air is rich for cosmogenic radionuclides, hence the tropospheric concentration of ^{7}Be is increasing in this season. It was found that ^{7}Be concentrations followed a pattern similar to that of the fallout fission products [Todorovic99]. They have entered the stratosphere during nuclear weapons tests.

Viezee and Singh [Viezee80] observed high positive correlation between the ^{7}Be concentrations and the occurrence of tropospheric low-pressure troughs. This supports the postulate that tropopause folding events are dominant stratosphere to troposphere exchange mechanism. These intrusions are not delivered uniformly with time, but rather in short pulses [Dutkiewitz85]. Annually averaged exchange rate in the northern hemisphere is about 20 to 30% greater than in the southern hemisphere. The seasonal behavior of stratosphere to troposphere exchange is highly dependent upon latitude [Viezee80].

Also another observation indicates the stratospheric input of ^{7}Be into the troposphere. The measured annual deposition of ^{7}Be was found by Bleichrodt and van Abkoude [Bleichrodt63] to exceed the expected fallout of ^{7}Be that is produced

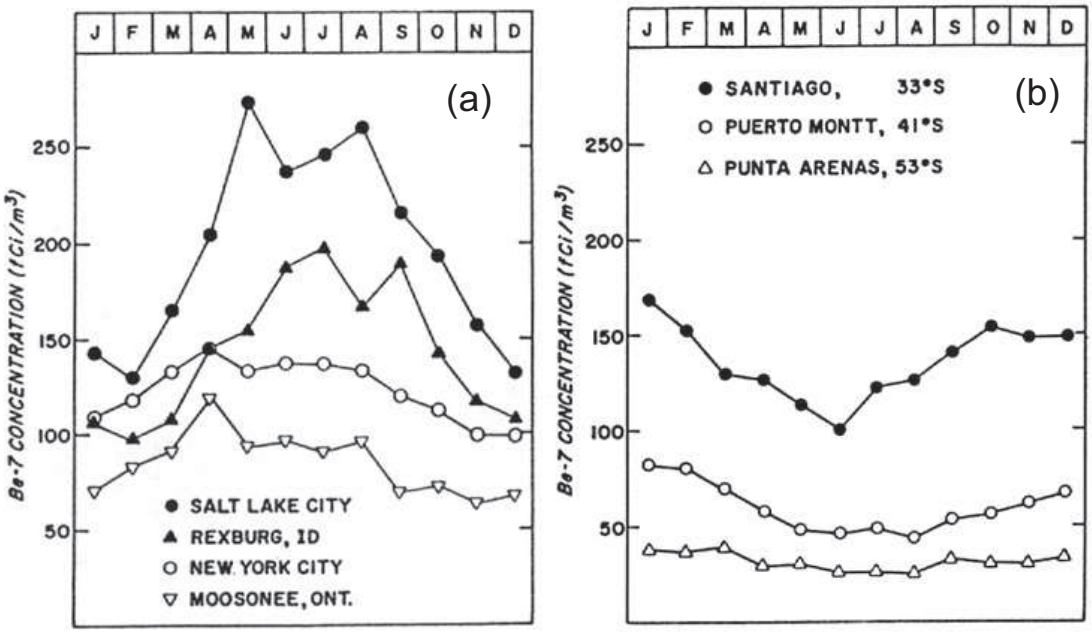

Figure 4.6: Mean monthly concentrations of ^{7}Be at four northern (a) and at three southern (b) hemisphere sites [Feely89].

in the troposphere only. The difference agrees with an estimated contribution of ^{7}Be originating from the stratosphere. Dutkiewicz and Husain [Dutkiewitz85] analyzing the ^{7}Be/^{90}Sr ratio showed that on annual basis the stratosphere contribute approximately 25% of the ^{7}Be in surface air.

Feely [Feely89] measured for many sites all over the world the highest concentrations of ^{7}Be during the warmer seasons and lowest during the cooler seasons. In Figure 4.6 the mean monthly ^{7}Be concentrations for four sites in North America show elevated values during the warmer mid-year months (a) and similar data are plotted for three south American sites (b). Again the highest concentrations occur during the warmer months, here at the end and beginning of the calendar year. The increased rate of vertical transport within the troposphere enhanced by high temperatures is the important factor in producing peak concentrations during warmer months. This effect is stronger at middle latitudes. The more detail information is in section 2.2.

The ^{7}Be concentrations for Arctic sites show a strong seasonal variation, with peak concentrations in the late winter or early spring [Feely89] as can be seen in Figure 4.7. These maxims coincide with the arrival of haze layers that are believed to be derived from air pollutants emitted in the middle latitudes of Asia, Europe and North America [Rahn81]. This agrees with the presumption that cosmogenic radionuclides enter the lower troposphere of the Arctic region as a result of horizontal advection within the lower layers of the troposphere. The stability of polar air masses restrain the vertical transport of ^{7}Be from upper layers. In this sense, although in polar regions of polar stratosphere is the production of

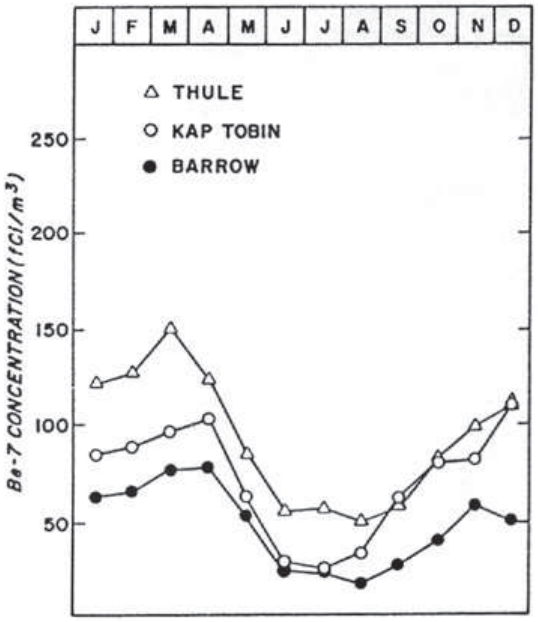

Figure 4.7: Mean monthly concentrations of ^{7}Be at three Arctic sites [Feely89].

cosmogenic radionuclides the highest, the concentrations of ^{7}Be are at relatively low levels.

Washout effect

Several sites localized in climatic zones typical of strong seasonal variations in the precipitation exhibit an inverse relationship between the rainfall rate and the ^{7}Be concentrations indicating the importance of washout of the atmospheric aerosol particles [Feely89]. For example, precipitation has proved to be the most important factor in controlling the concentration and deposition of ^{7}Be in the atmosphere in Monaco showing high correlation coefficient (R = 0.94) [Lee02].

Brown *et al.* [Brown89] found that the dry deposition of ^{7}Be is less than 10% of the amount deposited by rain. According to Knies *et al.* [Knies94] are concentrations of cosmogenic radionuclides (^{7}Be, ^{10}Be, ^{36}Cl) in precipitation through a single event correlated. Typically decrease from high values at the beginning of an event to lower values at the end.

4.1.3 Anthropogenic ^{7}Be

According to Bleichrodt and Van Abkoude [Bleichrodt63a] was the anthropogenic ^{7}Be produced by the Soviet nuclear test explosions in September and October 1961. If LiD was used for nuclear devices, ^{7}Be was probably produced by nuclear reactions of Li. The most likely reactions are $^{6}Li(n, {}^{3}H)^{4}He$ followed by $^{6}Li(^{3}H, 2n)^{7}Be$, $^{6}Li(D, n)^{7}Be$, and $^{7}Li(D, 2n)^{7}Be$. Use of Li in the Soviet bombs is also

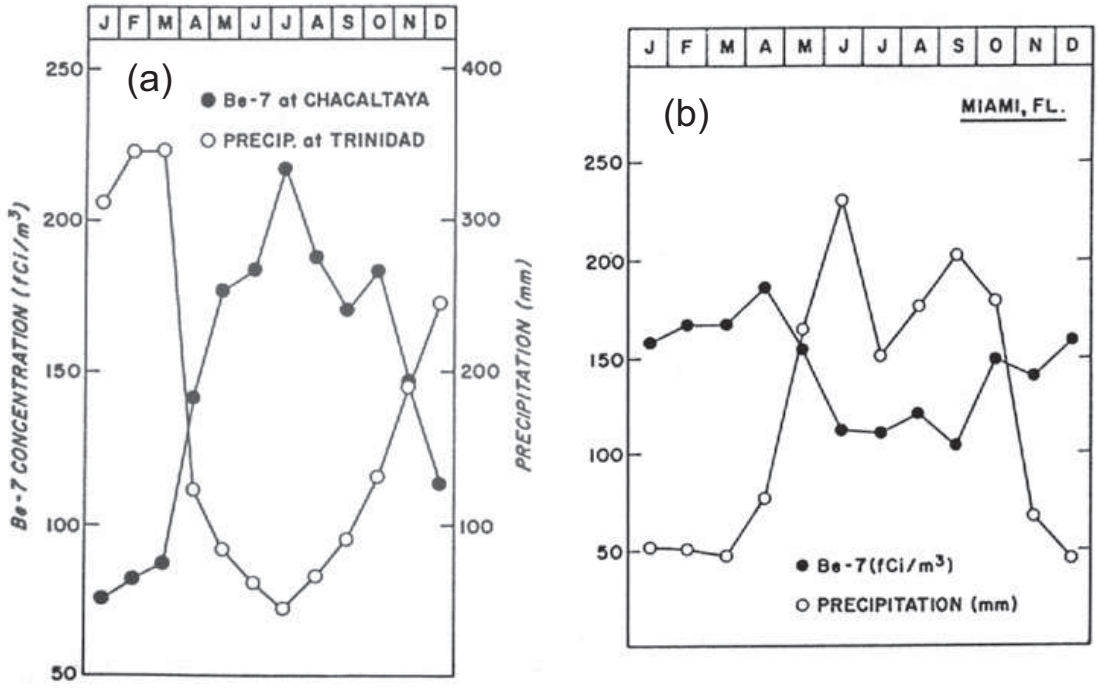

Figure 4.8: Mean monthly concentrations of ^{7}Be and mean monthly precipitation at Bolivia (a) and at Florida (b) [Feely89].

suggested by an increased Li twilight emission at Saskatoon during November 1961 [Sullivan62] and at Uppsala during November 1962 [Stoffregen63]. Since nuclear-test-ban treaty in 1963 there are no emissions of the anthropogenic ^{7}Be into the atmosphere.

4.2 Radionuclide ^{210}Pb

Radionuclide ^{210}Pb is β-emitter with the half-life of 22 years. Atmospheric ^{210}Pb is created through the emanation of ^{222}Rn from continental lands free from glaciers and permafrost. Generally speaking, atmospheric ^{210}Pb levels are related to the size of land-masses [Rangarajan86]. Since the source of ^{210}Pb is solely in the surface continental air, its concentrations are greatest near the land surface and decrease with both altitude and distance from land. Vertical profile of ^{210}Pb up to 16 km of altitude is presented in Figure 4.9. ^{210}Pb is also released from industrial processes such as the sintering of ores in steelworks, the burning of coal or the production and use of agricultural fertilizers.

^{210}Pb is of considerable interest in geophysical applications, like in modeling various bio-geochemical cycles of lacustrine, estuarine and coastal marine environments as well as soils, peatlands, polar and glacial ices [El-Daoushy88]. Moreover, the concentration ratio of ^{210}Pb to other ^{222}Rn decay products can be used to obtain information on the residence time of aerosols [Papastefanou06], [Baskaran01].

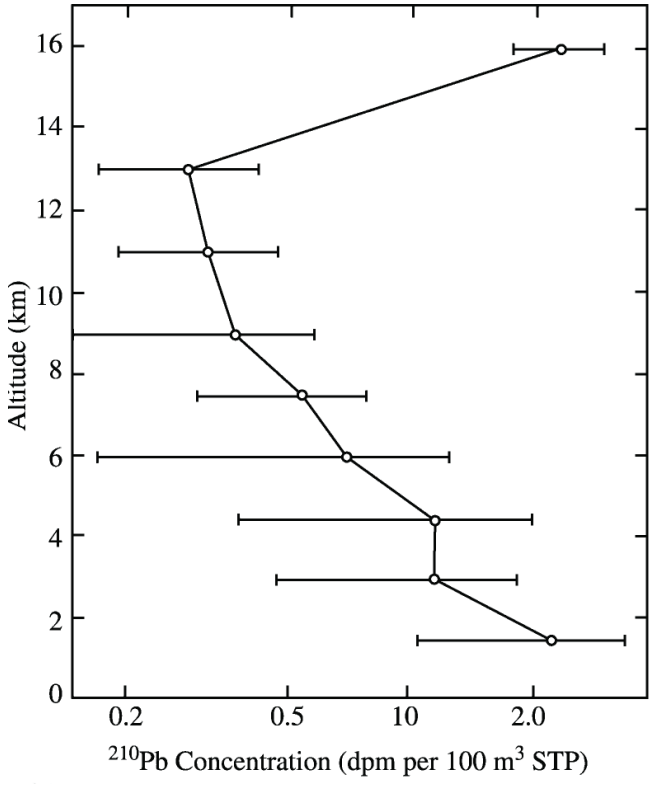

Figure 4.9: Vertical distribution of ^{210}Pb in the atmosphere in the North American mid-continental region [Moore73].

^{210}Pb is also important as a source of ^{210}Po which contributes a significant portion of the natural radiation dose to man. However, their typical contribution to committed effective dose by inhalation is much less than their typical contribution by ingestion. It should be noted that inhalation of ^{210}Pb and ^{210}Po is enhanced in tobacco smokers, due to external deposition of ^{210}Pb on tobacco leaves from the atmosphere [Eisenbud97].

4.2.1 ^{222}Rn and its daughter products

^{222}Rn, a daughter product in the ^{238}U decay series, is a noble gas released from soil matrix. ^{222}Rn emanated from earth undergoes radioactive decay in the atmosphere and produces several short-lived daughter products (Figure 4.10), which attach to aerosol particles.

The exhalation rate of ^{222}Rn depends on the soil type and on its ^{226}Ra concentrations, however at a given location it can be considered roughly constant. Typical exhalation rate of ^{222}Rn from soil is about 2.10^{-4} Bq cm^{-2} s^{-1} [Gäggeler95]. It results in a radon inventory of the global atmosphere of approximately 1.5×10^{18} Bq. ^{222}Rn emanation is influenced by various meteorological conditions, mainly rain and soil moisture. Other factors, such as ground surface temperature, wind speed

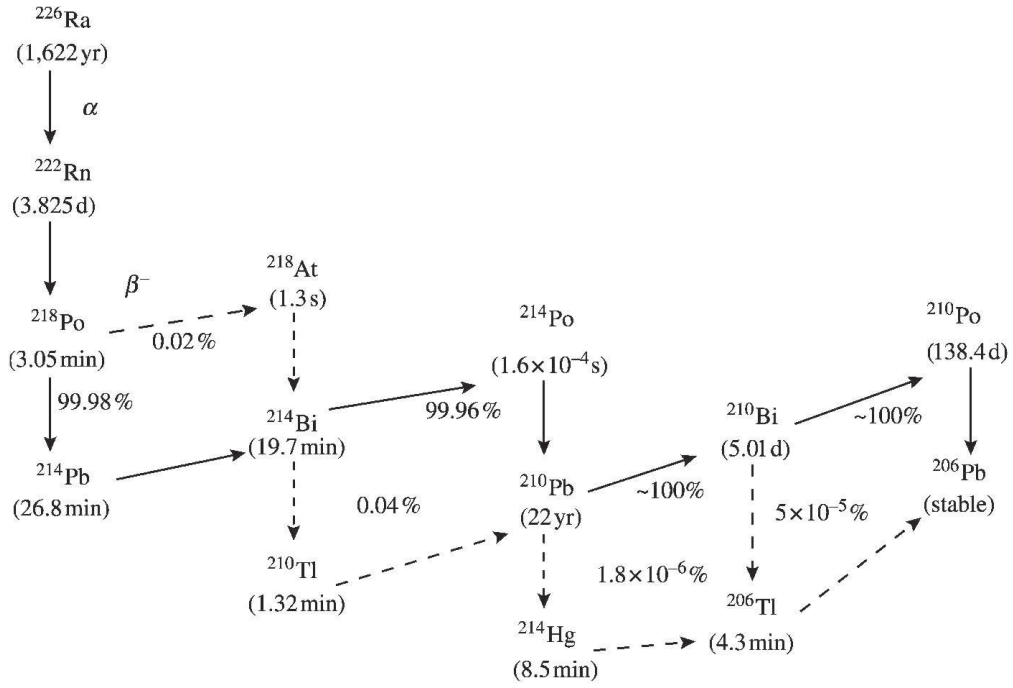

Figure 4.10: The decay chain for ^{222}Rn.

and atmospheric pressure have only a minor influence [Dueñas90]. Atmospheric radon itself is a chemically inert and not removed from the atmosphere by physical or chemical means. Because its half-life is much less than the mixing time of the atmosphere, it is a tracer of atmospheric transport and can be used for identifying air masses derived from continental areas.

^{222}Rn is lost from the atmosphere only by its radioactive decay and it is thus the source of all of the ^{214}Bi, ^{214}Pb, ^{214}Po, ^{210}Pb, ^{210}Bi, and ^{210}Po in air. The quantities of radon decay products on soil dust resuspended from the surface or volatilized from lava are small by comparison on a global scale, but may be comparable locally and episodically.

Air activity concentration of ^{222}Rn shows seasonal variations with maximum values in winter and minimum in summer. It also indicates diurnal variations with the maximum in the night hours and the minimum in the afternoon [El-Hussein01], [Holý01]. An example is given in Figure 4.12

The concentration and the temporal variation of ^{222}Rn and its decay products may provide information on atmospheric thermodynamic conditions as well as on the atmospheric processes that involve aerosols such as transport, dispersion, or removal rate. ^{222}Rn was used in several studies as an indicator of the origin of air masses or as a tool for the vertical stability determination.

The migration of ^{222}Rn trough soils into building materials can lead to indoor air concentrations that pose significant radiological hazards. ^{222}Rn and its products are the second most relevant cause of cancer diseases of respiration tract and lungs after smoking. Therefore, concentrations of ^{222}Rn and its decay products

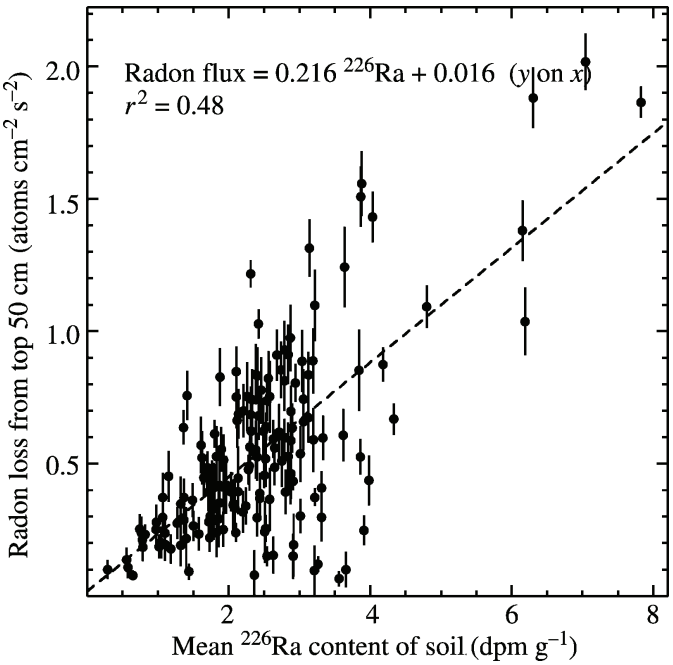

Figure 4.11: Radon loss rate from the upper 50 cm of soils versus the mean radium concentration. Bars indicate calculated 1σ error of the loss [Graustein90].

in the atmosphere are of concern for health purposes because they are the most important contributors to human exposure from natural sources [UNSCEAR00]. Also some of industries which process materials that contain naturally occurring radioactive material (NORM) are considered to be of potential significance with regard to occupational exposure. These are for example fossil fuel power stations, oil and gas extraction, metal processing, or phosphate industry.

4.2.2 Seasonal variations

The half-life of ^{222}Rn is 3.8 days. Although, the half-life of ^{210}Pb is 22.26 years, the residence time of ^{210}Pb in lower troposphere is much shorter, about one to two weeks [Poet72], [Papastefanou06]. It is caused by aerosols scavenging by precipitations and settling on Earth's surface by gravitational forces. Therefore, are the seasonal variations of ^{210}Pb and ^{222}Rn in the atmosphere somewhat similar although the particulate form of ^{210}Pb and gaseous form of ^{222}Rn. The factors that influence ^{210}Pb levels in atmosphere are [Rangarajan86]:

1. geographical, reflecting the mineral content of local soil and the continentality of the region,

2. climatological, since precipitations reduce emanation of radon and enhance scavenging of aerosols, and

3. anthropogenic and other factors may affect levels over long periods.

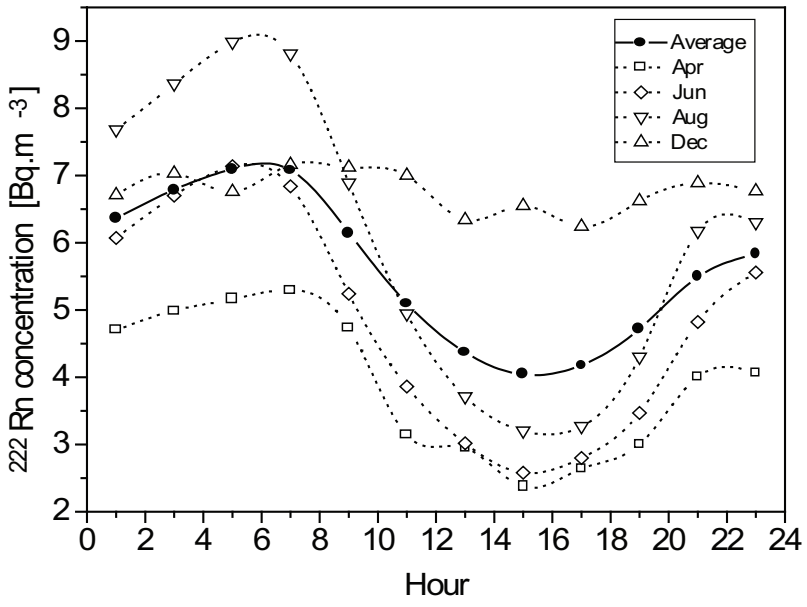

Figure 4.12: The mean diurnal courses of the ^{222}Rn activity concentration in Bratislava atmosphere (years 1991 - 2000) [Holý01].

The seasonal variation of ^{210}Pb has a pronounced peak in late autumn and winter and minimum in summer [Vecchi05]. The ^{210}Pb maxima may be attributed to frequent inversion conditions of the surface air layers, resulting in a build-up of radon and its daughters in low level air. However, in winter months, this process can be negated because of the low emanation of radon from the frozen and/or snow-covered soil [Hötzl87]. Lower activity concentrations of ^{210}Pb in summer months corresponds to higher intensity of vertical mixing within the troposphere at this season. Also the elevated precipitation scavenging of aerosols may contribute to the activity decrease. There was found a significant decrease of ^{210}Pb concentration in air with increase in rainfall [Likuku06] and relatively strong correlation (0.599) was found in Tokai-mura in Japan between deposition of ^{210}Pb and amount of precipitation [Ueno03].

4.3 Radionuclide ^{137}Cs

There were over 800 nuclear atmospheric tests performed from 1945 to 1980, about 300 of them in the southern hemisphere. Mainly the atmospheric nuclear explosions caused global environmental contamination when the radioactive material was carried away from the explosion site by air circulation. The nuclear debris reached even upper layers of atmosphere and contaminated the stratosphere. The

stratospheric residence time is very long, up to several years, and therefore stratosphere was for many years reservoir of radioactive debris from nuclear weapon testing. About 10 years were needed for clearance of stratosphere after the nuclear-test-ban treaty in 1963 [Warneck88]. Radionuclide ^{137}Cs (half-life of 30.14 years) is one of the products of these tests.

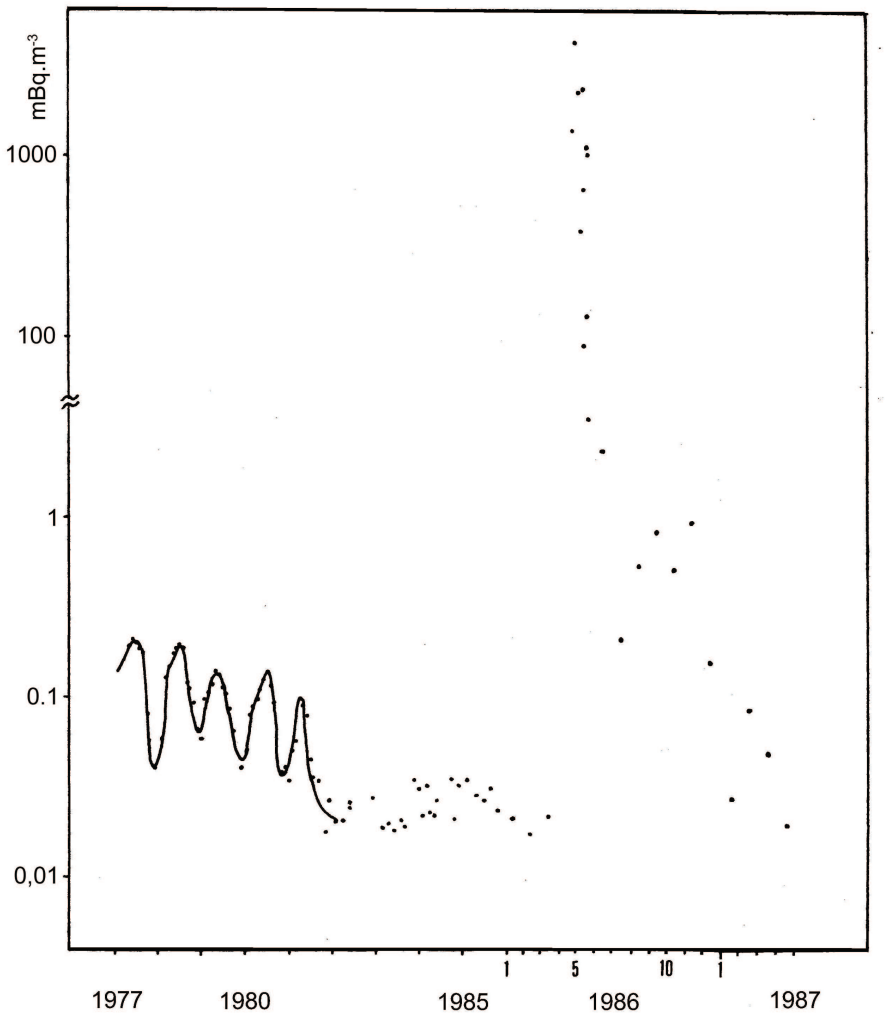

Figure 4.13: Monthly mean values of ^{137}Cs concentrations in the atmosphere of Bratislava before and after the Chernobyl accident [Povinec88].

Significant contribution of ^{137}Cs in the environment comes from the Chernobyl accident in May 1986. Although the deposition of radioactivity was essentially completed within several days, Chernobyl derived ^{137}Cs is even today detectable in small amounts. But today it is redistributed mainly by terrestrial mechanisms and not by the atmospheric mechanisms, which were formerly governing the deposition of worldwide fallout. The present deposition velocity of ^{137}Cs is similar to those of many stable elements such as Fe, Ca, Mg, Al, Mn, *etc.* Nowadays has the Chernobyl derived ^{137}Cs much more similarity to a normal stable element of

terrestrial origin than to a radionuclide derived from the stratosphere [Rosner96].

In surface soils remained significant levels of ^{137}Cs , from a few tens to some hundreds of Bq per kilogram [Papastefanou96]. Since ^{137}Cs is firmly absorbed into surface soil constituents, it has been used to study soil erosion and resuspension processes [Igarashi96]. Resuspension of particles from soil is governed by climatic conditions such as wind speed, ground humidity and movement of air masses [Lee02].

As can be seen in Figure 4.13, before the the year 1986 was the seasonal pattern of ^{137}Cs concentrations similar to the variations of cosmogenic radionuclides with pronounced spring maximums. The slow decrease of peak values from year to year caused by the stratospheric clearance effect is apparent. It the May 1986 the concentration increased four orders of magnitude as a result of he Chernobyl accident. The level of ^{137}Cs concentrations in the atmosphere was strongly affected also by the iron melting accident in May 1998 in the south of Spain (Algeciras).

4.4 Radionuclide ^{40}K

Of the three naturally occurring potassium isotopes, only ^{40}K is unstable, having a half-life of 1.3×10^{9} years. ^{40}K occurs to an extent of 0.0118% in natural potassium, thereby imparting a specific activity of approximately 30 kBq kg^{-1}. Person weighting 70 kg contains about 140 g of potassium, most of which is located in muscle. From the specific activity of potassium, it follows that the ^{40}K content of the human body is on the order of 4 kBq [NCRP87]. The potassium content in the body is under strict homeostatic control and is not influenced by variations in environmental levels. For this reason, the dose form ^{40}K within the body is constant [Eisenbud97].

Atmospheric concentrations of ^{40}K are very low, on the level of tens of μBq m^{-3}, for example Hötzl reported 12 μBq m^{-3} [Hötzl87]. Into the air comes potassium due to resuspension of surface soils.

Chapter 5

Materials and methods

5.1 Sampling

Atmospheric aerosols

Continuous week sampling of atmospheric aerosol was performed at the Department of Nuclear Physics and Biophysics of Faculty of Physics, Mathematics and Informatics, Comenius University Bratislava, since 2002. The sampling equipment undergo some reconstructions and upgrades. In 2004 was the new sampling device with mean flow rate 80 m^3 h^{-1} installed and the active deposition surface of air filter increased from 255 cm^2 to 400 cm^2. The aerosol particles are collected on the nitro-cellulose membrane filters PRAGOPOR. The pore size of the used filters is defined by manufacturer to 0.85 μm, and we estimated collection efficiency for approximately 100%. The 25 round shaped filters are exposed. After sampling campaign are filters placed one on top of each other, forming cylinder with height of about 3 mm.

The sampler device is situated at height of 2.85 m above the ground at the Meteorological station near the Faculty of mathematics, physics and informatics, Comenius University, Bratislava. It is quiet location with very low traffic influences. The filters are changed every week and about 10 000 - 15 000 m^3 of ambient air is pumped through the filters. Dust contents were determined by weighting the filters before exposure and after exposure under the same conditions. Before weighting were blank and exposed filters dried at 60°C for at least one hour (Figure 5.1). The difference between the two weights gives specific aerosol mass concentrations [μg m^{-3}]. At this meteorological station are simultaneously other meteorological parameters, like air temperature, atmospheric pressure, *etc.*, measured.

Precipitation

In the August 2004 rain collector with the active collection surface of 1 m^2 was mounted on the roof of one of the faculty buildings. The water was collected into the 25 l vessel in daily periods in order to eliminate the effect of evaporation during

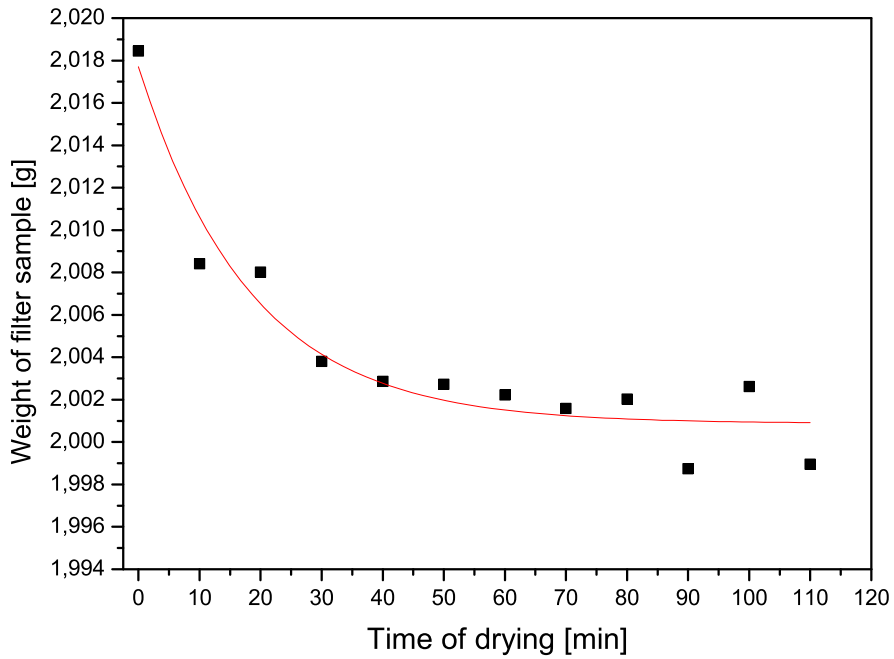

Figure 5.1: Weighting of the filter sample after the drying at 60°C.

the sampling campaign. In order to prevent the binding of particles on the walls of the sampling vessel the water is acidified using the HNO_3. The monthly samples were accumulated and evaporated to dryness. The method of evaporation at the boiling temperature showed 10% outflow of the aerosols. Another two techniques were tested, evaporation at maximum 60°C temperature and cold evaporation by ventilation. Both showed no significant outflow of the aerosols. The residual samples were after that transferred into the plexiglas container with radius of 1.3 cm and hermetically encapsulated. The detail information about the sampling technique and treatment of the samples can be found in [Korčák06].

5.1.1 Decay correction

For all radioactive nuclides is the decay law obligatory. Hence the time factor, especially for short-lived radionuclides is significant in the radioactivity evaluation process. The activity on filter samples have to be corrected for decay during the time of sampling t_1, during the time between sampling and measurement t_2, and during the time of measurement t_3.

$$A_{cor} = Ak_1k_2k_3 \tag{5.1}$$

The correction factors k_1, k_2, k_3 are calculated according following equations:

$$k_1 = \frac{t_1}{T} \cdot \frac{ln2}{1 - 2^{\frac{-t_1}{T}}} \tag{5.2}$$

$$k_2 = 2^{\frac{t_2}{T}} \tag{5.3}$$

$$k_3 = \frac{t_3}{T} \cdot \frac{ln2}{1 - 2^{\frac{-t_3}{T}}} \tag{5.4}$$

where T is the half-life of particular radionuclide.

Equation 5.2 is derived using the assumption that the activity concentration in air is constant during the sampling period and that the aerosols are deposited on the filter with a constant rate over the entire campaign. The aerosol collection efficiency was assumed to be 100%. This condition is described by equation 5.5.

$$\frac{dN(t)}{dt} = Cv - \lambda N(t) \tag{5.5}$$

where C is the concentration of radionuclide in atmosphere, v is the pumping rate, λ is the decay constant of radionuclide, t is time, and $N(t)$ is the number of radioactive nuclei on the filter at time t. At the end of sampling campaign (t_1) is on the filter $N(t_1)$ number of radioactive nuclei.

$$N(t_1) = \frac{Cv}{\lambda}(1 - e^{-\lambda t_1}) = N_{t_1} \tag{5.6}$$

Between sampling and measurement the number of nuclei is dependent only on radioactive decay.

$$N(t_2) = N_{t_1} e^{-\lambda t_2} \tag{5.7}$$

Combining 5.6 and 5.7 the radioactivity captured on filter A_f is given by:

$$A_f(t_2) = \lambda N(t_2) = Cv(1 - e^{-\lambda t_1})e^{-\lambda t_2} \tag{5.8}$$

The volume activity is

$$A = \lambda C \tag{5.9}$$

and pumping rate is $v = \frac{V}{t_1}$, therefore we can calculate

$$A = \frac{A_f(t_2)}{V} \cdot \frac{\lambda t_1}{1 - e^{-\lambda t_1}} \cdot \frac{1}{e^{-\lambda t_2}} = \frac{A_f(t_2)}{V} k_1 k_2 \tag{5.10}$$

The correction for the measurement period k_3 is calculated by the same way as for the k_1.

A significant uncertainty may result from the variability of the source term for the radionuclides with half-lives of the order of days or shorter. For the ^{7}Be is the relative standard uncertainty about 2% , for long-lived radionuclides like ^{210}Pb or ^{137}Cs is the uncertainty smaller than 0.1% [Makarewicz05].

5.1.2 Correction for sampled volume of air

The concentration of measured radionuclide in the atmosphere determines the minimum of sampled air volume needed. The lower concentrations, the larger volume of air has to be pumped trough the filter. The flowmeter is calibrated in standard conditions, the atmospheric pressure of 101 kPa and the air temperature of 20°C. But during the sampling over the different seasons of year are conditions much different from the standard ones. Hence, the difference in measured volume and pumped volume of air occurs.

From the equation of state we can derive relation between density, pressure and temperature of a gas:

$$\rho = \rho_0 \frac{pT_0}{p_0 T} \tag{5.11}$$

where ρ is the density of air, ρ_0 is density of air at temperature of 0°C (= 1.293 kg m^{-3}), p is atmospheric pressure, p_0 is atmospheric pressure at temperature 0°C (= 101 325 Pa), T is air temperature and T_0 is temperature of 0°C (= 273.15 K).

The flowmeter is calibrated at the temperature of 20°C and 101 325 Pa of atmospheric pressure. This corresponds to air density about 1.205 kg m^{-3}. The real pumped volume V_R we can calculate from the measured volume V_M by using correction factor k_ρ.

$$V_R = k_\rho V_M \tag{5.12}$$

Considering that $V_R = \frac{m}{\rho}$ and $V_M = \frac{m}{\rho_{20}}$ we can express the correction factor like in equation 5.13.

$$k_\rho = \frac{\rho_{20} p_0 T}{\rho_0 p T_0} = \frac{\rho_{20}}{\rho} \tag{5.13}$$

For example, we calculate the volume activity of ^{7}Be with and without the volume correction. During the sampling campaign 04/01/06-11/01/06 was the average temperature of air -0.6°C and the average atmospheric pressure was 100356.9 Pa. In these conditions using formulae 5.13 we get for k_ρ the value 0.94. The volume activity of ^{7}Be is 2.515 mBq m^{-3} and 2.678 mBq m^{-3} for measured and corrected (real) volume of sampled air, respectively. This corresponds to difference of about 6.5%.

For the calculation of activity concentration uncertainty we assumed the standard uncertainty of the volume sampled $\pm \triangle V/V = 5\%$.

5.2 Gamma-spectrometric measurement

After sampling the exposed filters have been analyzed on two HPGe detectors by standard gamma-spectrometry for determination of airborne radioactivity. Used semiconductor coaxial HPGe detectors are equipped with SILENA electronics. High volume HPGe detector produced by PGT Europe has 70 % relative efficiency (for 1332.5 keV, relative to NaI(Tl)) and 270 cm^3 of sensitive volume. The relative efficiency of HPGe detector with Be window produced by ORTEC is 6% (for

1332.5 keV, relative to NaI(Tl)), sensitive volume of 40 cm^3 and resolution is 370 eV and 625 eV at 5.9 keV for ^{55}Fe and 122 keV for ^{57}Co, respectively. For the spectra analysis was the EMCAPLUS software used.

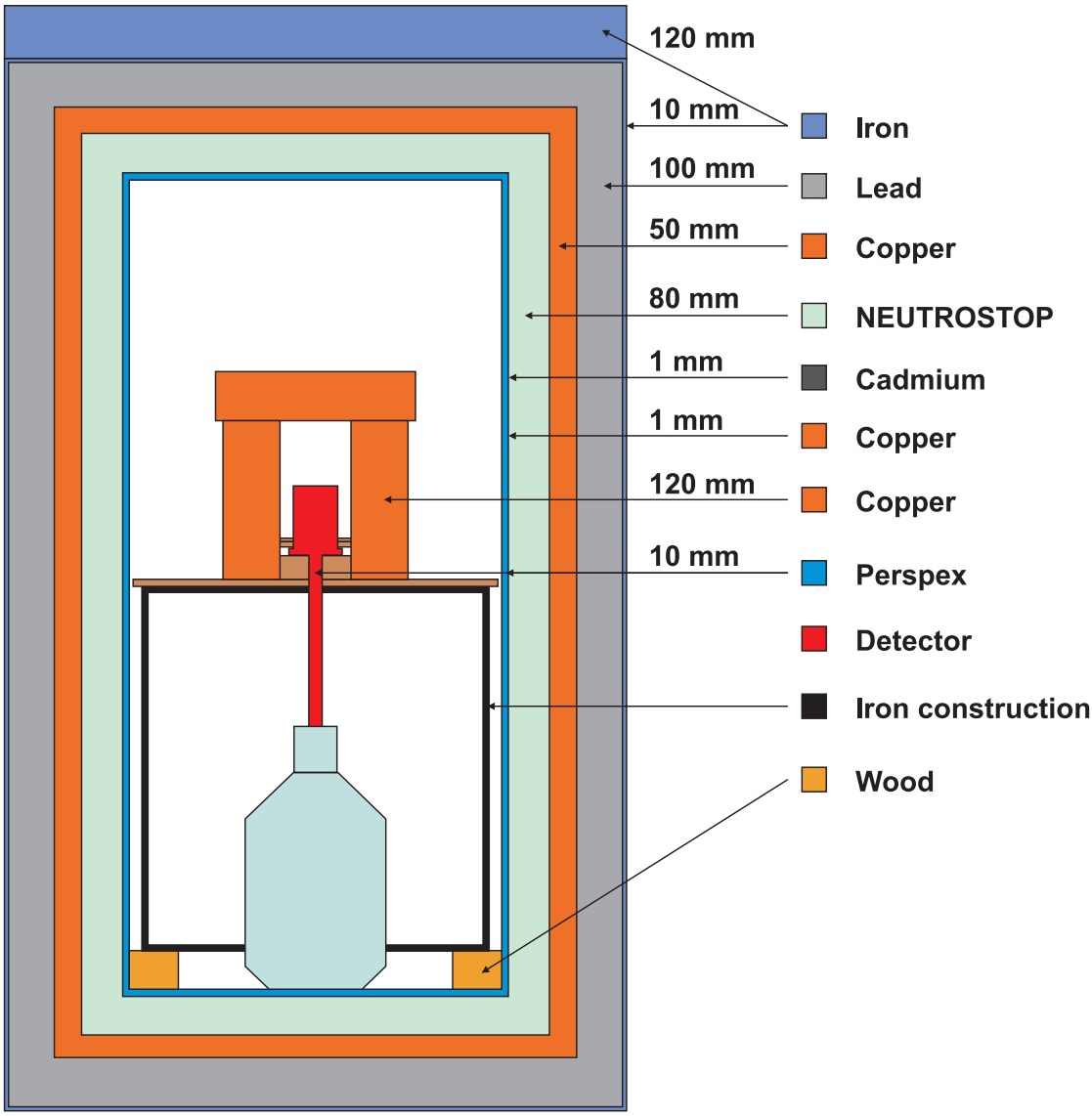

Figure 5.2: Cross section scheme of the large shield.

Both detectors are placed in the low-background shields in order to reach better detection limits. The high volume HPGe detector is inside of the large shield: 2 m high and 1.5×1.5m^2 of base. It is composed of the following layers (from the outside to the inside): 10 cm of lead, 10 cm of electrolytic copper, 10 cm of polyethylene with 3% of boron (NEUTROSTOP), 0.1 cm of electrolytic copper, and 0.1 cm of cadmium. On the inner side there is 1 cm of plexiglas. On the top, a layer of 12 cm of iron is added. The inner dimensions of the shield are 80×90×172 cm. In the past the shield was hermetically closed in order to decrease

the radon contribution and stabilize its content in the shield. But this arrangement was complicated for maintenance of the detector and was not suitable for other experiments taking place in the laboratory, like for example the anticoincidence measurements. Therefore an extra copper shield (12×20×30 cm) has been builded inside the large shield as shown in Figure 5.2. The copper has been used because of its low radioactive contamination by uranium and thorium and their decay products. This way was further reduction of the detector background achieved. The reduction of the background gamma-ray spectra measured outside and inside the large and small shield is shown in Figures 5.4 and 5.5, respectively. In both cases a background reduction of about two orders of magnitude has been reached.

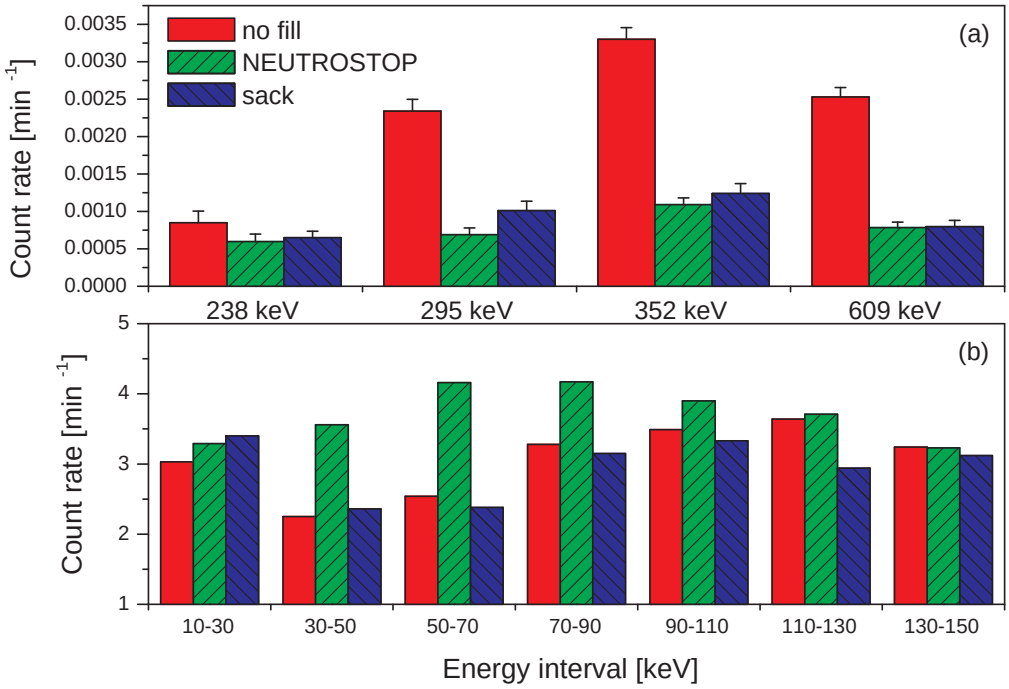

Figure 5.3: Variations of the count rate in the peaks (a) of ^{212}Pb (238 keV), ^{214}Pb (295 keV, 352 keV), and ^{214}Bi (609 keV), and in the low energy background spectra (b) of HPGe detector with Be window placed in the small shield.

The HPGe detector with Be window is placed inside of the small shield, which has similar composition of layers to the large shield, however, its inner dimensions are 38×38×62 cm only. For reduction of radon variations in this shield we tried to use the inactive material (NEUTROSTOP bricks) in order to displace the gaseous radon around the detector. The suppression of background peaks was good, but simultaneously has the count rate in low energy spectrum increased due to gamma-rays dissipation (Figure 5.3). Hence we replaced the bricks with the sack filled with old air [Merešová02]. This setup was finally used for the measurements.

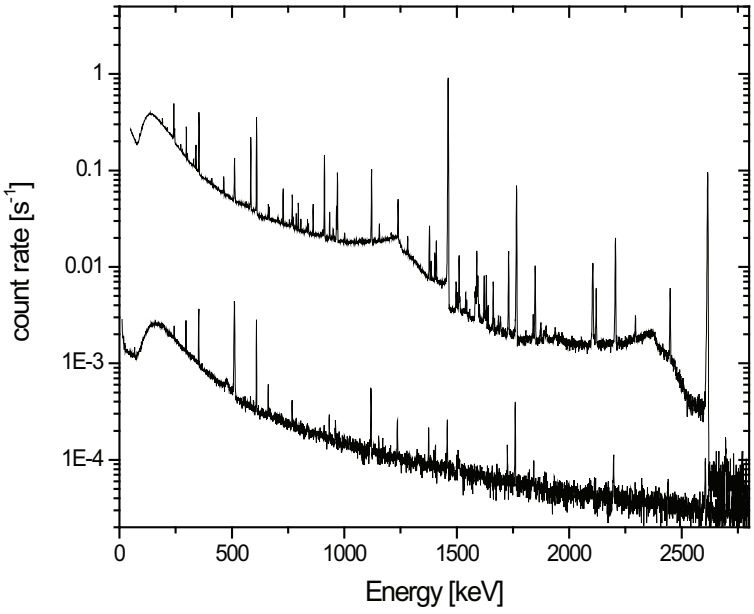

Figure 5.4: Gamma-spectra in and out of the large shield.

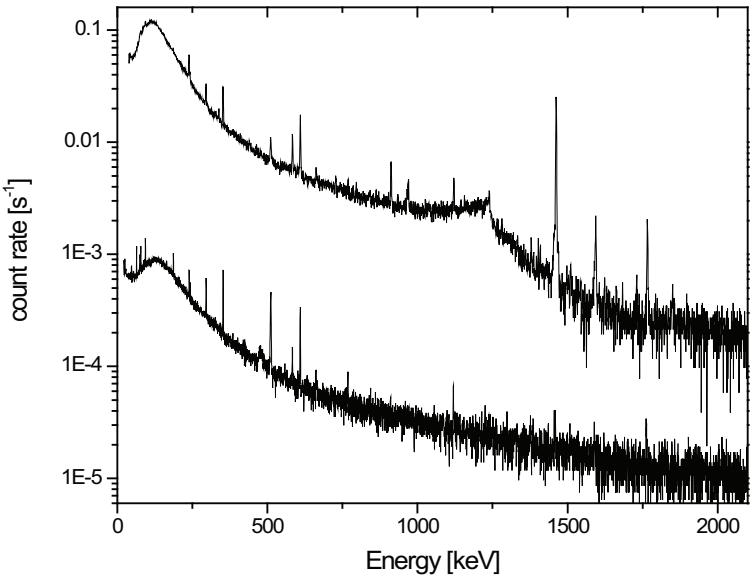

Figure 5.5: Gamma-spectra in and out of the small shield.

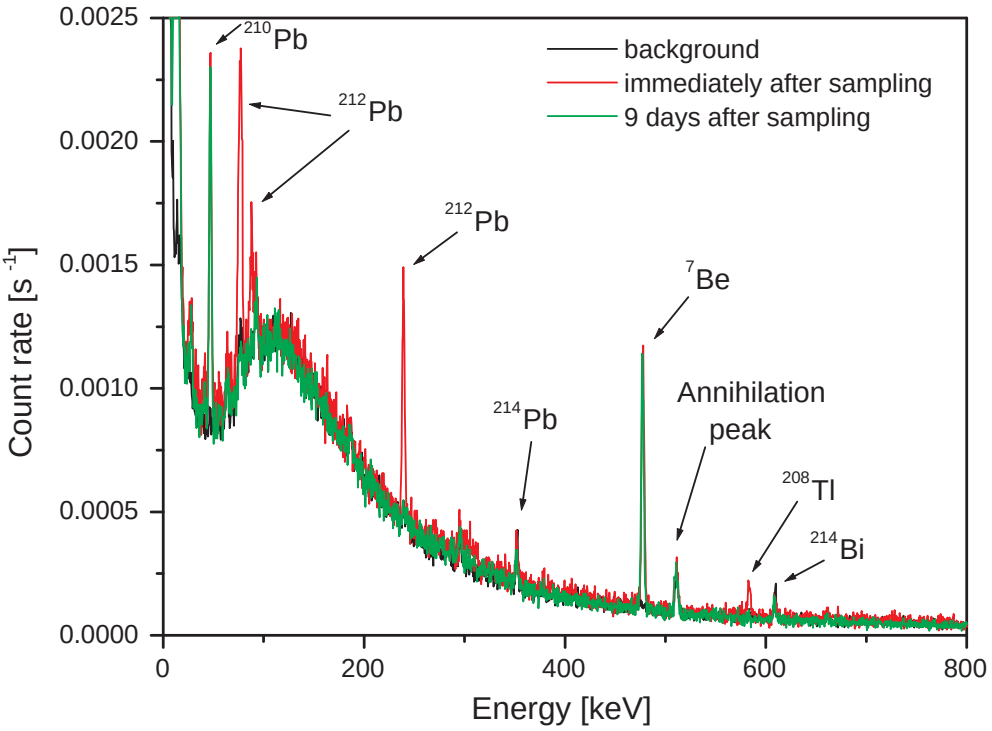

Figure 5.6: Gamma-spectrum of aerosol filter sample measured immediately after sampling (red) with peaks from ^{222}Rn and ^{220}Rn daughters. In the spectrum measured 9 days after sampling (green) are only few peaks from radionuclides with longer half-lives and annihilation peak present.

Energy calibration was performed with a set of standard point sources of ^{137}Cs, ^{133}Ba, ^{60}Co, ^{152}Eu and ^{54}Mn with activities ranged from 0.6 to 25 kBq and uncertainties from 1% to 3%. The efficiency calibration is discussed in next section.

The detector with a Be-window was utilized for determination of the 46.5 keV gamma-line from ^{210}Pb. The ^{7}Be concentration was calculated using the 477.6 keV gamma-line. Counting times were about 3000 minutes. A typical gamma-ray spectrum of an aerosol filter obtained by using a HPGe detector is shown in Figure 5.6. The black line represents background spectrum, the red line is spectrum counted immediately after sampling where are gamma-lines from short-lived decay products of radon and thoron present. The green line stands for spectrum measured after several days where no short-lived decay products are present. Here are the only significant peaks from ^{210}Pb, ^{7}Be and annihilation peak.

Since the atmospheric activity concentrations of ^{137}Cs and ^{40}K are very low, the cumulated monthly samples (cumulated four or five week samples) were used for the measurement. These cumulated samples have been measured by a large

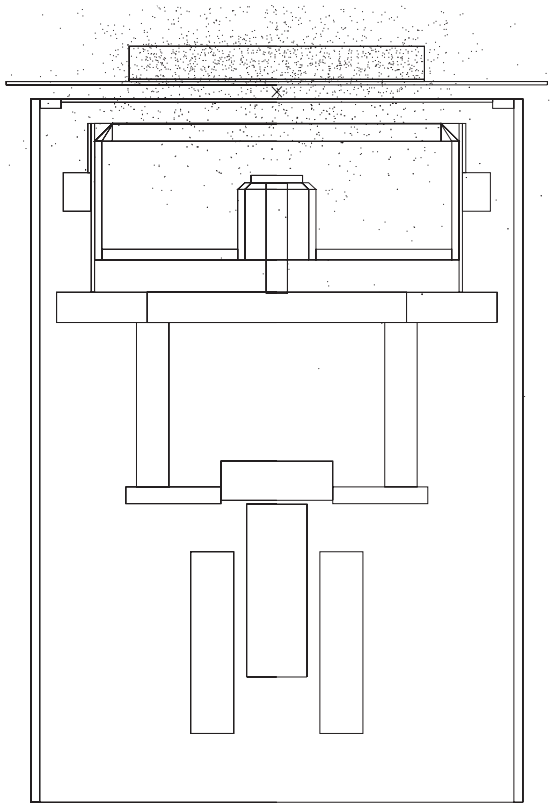

Figure 5.7: The model of HPGe(Be) detector with a filter sample. The dots correspond to points of first interaction of photons of energy 477 keV.

volume HPGe(270) detector with higher detection efficiency.

5.2.1 Detection efficiency

The photo-peak efficiency for geometry of filter and precipitation samples were calculated by Monte Carlo method using the code GEANT [Brun87]. The development of detector model was started by Garabík [Garabík97]. Quite often are Monte Carlo calculations applied to the determination of detection efficiency [Ewa01], [Sima]. This method is based on the simulation of individual photon histories. Each photon is tracked on its path from its origin inside the source trough the source material to and into the detector. The model was originally created for the efficiency calculations of large volume samples. The geometry of filter samples and evaporated precipitation samples was made additionally. In Figure 5.7 is shown the model of HPGe(Be) detector with a filter sample. The simulation using GEANT code already includes the effect of self-absorption in the sample, therefore no correction for mass density and atomic composition was needed.

Since the thickness of the so called "dead" germanium is not known, we have estimated the value by comparing the measured and calculated efficiencies for the

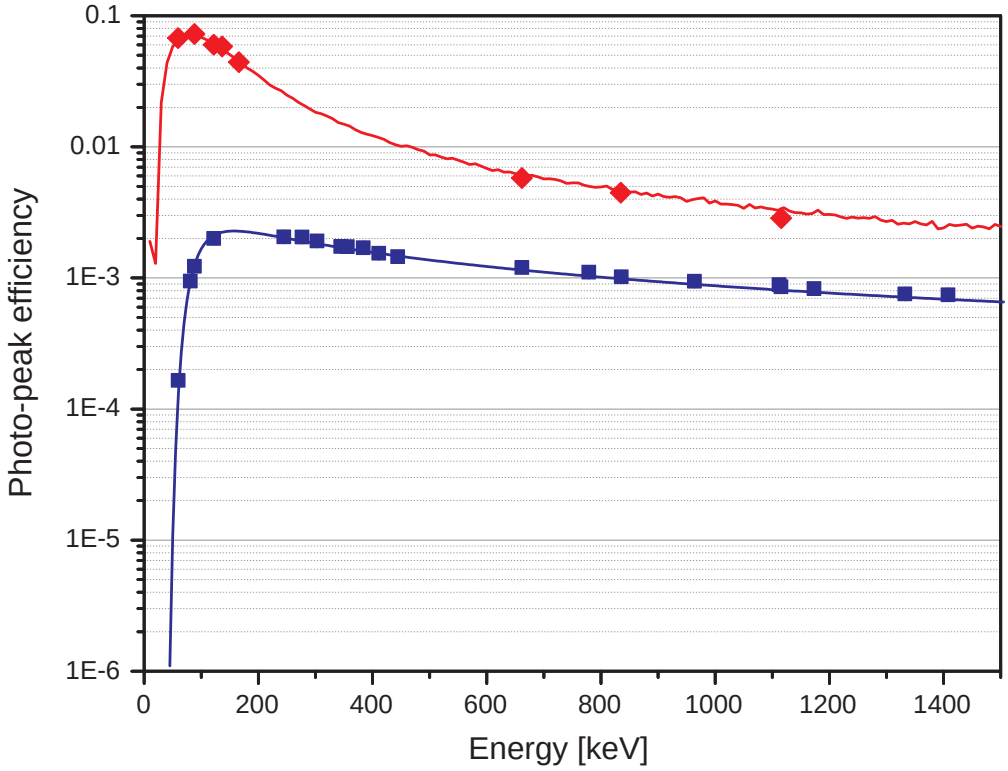

Figure 5.8: Comparison of photo-peak detection efficiency of HPGe(Be) calculated by GEANT model (lines) and experimental measurements (points) for standard point sources at a source-detector distance of 3 cm (red) and 25.5 cm (blue).

calibration solution of ^{210}Pb in a glass vial. This radionuclide was used for its low gamma energy (46.5 keV), which is more sensitive for the attenuation in the "dead" germanium layer.

For the verification of the GEANT model the values of photo-peak efficiency for point sources were calculated by the model and compared with experimentally obtained efficiency values. The agreement was good as can be seen in Figure 5.8.

In the Table 5.1 are the photo-peak efficiency values used for the activity calculations presented. The minimum detectable concentrations are calculated for volume of pumped air 14 000 m^3, time of measurement of the background 6 000 min and of the sample 3 000 min.

The efficiencies for the rainwater samples were determined the same way as for filter samples. The size of residue samples varied according the volume of rainwater, hence the efficiency was different for each individual sample.

Table 5.1: Photo-peak efficiency and minimum detectable concentrations (MDC) for determined radionuclides in aerosol filter samples

Radionuclide	Photo-peak efficiency	MDC [μBq m^{-3}]
^{210}Pb(HPGe(Be))	13.9%	0.15
^{7}Be(HPGe(Be))	2.8%	1.5
^{7}Be(HPGe(270))	7.0%	0.6
^{137}Cs(HPGe(270))	5.3%	0.09
^{40}K(HPGe(270))	3.0%	0.13

5.2.2 Activity calculation

The volume activity of radionuclide in air was calculated using following formula:

$$A = \frac{A_S}{V} = \frac{CPS}{I\varepsilon}\frac{1}{V} \tag{5.14}$$

where A_S is activity of filter sample [Bq], CPS is counts per second in particular photo-peak, I is photon emission probability of particular gamma-line, ε is photo-peak efficiency and V is volume of sampled air [m^3]. The above mentioned corrections for decay and correction for sampled volume are applied.

The total standard uncertainty of the method (calculated as sum of relative uncertainties in detection efficiency estimation, photo-peak counts estimation, sample volume estimation, *etc.*) was estimated below 6% for 95% confidence level. Minimum detectable concentrations MDC (Table 5.1) were derived from the lower limit of detection as $LLD = k^2 \pm 2LC$, where k is a coefficient of normal distribution corresponding to 95% confidence level and LC is the critical level depending on the counts of background photo-peak.

The volume activity of radionuclide in precipitation is calculated according the same formula 5.14, but A_S is activity of wet-precipitation residual sample and V stands for total volume of sampled water. Also the total deposition of radionuclide may be calculated [Bq m^{-2}]. In fact it is the value of A_S, since the active sampling surface is of a unit square meter. The same decay corrections are applied.

5.3 Neutron activation analysis

Activation analysis is a method for qualitative and quantitative determination of elements based upon the conversion of stable nuclei to other, mostly radioactive via nuclear reactions. In neutron activation analysis (NAA) the nuclear reaction occurs via bombardment of the analyzed material with neutrons. The induced radioactivity is consecutively measured.

All of the stable elements have properties suitable for production of radioactive isotopes although at different reaction rates. To carry out an NAA analysis

the sample is placed into a suitable irradiation facility at a constant, known neutron flux. This creates artificial radioisotopes of the elements present. Following irradiation the artificial radioisotopes decay via the emission of particles and photons. Each radionuclide is uniquely characterized by its decay constant and the type and energy of emitted radiation. Amongst the several types of radiation that can be emitted, gamma-radiation offers the best characteristics for the selective and simultaneous detection of radionuclides and thus of elements. The activation will result in a mixture of radionuclides, which can be analyzed by two different approaches:

1. The resulting radioactive sample is decomposed, and through chemical separations it is divided into several fractions: destructive or radiochemical neutron activation analysis.

2. The resulting radioactive sample is kept intact, and the measurements are made at different decay intervals taking advantage of the differences in decay rates of individual radionuclides: non-destructive or instrumental neutron activation analysis (INAA).

The second one is the most common method of NAA and found usage in many fields of science, mostly environmental studies, archaeology, material science, or biotechnologies. Particularly advantage is taken of the fact that the samples do not have to undergo any chemical treatment, neither prior, nor after the activation (non-destructive analysis). Another benefit is that light elements such as H, C, N, O, Si which in many materials belong to the major matrix components, do not produce radioactive products upon neutron activation. Therefore do not interfere with the determination of the other radioisotopes and it enables the observation of trace elements at very low detection limits, mg kg^{-1} to μg kg^{-1} in matrices composed of the light elements. The good resolution of gamma-spectrometric system allows high selectivity and simultaneous determination of many radionuclides to be interpreted as multi-element determination.

On the other hand the major imperfection of NAA is the inability to determine some elements like Cu, Cd, Tl, Pb, Bi. The reason can be either one, or a combination of very low activation cross sections, activation products with very short half-lives and the emission of the radiation not suitable for gamma-spectrometry detection. The next drawback to the use of NAA is the fact that even though the technique is essentially non-destructive in the most of the cases the irradiated sample usually will remain radioactive for many years after the initial analysis, requiring handling and disposal protocols for low-level to medium-level radioactive material. Also the number of suitable activation nuclear reactors is declining and with a lack of irradiation facilities the technique becomes more expensive.

Thermal neutron activation analysis takes advantage of the high intensity of neutrons available from the thermalization of fission neutrons and the large thermal neutron cross sections for most isotopes. Epithermal neutron activation analysis

(ENAA) is a useful extension of INAA. The thermal neutrons are effectively removed by means of a filter consisting of some material with very high neutron absorption cross section, such as boron, cadmium, or gadolinium. The method is based on the fact that some elements have isotopes with resonances in the epithermal neutron region. This gives certain advantages over conventional INAA for several trace elements in terms of improvement in precision and lowering of detection limits, because of the reduction of high matrix activity. The ratio of resonance activation integral to thermal neutron cross section I_0/σ_0 is about 0.5 for nuclides without resonance in epithermal region and with resonance it may reach 100. It enhances the activation of a number of trace elements relative to the major matrix elements.

Analysis of airborne particulate matter is common air pollution study. Air filter analysis is an area where INAA can hardly be replaced by any other analytical technique. This is because of the total mass of the aerosol collected on a filter is usually very small, and thus prefers direct non-destructive methods rather than those depending on dissolution of the sample preceding to analysis [Frontasyeva00b].

Our air filter samples were irradiated on Department of Activation Analysis and Radiation Research at Frank Laboratory of Neutron Physics, Joint Institute for Nuclear Research (JINR) in Dubna, Russia. For this purpose the reactor IBR-2 and the REGATA experimental setup was used. This setup allows to carry multi-elemental analysis of many sample types using conventional and epithermal neutron activation. Because of a high resonance neutron flux of IBR-2 reactor ENAA is especially advantageous for determining many rare-earth elements and heavy metals due to their high resonance activation integral to thermal neutron activation cross section ratio. The combination of epithermal and conventional activation analysis on IBR-2 reactor, supplemented by atomic absorption spectrometry (AAS) for the elements Pb, Cd, and Cu, allows determine about 45 elements [Frontasyeva97].

The procedure in INAA is characterized by three steps, activation via irradiation with reactor neutrons, measurement of the induced gamma-radiation after one or more decay times and interpretation of the resulting gamma-spectra in terms of elements and its concentration.

5.3.1 Activation

The purpose of activation is to convert stable nuclei into radioactive nuclei emitting radiation that can be used for analytical purposes. Crucial is the knowledge of reactions that may take place during irradiation, otherwise we are not able to identify the relation between the observed radionuclide, its target nucleus, and associated element. For quantitative determination the reaction rates have to be known. After the nucleus captures a neutron during activation the nuclear mass is changed. After the capture the excess energy is promptly emitted in form of photons and particles. The newly formed nucleus may be unstable (radioactive)

and already during activation it starts to decay to a stable state. In most cases and X-radiation is emitted simultaneously. Most common reaction occurring in NAA is the (n,γ) reaction, but also reactions such as (n,p), (n,α), (n,n') and (n,2n) are important. Some nuclei, like ^{235}U are fissionable by neutron capture and then reaction (n,f) may run. The reaction rate R is given by

$$R = \int_0^\infty \nu n(\nu)\sigma(\nu)d\nu \tag{5.15}$$

where ν is the neutron velocity [m s^{-1}]; $\sigma(\nu)$ is the neutron cross section [m^2] for neutrons with velocity ν; $n(\nu)d\nu$ is the neutron density [m^{-3}] of neutrons with velocities between ν and $\nu + d\nu$ considered to be constant in time.

The production of radioactive nuclei is described by

$$\frac{dN}{dt} = RN_0 - \lambda N \tag{5.16}$$

where N_0 is the number of target nuclei; N is the number of radioactive nuclei; λ is the decay constant [s^{-1}]. The disintegration rate D of the produced radionuclide at the end of the irradiation time t_{ir} is

$$D(t_{ir}) = N(t_{ir})\lambda = N_0R(1 - e^{-\lambda t_{ir}}) \tag{5.17}$$

where we assume that $N = 0$ at $t = 0$ and N_0 is constant. The cross section and neutron flux are energy dependent. In research reactors can be generally three types of neutrons distinguished:

1. Fission or fast neutrons of an energy range up to at least 15 MeV, with the most probable energy at about 1 MeV;

2. Neutrons of intermediate energies, which are in the process of slowing down in the reactor. Usually are called resonance, and include neutrons with energies from 1 eV to 1 MeV;

3. Thermal neutrons, which are in thermal equilibrium with the moderator. The most probable energy is 0.025 eV.

Thermal neutron fluxes are typically highest, as can be seen on Figure 5.9 The epithermal (resonance and fast) neutron fluxes strongly depend on the reactor configuration and the choice of the moderator. Reactions of the (n,γ) and (n,f) type have the highest cross section for thermal neutrons. The reactions such as (n,p), (n,α), (n,n') and (n,2n) mainly occur with fast neutrons at cross sections 2 or 3 orders of magnitude lower [Bode96].

Upon irradiation a thermal neutron interacts with the target nucleus via a non-elastic collision, causing neutron capture. This collision forms a compound nucleus which is in an excited state. The excitation energy within the compound nucleus is formed from the binding energy of the thermal neutron with the target

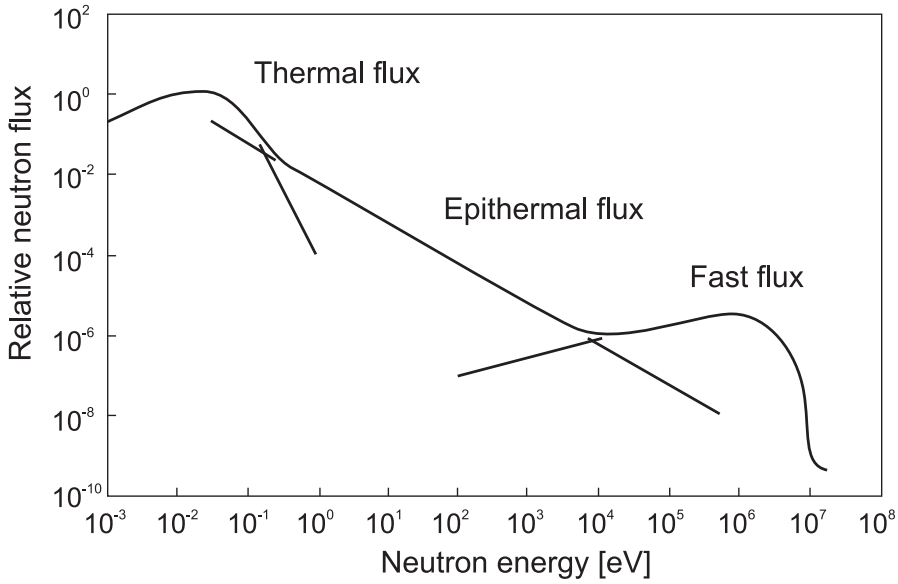

Figure 5.9: Schematic representation of the neutron flux spectrum in a thermal nuclear reactor. Adopted from [Bode96].

nucleus. This excited state is unfavorable and the compound nucleus will almost instantaneously de-excite into a more stable configuration through the emission of a prompt particle and one or more characteristic prompt gamma photons. In most cases this more stable configuration yields a radioactive nucleus. The newly formed radioactive nucleus now decays by the emission of particles and one or more characteristic delayed gamma photons. This decay process is at much slower rate than the initial de-excitation and depends on unique half-life of the radioactive nucleus.

The activation cross section for thermal neutrons is inversely proportional to the neutron velocity ($\frac{1}{\nu}$ law). In the epithermal region the cross section can be very high for neutrons of a discrete energy. These resonance peaks are used for determination of some trace elements, in particular rare earth elements.

The energy dependence of the cross section and neutron flux can be taken into account in equation 5.15 by dividing the neutron spectrum into a thermal and an epithermal region. The boundary line is at En = 0.55 eV, the so-called cadmium cut-off energy. The integral in 5.15 can be rewritten as

$$R = \int_0^{\nu_{Cd}} \nu n(\nu)\sigma(\nu)d\nu + \int_{\nu_{Cd}}^{\infty} \nu n(\nu)\sigma(\nu)d\nu \tag{5.18}$$

The first term can be integrated

$$\int_0^{\nu_{Cd}} \nu n(\nu)\sigma(\nu)d\nu \simeq \nu_0\sigma_0 \int_0^{\infty} \nu n(\nu)d\nu = n\nu_0\sigma_0 \tag{5.19}$$

where

$$n = \int_0^{\infty} n(\nu)d\nu \tag{5.20}$$

is called the thermal neutron density and $\Phi_{th} = n\nu_0$ is the conventional thermal neutron flux [$m^{-2} \cdot s^{-1}$], for energies up to the Cd cut-off. σ_0 is the thermal neutron activation cross section [m^2]; ν_0 is the most probable neutron velocity at 20°C: 2200 m s^{-1}. The second term is re-formulated in terms of neutron energy rather than neutron velocity and the infinite dilution resonance integral I_0 (it is also a cross section) is introduced:

$$\int_{\nu_{Cd}}^{\infty} \nu n(\nu) d\nu = \Phi_{epi} \int_{E_{Cd}}^{E_{max}} \frac{\sigma(E_n) dE_n}{E_n} = \Phi_{epi} I_0 \tag{5.21}$$

where

$$I_0 = \int_{E_{Cd}}^{E_{max}} \frac{\sigma(E_n) dE_n}{E_n} \tag{5.22}$$

Φ_{epi} is the conventional epithermal neutron flux per unit energy interval, at 1 eV. In real practise the epithermal neutron flux is not precisely proportional to $\frac{1}{E_n}$, but small deviation has to be accounted by introducing an epithermal flux distribution parameter α:

$$I_0(\alpha) = \int_{E_{Cd}}^{E_{max}} \frac{\sigma(E_n) dE_n}{E_n^{(1+\alpha)}} \tag{5.23}$$

The expression 5.18 can be rewritten as

$$R = \Phi_{th}\sigma_0 + \Phi_{epi} I_0(\alpha) \tag{5.24}$$

Expressing the ratio of the thermal and the epithermal neutron flux as $f = \frac{\Phi_{th}}{\Phi_{epi}}$ and the ratio of the resonance integral and the thermal activation cross section as $Q_0(\alpha) = \frac{I_0(\alpha)}{\sigma_0}$, an effective cross section can be defined:

$$\sigma_{eff} = \sigma_0 (1 + \frac{Q_0(\alpha)}{f}) \tag{5.25}$$

Afterwards is the equation 5.21 simplified

$$R = \Phi_{th}\sigma_{eff} \tag{5.26}$$

5.3.2 Measurement

The nuclear transformations are established by measurement of the number of nuclear decays. In INAA it is performed using gamma-spectrometry. Germanium semiconductor detectors have the best energy resolution, which is especially demanded for unambiguous radionuclide identification. The number of activated nuclei $N(t_{ir}, t_d)$ present at the start of the measurement is given by

$$N(t_{ir}, t_d) = \frac{RN_0}{\lambda} (1 - e^{-\lambda t_{ir}}) e^{-\lambda t_d} \tag{5.27}$$

and the number of nuclei ΔN disintegrating during the measurement is given by

$$\Delta N(t_{ir}, t_d, t_m) = \frac{RN_0}{\lambda}(1 - e^{-\lambda t_{ir}})e^{-\lambda t_d}(1 - e^{-\lambda t_m}) \tag{5.28}$$

where t_d is the decay time, time between the end of the irradiation and the start of the measurement; t_m is the duration of measurement. Replacing the number of target nuclei N_0 by $\frac{N_{Av}\theta w}{M}$ and using the equation 5.23, the resulting net area A of a peak in the spectrum corresponding with a given photon energy is approximated by the activation formula:

$$A = \Delta N\gamma\varepsilon = \Phi_{th}\sigma_{eff}\frac{N_{Av}\theta w}{M}(1 - e^{-\lambda t_{ir}})e^{-\lambda t_d}(1 - e^{-\lambda t_m})\gamma\varepsilon \tag{5.29}$$

where N_{Av} is Avogadro's number [mol^{-1}]; θ is the isotopic abundance of the target isotope N_0; w is the mass of the irradiated element [g]; M is the atomic mass [g mol^{-1}]; γ is the probability of disintegrating nucleus emitting a photon of this energy; ε is the photopeak efficiency of the detector.

NAA is a comparative technique. Element contents are determined on the basis of certified reference materials and flux comparators. Standards are prepared from certified solutions of known concentration of the elements of interest. The procedure generally used to calculate concentration (i.e., ppm of element) in the unknown sample is to irradiate the unknown sample and a comparator standard together in the reactor. If both are measured using the same detector, then one needs to correct the difference in decay between the two, but do not need the photo-peak efficiency correction. The activities are usually decay corrected for sample and reference material back to the end of irradiation using the half-life of the measured isotope. The equation used to calculate the concentration of an element of interest in the unknown sample is:

$$\rho = \frac{(\frac{A}{t_m e^{-\lambda t_m}(1-e^{-\lambda t_m})w})_{sample}}{(\frac{A}{t_m e^{-\lambda t_m}(1-e^{-\lambda t_m})w})_{standard}} \tag{5.30}$$

where ρ is concentration [g g^{-1}]; w is the mass [g].

For the full multi-element INAA it is virtually impossible to produce a multi-element standard containing known amounts of all 70 detectable elements with sufficient accuracy in a volume closely matching the shape and the size of the samples. In this case the absolute calibration has to be used. The physical parameters θ, N_{Av}, M, σ_{eff}, γ, λ are taken from literature. The other parameters A, w, Φ, ε, t_{ir}, t_d, t_m are determined, calculated or measured for given experimental setup.

5.3.3 Reactor IBR-2 and system REGATA

For purpose of irradiation of our samples we used the experimental pulsed fast reactor IBR-2 at JINR in Dubna, Russia. The main parameters of IBR-2 reactor are in Table 5.2.

Table 5.2: Main parameters of pulsed fast IBR-2 reactor in JINR Dubna

Power	Mean 2 MW, in pulse 1500 MW
Pulse frequency	5 Hz
Thermal neutron flux on moderator surface [cm $^{-2}$ sec $^{-1}$]	For extracted beams 8×10^{12}, in pulse 5×10^{15}
Thermal neutron pulse width	320 μs
Moderator	Water (300 K), flat and of grooved type, cold methane for operations in the range 20-50 K
Number of channels	14 horizontal, 2 vertical

There are four irradiation channels designated for INAA at irradiation facility (Beam 3 in Figure 5.12) and provide activation with thermal, epithermal and fast neutrons [Frontasyeva00a]. Reactor is equipped with fast pneumatic transfer system REGATA (Russian - European GAte To Asia). The layout is given in Figure 5.10. It consists of four channels for irradiation (Ch1 - Ch4), the pneumatic transport system (PTS) and three gamma-spectrometers located at three rooms on the ground floor of the reactor IBR-2. Channels Ch3 and Ch4 are not connected to REGATA. The samples are in this case introduced into the channel before the reactor cycle. Two channels are screened for activation with epithermal neutrons [Frontasyeva97]. The neutron spectra with and without the Cd coat are shown in Figure 5.11 [Peresedov96]. The main parameters (for reactor's power 2 MW) of the irradiation channels are presented in Table 5.3.

Table 5.3: Neutron flux density, temperature T inside the channels, diameter and length of irradiation channels Ch1 - Ch2 [Frontasyeva00a]

Irradiation site	Neutron flux density [cm^{-2} s^{-1}]			T [°C] Inside Ch	Ch diameter [mm]	Ch length [mm]
	Thermal	Epithermal	Fast			
Ch1	Cd-coated	3.31×10^{12}	4.32×10^{12}	70	28	260
Ch2	1.23×10^{12}	2.96×10^{12}	4.10×10^{12}	60	28	260

The channels Ch3, Ch4 are cooled by water, and the channels Ch1, Ch2 are cooled by air. That is why the temperature in channels Ch3 and Ch4 is lower than the temperature in channels Ch1 and Ch2 in spite of the greater neutron flux density. The time of sample irradiation in channels Ch3, Ch4 depends on the operation cycle duration of the reactor and is equal to 10-12 days. The irradiation channels Ch1 and Ch2 are the same, but Ch1 is Cd-coated. Each channel consists

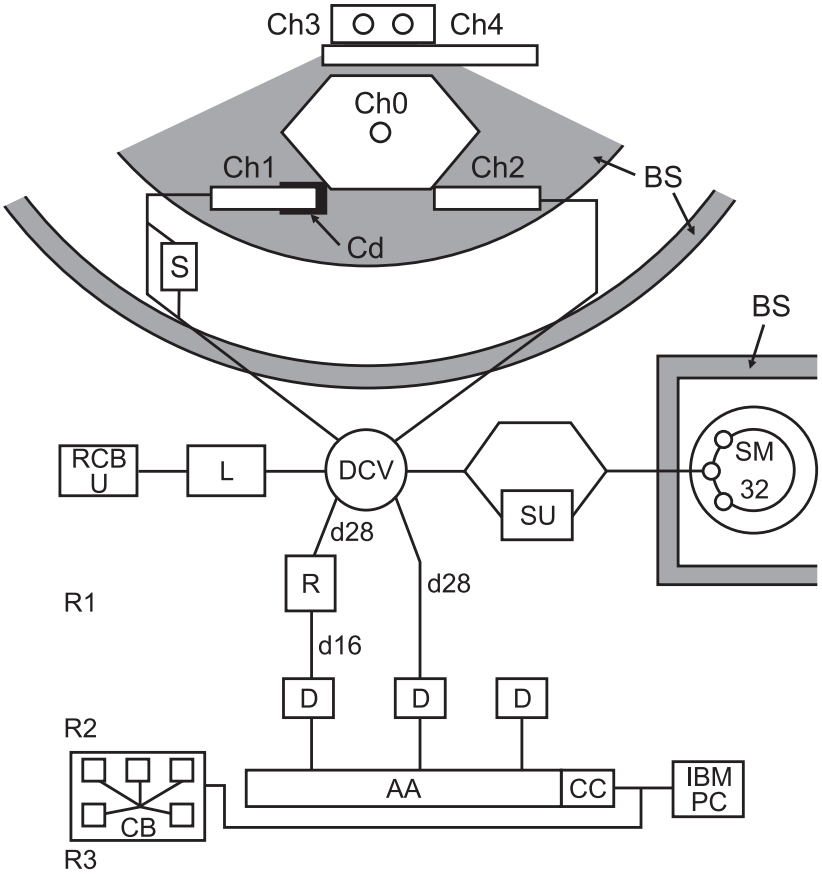

Figure 5.10: The REGATA experimental setup: Ch1 - Ch4 - irradiation channels, S - intermediate storage, DCV - directional control valves, L - loading unit, RCB - radiochemical glove-cell, U - unloading unit, SU - separate unit, SM - storage magazine, R - repacking unit, D - Ge(Li) and HPGe detectors, AA - amplitude analyser, CB - control board, CC - CAMAC controller, BS - biological shield, R1-R3 - the rooms where the system is located [Frontasyeva00a].

of two concentric pipes made from stainless steel. They are placed into an aluminium box filled with biological shield. Samples are transported through one of the pipes (flight pipe) of 28 mm in diameter and compressed air flows through the second pipe.

Samples are irradiated in transport containers made of polyethylene, teflon and aluminium. The irradiation time of a polyethylene container is limited by radiation and temperature resistance of polyethylene and is equal to 30 minutes, both for Ch1 and Ch2 at 2 MW power of the reactor. A teflon container is used for irradiation up to 5 hours. Aluminium containers are used for longer irradiation. The internal volume of the polyethylene container is equal to approximately 4 cm^3, and the volume of the aluminium container is 1.5 times lager. Up to 7 containers can be simultaneously loaded in each channel.

The pneumatic system transports containers by compressed air (0.3-0.6 MPa).

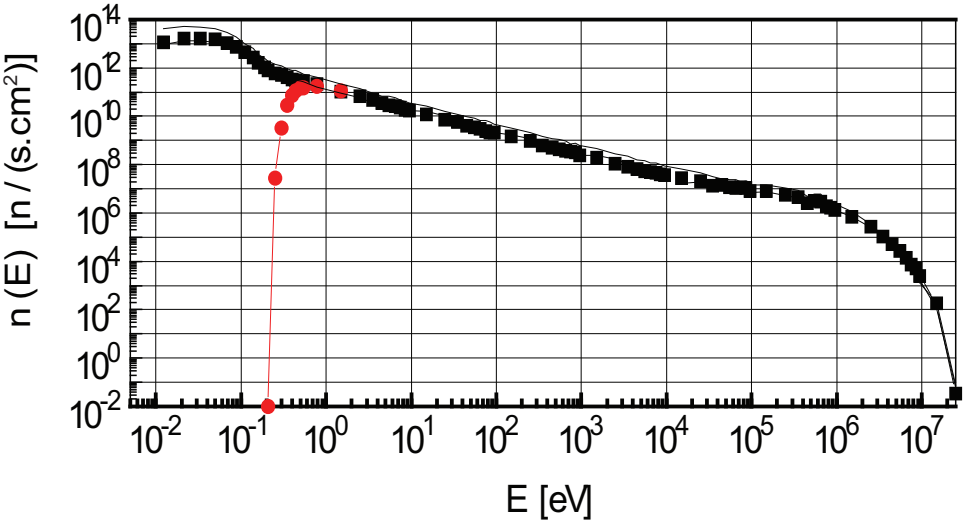

Figure 5.11: Neutron energy spectra in irradiation channels Ch1 (red) and Ch2 (black) [Peresedov96].

All its units are located far from the reactor core (50-60 m). The polyethylene containers are transported to irradiation site for 7-20 seconds, the aluminium containers flight faster, 3-7 seconds. The intermediate storage (S), for up to 15 containers, is used to reduce the activity of aluminium containers after long irradiation. It is located between two rings of the biological shield of the reactor. High activity samples are stored in the storage (SM) with a capacity of 32 cells surrounded by the shield from lead and concrete block.

When short-lived isotopes are determined, a small polyethylene capsule is placed into a transport container. To extract a small capsule from a transport container the special repacking unit (R) is used.

PTS has loading (L) and unloading (U) units to load and to unload containers from the system. To provide radiation safety, the unloading unit is placed into a glove-cell. All devices of the pneumatic system are equipped with photosensors and end-switches to indicate the container position in the system and to correct operation of all mechanisms. Acoustic detectors placed on the flight pipes of irradiation channels behind the first ring of a biological shield allow to determine the time of a container arrival and departure. There are many noise pulses during the transport of a container in the flight pipe intended to clear the irradiation timer. The knock of the capsule at the bottom of the channel forms the last clearing pulse. After this pulse the irradiation timer starts counting the time of irradiation. Such positioning of acoustic detectors protects them from radiation damage.

The neutron flux is controlled by monitors (Au, Zr, *etc.*). The reduction of the neutron flux density along the channel length is gradual, but significant, up to

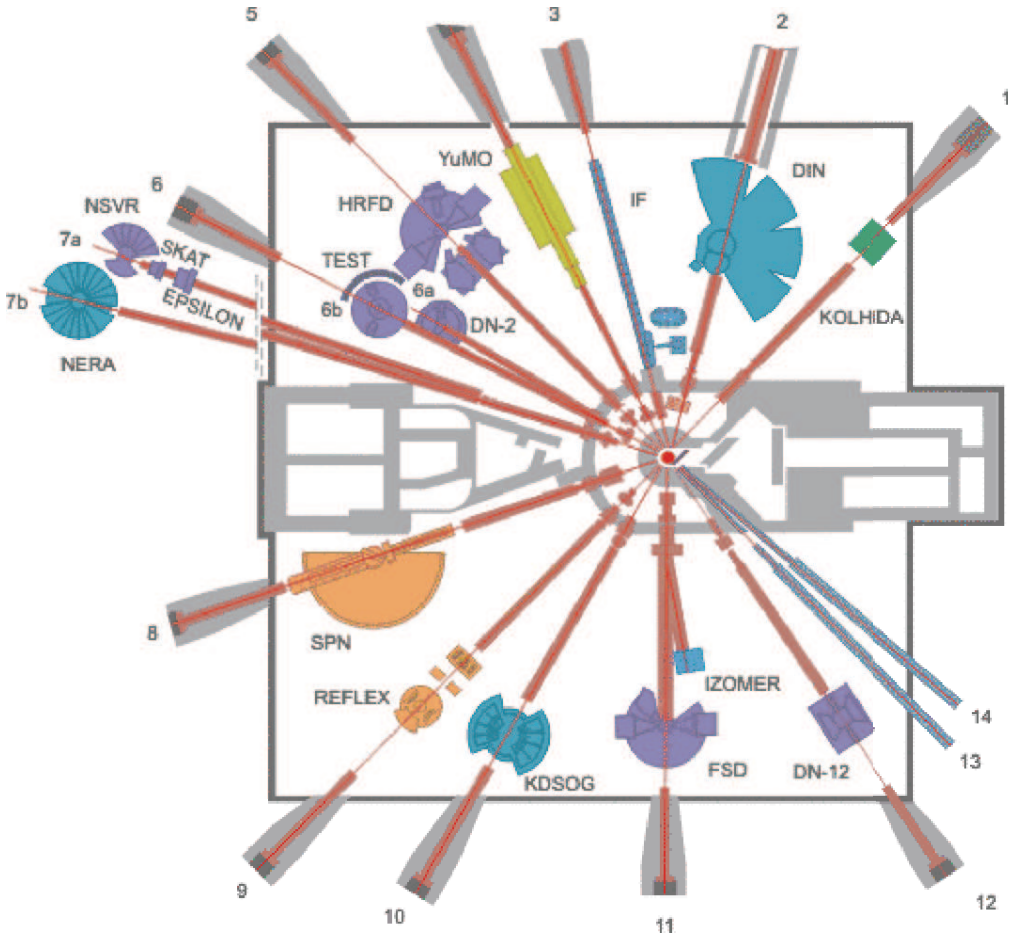

Figure 5.12: Layout of neutron channels in pulsed fast reactor IBR-2 at JINR Dubna.

30-50 %. It should be taken into consideration while data processing.

The induced activity is measured using gamma-spectrometers with Ge(Li) and HPGe detectors equipped with ORTEC electronics. The software developed at JINR is used for data processing [Ostrovnaya93].

But REGATA is just small research activity at the experimental nuclear reactor IBR-2 in JINR. There are also other instruments installed and many experiments took place at this site. Figure 5.12 shows the reactor scheme with 14 neutron beams used for several experiments:

B1: KOLHIDA - Nuclear physics facility
B2: DIN-2PI - Time-of-flight spectrometer of direct geometry
B3: IF - Irradiation facility
B4: YuMO - Small angle scattering spectrometer
B5: HRFD - High resolution Fourier diffractometer
B6a: DN-2 - Multipurpose diffractometer
B6b: TEST - Test spectrometer
B7a: EPSILON/SKAT and NSHR - Strain/stress and texture diffractometers

B7b: NERA-PR - Multicrystal inverted geometry spectrometer
B8: SPN - Spectrometer of polarized neutrons
B9: REFLEX-P - Neutron reflectometer with polarized neutron beam
B10: KDSOG-M - Inverse geometry spectrometer
B11: ISOMER - Delayed neutron facility
B11a: FSD - High resolution Fourier Stress Diffractometer
B12: DN-12 - High pressure diffractometer

5.3.4 Treatment of samples

INAA is considered to be a non-destructive technique although some damage may occur due to thermal heating, radiolysis and radiation.

Filters (~ 0.4 g) were pressed into the form of small tablet with diameter 10 mm and packed in polyethylene foil bags for short-term irradiation. The special effort has to be taken to avoid contamination of the samples. Since the highest interest is on the determination of heavy metals, also the device for pressing is made from plastic.

To determine the short-lived isotopes of Na, Mg, Al, Cl, K, Ca, Mn, Br, I and other, the channel 2 (Ch2) was used (conventional NAA). Samples were irradiated for 10 minutes and immediately measured for 5 min and second time for 20 min. The time of irradiation depends on the type of sample and the element composition supposed. It can vary from 3 to 20 minutes for the short-lived isotopes determination.

After determination of short-lived isotopes were the samples repacked into aluminium containers. Elements yielding long-lived isotopes were determined using the epithermal NAA in Cd-screened channel 1 (Ch1). Samples were irradiated for 1 hour and measured twice after 4-5 days and 20 days of decay, respectively. We have to wait at least 3 days to decay the activated aluminium container (^{24}Na, $T_{1/2} = 15$ hours) because of the radiation protection requirements.

Table 5.4 shows selected activated radionuclides, their half-lives, gamma peaks, the type of measurement used for element determination and accuracy of determination.

Data processing was carried out using software developed in FLNP JINR, and element contents were determined on the basis of certified reference materials and flux comparators [Frontasyeva00a]. For short-term irradiation in Ch2 a comparator of Au (10 μg) was employed. For Quality control to provide QC content of elements yielding short- and long-lived isotopes was determined using certified reference materials: Lichen 336 IAEA and Cabbage IAEA-359 (International Atomic Energy Agency, Austria), and standard reference material SRM-1573a (Tomato leaves) from the NIST (National Institute of Standards and Technology, USA). For long irradiation the three reference materials were packed together with samples in each transport container. The reference material showing least deviation between measured and certified values of elemental content was chosen.

Table 5.4: Overview on elements in aerosol filter samples determined by INAA

Element determined	Radionuclide	Half-life	Energy [keV]	Measurement*	Accuracy [%]
Na	^{24}Na	14.91 h	1368.5	B	10
Al	^{28}Al	2.241 m	1778.9	A	6
Cl	^{38}Cl	37.24 m	2167.7	B	29
K	^{42}K	12.36 h	1524.7	B	19
Ca	^{49}Ca	8.718 m	3084	A	14
Sc	^{46}Sc	83.83 d	889	D	32
Ti	^{51}Ti	5.76 m	320	A	34
V	^{52}V	3.743 m	1434.4	A	18
Cr	^{51}Cr	27.7 d	320	D	36
Mn	^{56}Mn	2.578 h	1810.7	B	5
Fe	^{59}Fe	44.5 d	1099.1	D	23
Ga	^{72}Ga	14.1 h	629.9	C	14
As	^{76}As	1.097 d	559.1	C	5
Se	^{75}Se	119.8 d	264.1	D	58
Br	^{80}Br	17.7 m	617	B	13
Rb	^{86}Rb	18.66 d	1076.6	D	59
In	^{116m}In	54.1 m	1294	B	25
Sb	^{122}Sb	2.7 d	564.2	C	51
I	^{128}I	24.99 m	442.7	A	7
Cs	^{134}Cs	2.062 y	795.8	D	65
Ba	^{139}Ba	83.1 m	165.8	B	45
La	^{140}La	1.678 d	1596.2	C	52
Sm	^{153}Sm	46.7 h	103.2	C	40
Dy	^{165}Dy	2.334 h	94.7	B	40
Tm	^{170}Tm	128.6 d	84.3	D	79
W	^{187}W	23.9 h	685.7	C	60
Au	^{198}Au	2.694 d	411.8	C	49
Hg	^{203}Hg	46.6 d	279	D	64
Th	^{233}Pa	27 d	312	D	40
U	^{239}U	23.5 m	74.7	B	27

*A: conventional NAA, short irradiation, first measurement
B: conventional NAA, short irradiation, second measurement
C: epithermal NAA, long irradiation, first measurement
D: epithermal NAA, long irradiation, second measurement

Chapter 6

Results and Discussion

6.1 Radioactivity of atmospheric aerosols

The sampling of atmospheric aerosol particles started in the March 2001. Up to the September 2007, 245 sets of aerosol filters were sampled. The nitro-cellulose filters with pore sizes of 0.85 μm were used, only one sampling (13.1.-18.1.05) was performed using the textile filter. The correction for the collection efficiency of these filters was applied. Three campaigns were realized in the location of the Slovak Institute of Metrology, in order to evaluate the radiation background radiation of this site. Since the location of the Slovak Institute of Metrology is in vicinity of our faculty (about 2.5 km), we have included also these results to the data set.

Table 6.1: Number of samples (NS) analyzed, range, average and median of activity concentrations of ^{7}Be, ^{210}Pb [mBq m^{-3}], in ground level air for the period of March 2001 - September 2007, and ^{137}Cs, ^{40}K [μBq m^{-3}] for the period of October 2003 to April 2007

	NS	Range	Average	Median	SD
^{7}Be	245	0.2 - 5.1	2.5 $\pm$ 0.1	2.4	1.0
^{210}Pb	245	0.13 - 3.07	0.77 $\pm$ 0.04	0.64	0.45
^{137}Cs	56	0.10 - 1.25	0.52 $\pm$ 0.10	0.50	0.29
^{40}K	56	1.2 - 13.0	5.2 $\pm$ 0.9	4.8	2.8

The activity concentrations of the ^{7}Be and ^{210}Pb in Bratislava atmosphere for the time period of March 2001 - September 2007 are presented in Figure 6.1 and Table 6.1. The activity concentrations of ^{7}Be ranged from 0.2 to 5.1 mBq m^{-3}, with the average value of 2.5 $\pm$ 0.1 mBq m^{-3}. The range of ^{210}Pb activity concentrations for this period was 0.1 to 3.1 mBq m^{-3}, with the average of 0.77 $\pm$ 0.04 mBq m^{-3}. The detail information of data are given in Appendix A. The running results were

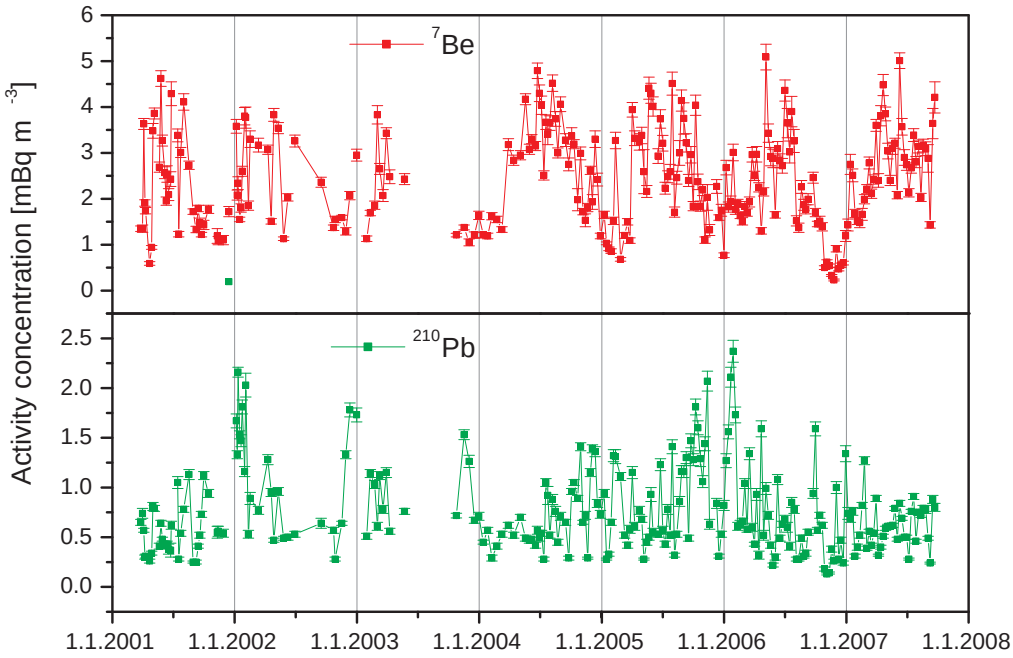

Figure 6.1: Activity concentrations of ^{7}Be and ^{210}Pb in Bratislava ground level air from March 2001 to September 2007.

presented in several papers and conferences [Sýkora03], [Merešová04a], [Merešová06], [Merešová05-06a], [Sýkora07].

The observed range and average values (Table 6.1) can be considered as representative at ground level air in our geographical region. Our results are generally in agreement with data reported in the literature [Winkler98], [Kuča03], [Vecchi05], [Cannizzaro04], [Todorovic05], [Hötzl87]. Due to irregular sampling campaigns were the monthly average values calculated only for the period of October 2003 - September 2007 (Figure 6.2).

Frequency distributions of ^{7}Be and ^{210}Pb concentrations presented in Figure 6.3 follow log-normal distribution:

$$y = y_0 + \frac{A}{\sqrt{2\pi}wx} e^{\frac{-(x/x_c)^2}{2w^2}} \tag{6.1}$$

The class intervals for ^{7}Be and ^{210}Pb concentrations were set to 0.5 and 0.2 mBq m^{-3}, respectively. Similar results are reported in the literature [Likuku06], [Todorovic05], [Dueñas99]. The geometric means of ^{7}Be and ^{210}Pb concentrations are 2.38 and 0.62 mBq m^{-3}, respectively. The geometric standard deviations (w is peak width) are 0.52 mBq m^{-3} for ^{7}Be and 0.45 mBq m^{-3} for ^{210}Pb.

The average activity concentrations of ^{137}Cs and ^{40}K in air are very low, therefore the cumulated monthly samples were used for the activity determina-

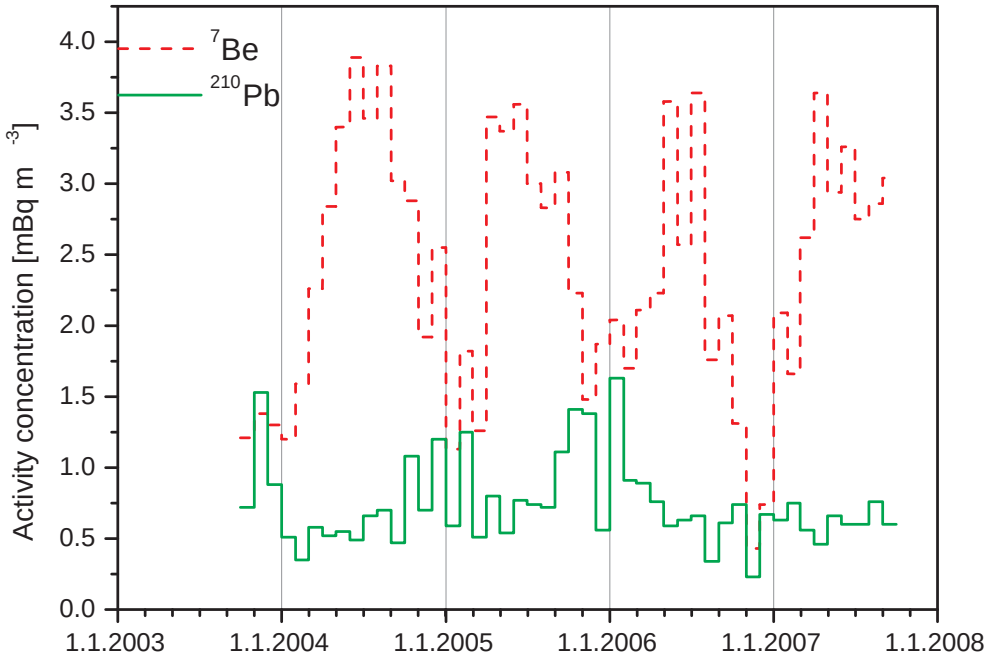

Figure 6.2: Monthly average activity concentrations of ^{7}Be and ^{210}Pb in Bratislava ground level air from October 2003 to September 2007.

tion. Values of ^{137}Cs and ^{40}K reached the level of 0.52 ± 0.10 μ Bq m^{-3} and 5.2 ± 0.9 μBq m^{-3}, respectively. The observed value of ^{137}Cs concentration was in average seven orders of magnitude lower than the maximum value 6 Bq m^{-3} measured on 1^{st} May 1986 in the territory of the Slovak Republic as reported by UNSCEAR [UNSCEAR88]. The decrease reflects a removal half-time of about 15 months [Cabáneková98], [Papastefanou96].

In the past, there has been correlation between ^{7}Be and ^{137}Cs concentrations observed. The stratosphere was reservoir of both radionuclides: the cosmogenic ^{7}Be produced by spallation of light nuclei atmospheric with cosmic rays, and the ^{137}Cs originating from numerous nuclear weapon tests. Since the nuclear test ban treaty the activity concentration in stratospheric reservoir has decreased to insignificant level and the present very low concentration of ^{137}Cs is the reason of no correlation found between ^{7}Be and ^{137}Cs. It has to be noted that the potential seasonal variations are ranging within the uncertainty of determination. However, Kozak *et al.* using the isotopic ratio ^{134}Cs/^{137}Cs concluded that Chernobyl radiocesium (most likely resuspended) from year to year plays less and less important role in the total radiocesium content in the air. Some of the observed ^{137}Cs came most likely from the stratosphere as the remain of the global fallout, or form other

sources like for example nuclear fuel reprocessing plants [Kozak97].

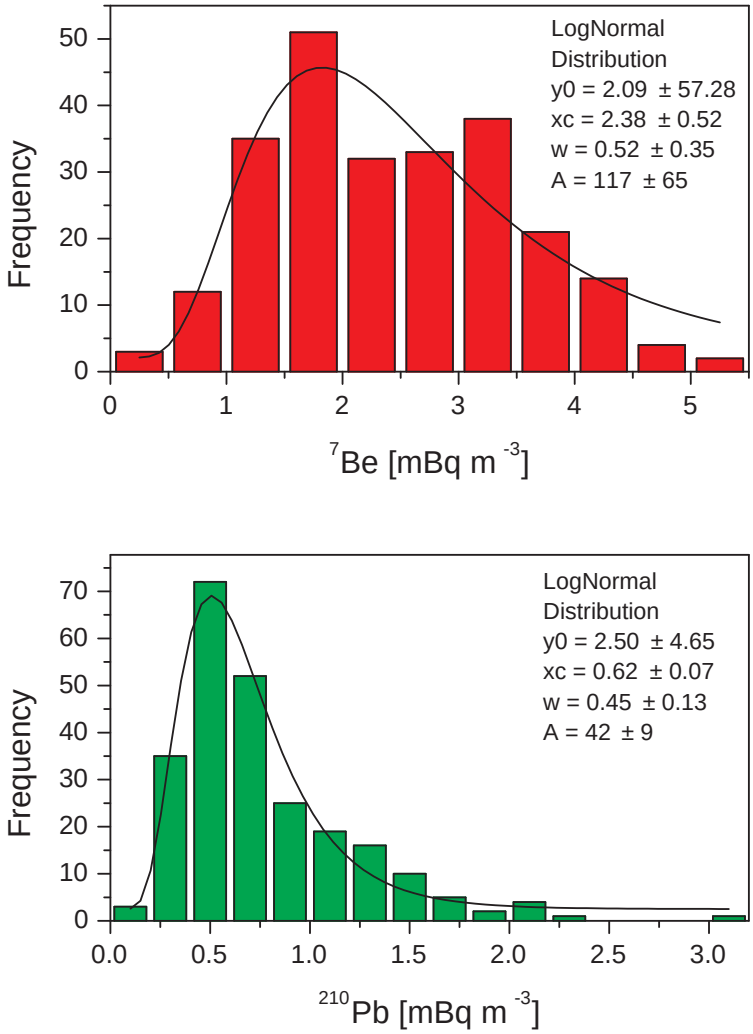

Figure 6.3: Frequency histograms of ^{7}Be and ^{210}Pb concentration.

6.1.1 Seasonal variations

The activity concentrations of ^{7}Be and ^{210}Pb exhibit the pattern of seasonal variations with mutually inverse trends (Figure 6.4), but no significant correlation was observed. In our region is the ^{7}Be concentration higher in spring comparing to autumn and winter season. It is connected to the air-mass transport from the stratosphere to the troposphere induced by the heating of the Earth's surface. The rising temperature enhances the exchange of matter between the air reservoirs with consequent transport of cosmogenic radionuclides to lower levels of the atmosphere.

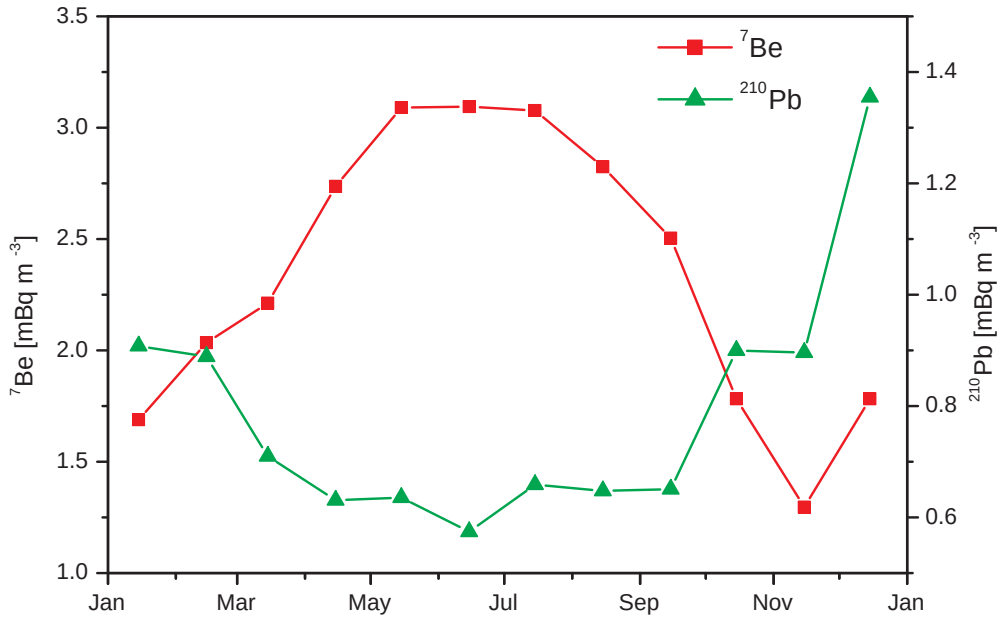

Figure 6.4: Seasonal variations of ^{7}Be and ^{210}Pb activity concentrations for period October 2003 - September 2007.

The intrusions of stratospheric air into the troposphere are processes occurring during the upward movement of tropopause. On the contrary in cold months these exchange processes are reduced and the supply of ^{7}Be produced in higher layers of atmosphere declines.

The concentrations of ^{210}Pb reach higher values in autumn and winter months, what is attributed to frequent inversion conditions of the surface air layers [Holý098]. The decrease of the ^{210}Pb concentration in warm spring and summer season is a result of intensive air mixing.

6.1.2 Comparison to meteorological parameters

The correlation study has been carried out between atmospheric concentrations of radionuclides ^{7}Be and ^{210}Pb and actual meteorological conditions: the air temperature, the atmospheric pressure, relative humidity of air, cloudiness, and the amount of precipitation. The linear correlation coefficients are presented in Table 6.2. Temperature is the variable most strongly correlated to the activities of ^{7}Be (Figure 6.5). High temperatures often lead to the setting up of upward convection currents in the atmosphere and enhances mixing of surface layers with air from upper levels. On the contrary, negative correlations are observed for ^{7}Be with humidity and cloudiness. Its because air temperature and these two parameters show an opposite behavior.

Table 6.2: Linear correlation coefficients between activity concentrations of ^{7}Be and ^{210}Pb and selected meteorological parameters

Radionuclide	Temperature	Pressure	Humidity	Precipitation	Cloudiness
^{7}Be	0.51	0.11	-0.49	-0.10	-0.43
^{210}Pb	-0.31	0.08	0.24	-0.28	-0.08

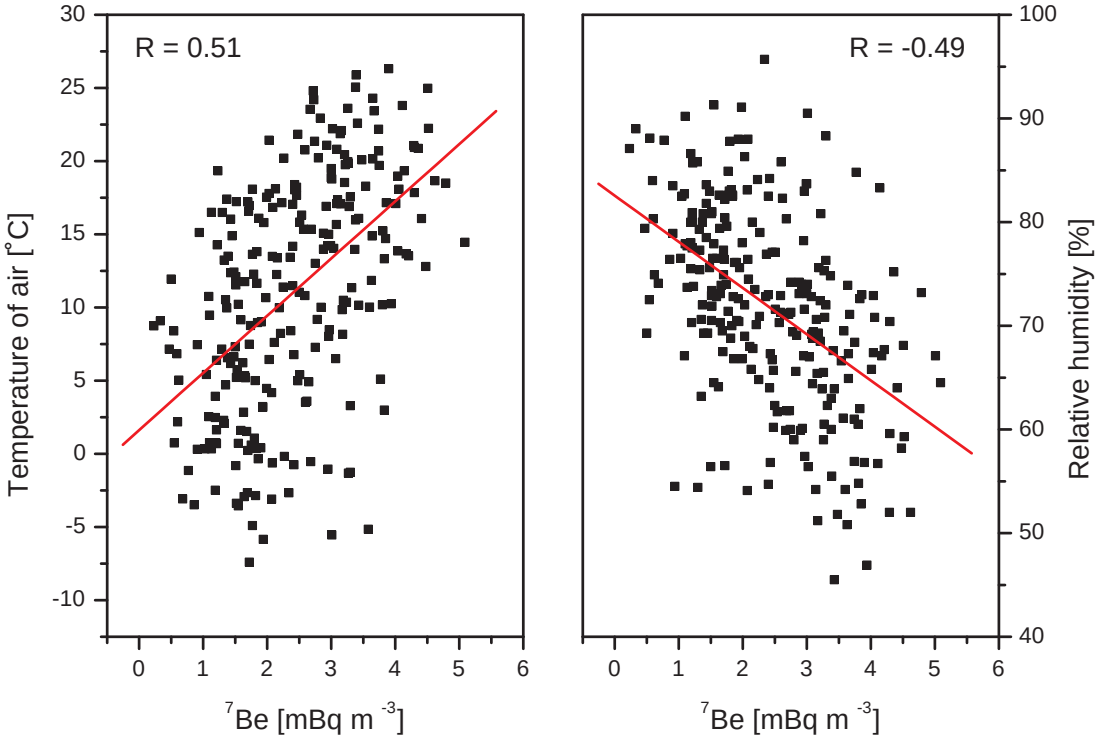

Figure 6.5: Correlation between ^{7}Be activity concentrations and temperature of air and relative humidity.

It has to be considered that the week measurement duration is quite long compared with the typical time scale of variations of meteorological parameters so that the correlation might be slightly better.

In order to quantify the temporal behavior of ^{7}Be and ^{210}Pb activity concentrations, we analyzed the harmonic components of the data (from October 2003 to September 2007). In Figure 6.6 are periodograms of ^{7}Be and ^{210}Pb together with periodograms of some meteorological parameters based on a Fourier analysis presented. The Danielson-Lanczos method was applied [Danielson42].

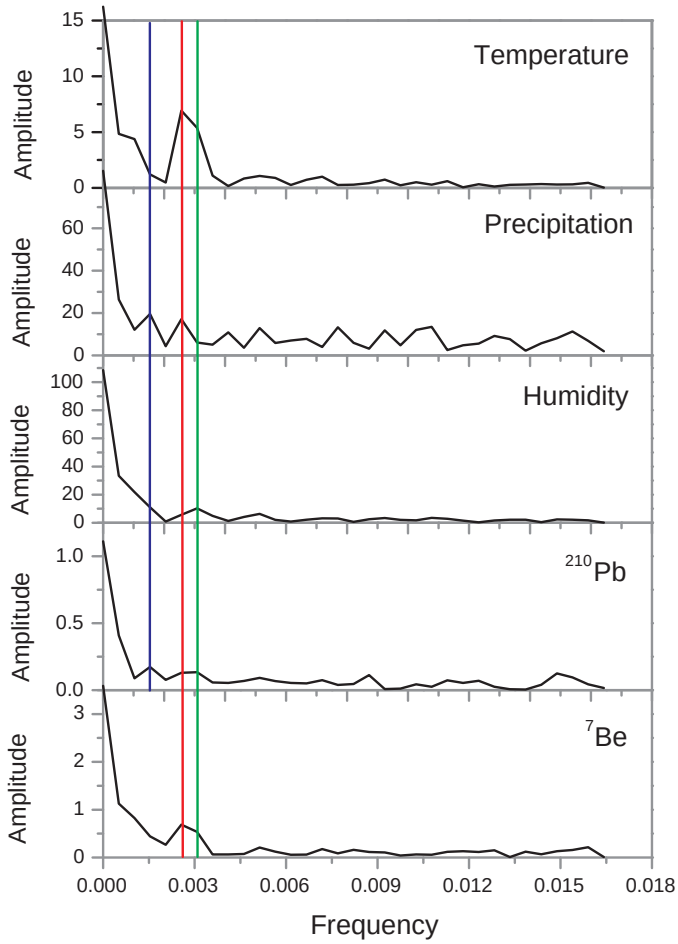

Figure 6.6: Periodograms of ^{7}Be, ^{210}Pb, relative humidity, monthly precipitation, and air temperature in Bratislava for time period from October 2003 to September 2007.

For ^{7}Be are observed two dominant frequencies 0.0026 and 0.0031, which correspond to periods of 390 and 325 days, respectively. This indicates that there are periodical phenomena with period approximately one year affecting the ^{7}Be activity concentrations in the ground level air. Fourier transformation of the temporal variations of air temperature, amount of precipitation, and humidity as well shows similar frequencies. Together with the linear correlation coefficient (Table 6.2), these observations indicate that the process of vertical mixing of the air induced by elevated temperature of air is responsible for approximately annual periodic component observed in the variation of ^{7}Be in the atmosphere.

Similar dominant frequencies corresponding to one-year period are observed in the case of ^{210}Pb activity concentrations.

6.1.3 ^{7}Be /^{210}Pb concentration ratio

In the absence of atmospheric motion and scavenging by precipitation, radionuclides ^{7}Be and ^{210}Pb would remain where they are produced, the upper troposphere and stratosphere and the ground level atmosphere over lands, respectively. But in the real atmosphere, ^{7}Be is mixed downward and ^{210}Pb upwards, and both are removed by precipitation. They are distributed by eddy mixing. The two radionuclides from different production processes are mixed well in the northern free troposphere air mass due to relatively long residence time of sub-micrometer particles.

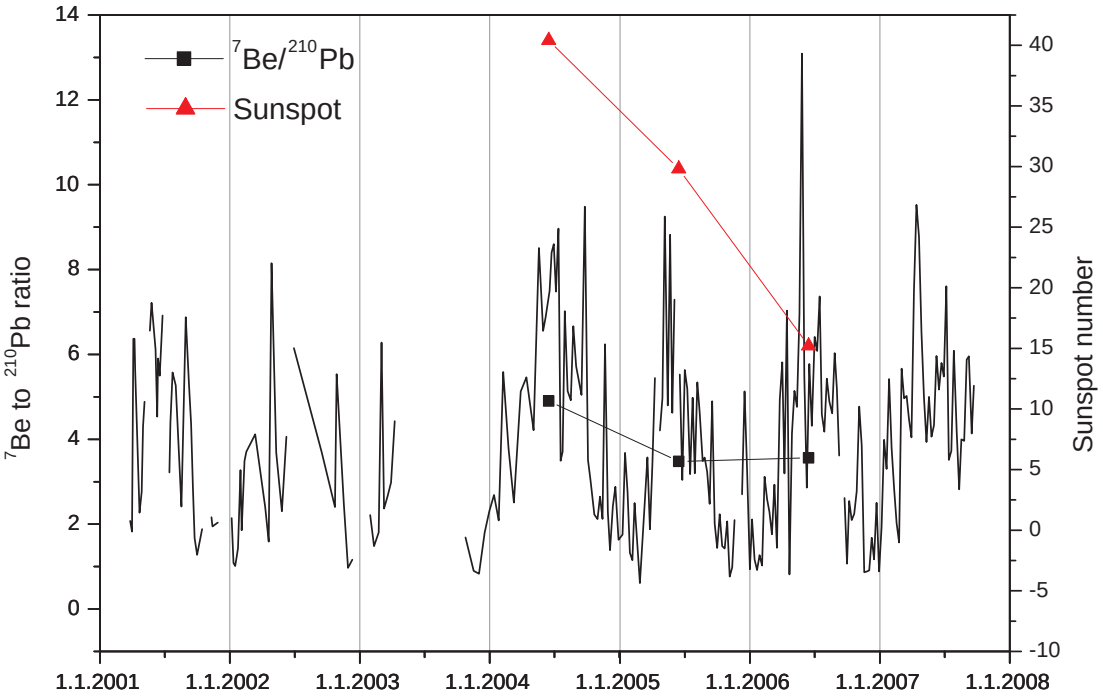

Figure 6.7: Temporal variations of ^{7}Be/^{210}Pb concentration ratio and annual averages (black) of ratios are compared to annual average sunspot numbers (red) for years 2004 - 2006.

Ratio of ^{7}Be and ^{210}Pb, due to their different origin, should depend on the altitude from which the air was transported, on continental influences and on removal processes. Changes in ^{7}Be/^{210}Pb with time and space reflect both vertical and horizontal transport in the atmosphere. In this way the ratio serves as the parameter of the air masses transport history [Todorovic05]. Over continents, seasonal variation in the stability of the atmosphere has a dominant influence on the ^{7}Be/^{210}Pb ratio. Surface heating in the summer increases convective mixing, which reduces ^{210}Pb in surface air by mixing it trough a larger volume and simul-

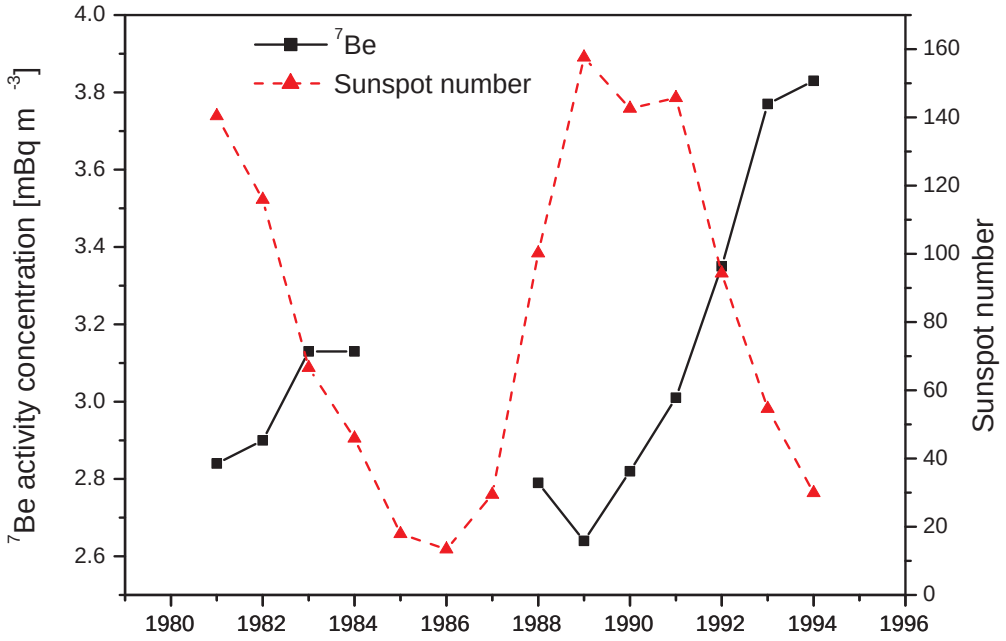

Figure 6.8: Temporal variations of annual average activity concentrations of ^{7}Be (black) and annual average sunspot numbers (red) for years 1981 - 1994.

taneously increases the transport of ^{7}Be to the surface. Winter stability tends to isolate surface air from the ^{7}Be source and keep ^{222}Rn and ^{210}Pb near the Earth surface. High ratio indicates intrusions of air mass from high latitudes, low value stands for surface air.

The values of ^{7}Be/^{210}Pb concentration ratio varied from 0.98 to 7.88 exhibiting the summer maxims and winter minimums as shown in Figure 6.7. The spring peak values indicate stratospheric intrusions bringing air rich for cosmogenic nuclides from upper atmospheric layers.

One of the causes of inter-annual variation of ^{7}Be/^{210}Pb ratios is that ^{7}Be production, depending on sun activity, shows a typical change according the 11-year solar cycle, whereas ^{210}Pb production shows no inter-annual change. As can be seen in Figure 6.7 the expected inverse correlation with the index of sunspot number is not observed. But period of three years is short for more reliable conclusions. Figure 6.8 obviously describes the inverse relation between the ^{7}Be activity concentration in the atmosphere and the sunspot number index. The period 1981 - 1994 covers the end of 21^{st} solar cycle and almost whole 22^{nd} solar cycle. The ^{7}Be data originates from the past study at our department [Ďurana96] and the sunspot numbers were taken from the National Geophysical Data Center [NGDC].

6.1.4 Tropopause height effect

The average values of tropopause height show certain variations with maximum in summer and minimum in winter. The data of tropopause height were supplied by the Slovak Hydrometeorological Institute. From Figure 6.9 is the relation to the ^{7}Be concentrations in atmospheric aerosols obvious. The changes of radioactivity correlate with the changes in the height of tropopause with a correlation coefficient of 0.35 for monthly average values from December 2003 to December 2006.

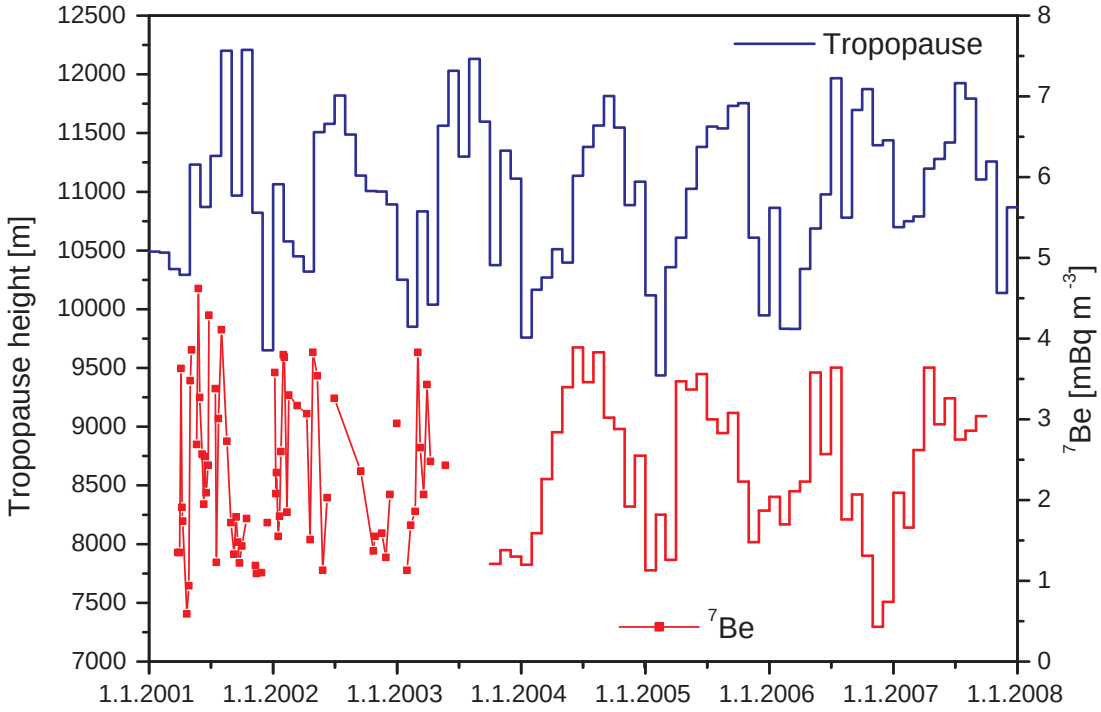

Figure 6.9: Variations of month average values of tropopause height and of ^{7}Be concentrations in the atmosphere from 2001 to 2007.

The similar result was observed by Todorovic [Todorovic97] in years 1968-1971, but instead of ^{7}Be the concentrations of ^{137}Cs were discussed. The increase in tropopause height during spring and early summer due to heating of the Earth's surface enhances the exchange of air masses from the stratosphere to troposphere. The falling of radioactive debris containing ^{137}Cs from the stratosphere into troposphere is a process occurring during the changes in tropopause height and not an immediate event connected with the height itself. The variations of stratospheric long-lived radionuclides follow the changes in tropopause height with a certain delay due to meteorological conditions in the troposphere and to the relative position of the sampling location regarding the point of stratospheric break through

into the troposphere [Todorovic97]. The same considerations could by applied also to ^{7}Be since the cosmogenic radionuclides originate from the stratosphere. Nowadays is the seasonal pattern of ^{137}Cs insensible. After the nuclear-test-ban treaty in 1963, which banned nuclear tests in the atmosphere, underwater and in space, almost all stratospheric nuclear debris was decayed and/or removed from its reservoir.

There are different theories on the dynamics of the exchange of air masses between troposphere and stratosphere. One of them considers these exchanges as connected with the so-called breaks in tropopause with the streams created on the breaking points. Another model connects the phenomenon with seasonal variations in tropopause height [Mahover83]. As can be seen in Figure 6.9, during the winter 2006 (November - December) were the lowest concentrations of ^{7}Be measured. At the same time, with a certain delay (January - March 2007), were relatively high levels of tropopause height observed. The tropopause have not fallen on usual level, the air masses from the stratosphere were not transferred downwards and therefore the level of cosmogenic radionuclides decreased rapidly.

6.2 Radioactivity in precipitation

Although was the sampling of precipitations started in June 2004, the reasonable results of activity concentration in rainwater and depositional fluxes are available since the July 2005. The one year period was needed for improvement of the sampling technique and the treatment of the samples collected. Also additional measurements were performed, in order to evaluate all influencing factors. Detailed information can be found in Section 5.1.

6.2.1 Activity concentration

The total activity of a radionuclide in precipitation depends on the mass of aerosol particles that scavenged and the volume of rainwater in which it is accumulated. The combination of these factors results in the large variability of the radionuclide concentrations observed. The results of ^{7}Be, ^{210}Pb, ^{137}Cs, and ^{40}K activity concentrations in precipitation are presented in Table 6.3. Further details are in Appendix B.

The ^{7}Be content in the rainwater can provide information on cloud thickness and height. For a cloud located at height above 1-2 km the concentration of ^{7}Be in the precipitation sample is significantly greater than for a cloud located below this height where is the ^{7}Be atmospheric concentration quite small [Talpos97].

No significant correlation between activity concentrations and amount of precipitation was found (Table 6.4). The reason of this observation may be that not the single event samples but the accumulated monthly precipitation samples were analyzed in our measurements. However, the decreasing trend of activity concentration with increasing precipitation amount is obvious as can be seen in Figure

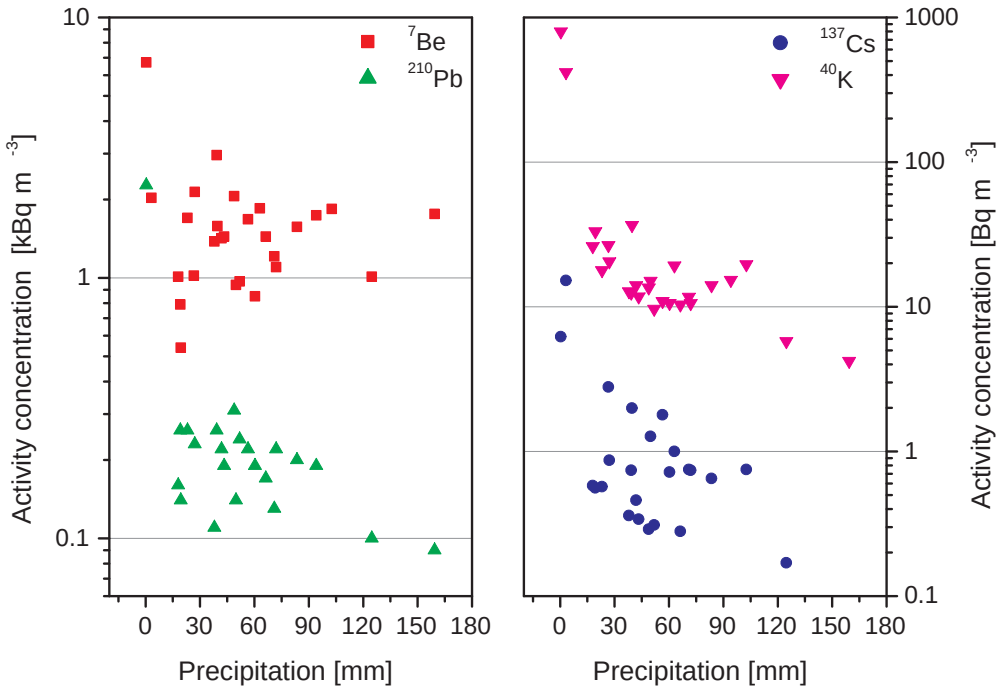

Figure 6.10: Decrease of radionuclides activity concentrations with the increased amount of precipitation.

6.10.

Although, we did not realized the measurements of sequential samplings of single precipitation events, there are several investigations showing that the precipitation scavenging effectiveness is decreasing during a precipitation event. ^{7}Be activity concentration decreased by 2.5-3 times between the first and the second part of the event, while ^{137}Cs activity concentrations decreased by 3-7 times, respectively [Ioannidou06]. Knies *et al.* observed correlation of ^{7}Be, ^{10}Be, and ^{36}Cl trough a single precipitation event with decrease from high values at the beginning to lower values at the end of an event [Knies94]. These observations may be explained by following. The raindrops remove the major amount of aerosol particles together with radionuclides attached in the first part of precipitation event. And not only the additional increase in the rainfall will not result in an additional increase of radionuclide concentration but also further rainwater dilutes airborne activity in the sample. Generally, the concept of the concentration should be used with careful consideration on the factors determining it.

The scavenging mechanism of atmospheric aerosols depends on the precipitation rate and precipitation type, whether it is rain or snow. Generally are the snowfall events more effective in respect of rainfall events of the same precipitation rate [Ioannidou06].

Table 6.3: Number of samples (NS) analyzed, ranges, averages, medians, and standard deviations of ^{7}Be, ^{210}Pb [kBq m^{-3}], ^{137}Cs, and^{40}K [Bq m^{-3}] activity concentrations in precipitation for the period July 2005 - September 2007 in Bratislava

	NS	Range	Average	Median	SD
^{7}Be	27	0.54 - 6.72	1.66 ± 0.06	1.44	1.14
^{210}Pb	27	0.09 - 2.27	0.27 ± 0.22	0.19	0.41
^{137}Cs	24	0.17 - 15.21	1.64 ± 0.55	0.73	3.15
^{40}K	26	4.2 - 798.9	61.5 ± 16.2	14.1	169.9

Table 6.4: Correlation coefficients between the total monthly amount of precipitation and concentrations of radionuclides

	Precipitation	^{7}Be	^{210}Pb	^{137}Cs	^{40}K
Precipitation	1.00	-0.23	-0.39	-0.47	-0.43
^{7}Be		1.00	0.92	0.37	0.83
^{210}Pb			1.00	0.95	0.99
^{137}Cs				1.00	0.71
^{40}K					1.00

High correlation was found among the activity concentrations of individual radionuclides. This observation suggests similar behavior of aerosol particles carrying the radionuclides. On the other hand were low correlation coefficients (0.41 and -0.12, respectively) found between activity concentrations of ^{7}Be and ^{210}Pb in precipitation and in the atmosphere. This indicates low importance of the radionuclide concentration in the atmosphere to the scavenging efficiency.

6.2.2 Deposition

Monthly wet depositions of ^{7}Be, ^{210}Pb, ^{137}Cs, and ^{40}K in Bratislava are plotted in Figure 6.11, together with the total monthly precipitation amount. Monthly wet depositions of ^{7}Be and ^{210}Pb ranged from 2.8 to 279.8 Bq m^{-2} and from 0.9 to 17.8 Bq m^{-2}, respectively. Simultaneously the ^{137}Cs and ^{40}K depositions in precipitation varied from 2.5 to 101.0 and from 328 to 1987 mBq m^{-2}, respectively. Table 6.5 summarizes the ^{7}Be, ^{210}Pb, ^{137}Cs, and ^{40}K monthly depositions for the investigated period. The detail information about the data are given in Appendix B.

Monthly wet depositions of radionuclides are relatively highly correlated with total monthly precipitation. Table 6.6 presents the correlation coefficients. Figure

Table 6.5: Number of samples (NS) analyzed, ranges, averages, medians, and standard deviations of ^{7}Be, ^{210}Pb [Bq m^{-2}], ^{137}Cs, and ^{40}K [mBq m^{-2}] monthly depositions for the period July 2005 - September 2007 in Bratislava

	NS	Range	Average	Median	SD
^{7}Be	27	2.75 - 279.8	79.4 ± 1.7	62.6	61.9
^{210}Pb	27	0.93 - 17.8	7.92 ± 0.30	7.17	4.58
^{137}Cs	24	2.54 - 101.0	38.1 ± 11.5	26.4	27.5
^{40}K	26	328 - 1987	794 ± 204	667	399

Table 6.6: Correlation coefficients between the total monthly amount of precipitation and monthly depositions of radionuclides

	Precipitation	^{7}Be	^{210}Pb	^{137}Cs	^{40}K
Precipitation	1.00	0.91	0.68	0.31	0.33
^{7}Be		1.00	0.75	0.36	0.39
^{210}Pb			1.00	0.38	0.54
^{137}Cs				1.00	0.63
^{40}K					1.00

6.12 shows the relation between monthly deposition of ^{7}Be and ^{210}Pb and monthly precipitation amount. Also ^{7}Be and ^{210}Pb monthly depositions are significantly correlated with each other. Therefore, it can by stated that the two radionuclides are deposited by similar removal processes, mainly by wet deposition. The direct proportion to the local precipitation amount was observed also in the literature [Brown89], [Ioannidou06].

Depositions of ^{137}Cs and ^{40}K have a lower dependency on the monthly precipitation. Even lower values of correlation coefficients for ^{137}Cs and^{40}K (-0.054 and 0.059) were observed in Japan [Ueno03]. Rosner *et al.* [Rosner96] estimated the ^{137}Cs deposition dry-to-total ratio of 0.65. Also Ioannidou and Papastefanou [Ioannidou06] reported the fraction of dry-to-total deposition of ^{137}Cs 3-4 times higher than that of ^{7}Be. Ueno *et al.* deduced that the dry deposition is dominant for larger particles to which are these radionuclides mostly attached. Nowadays most of ^{137}Cs in the atmosphere comes from the surface soil resuspension after the Chernobyl fallout. Radionuclide ^{40}K is soil derived.

The annual total wet-depositions of ^{7}Be,^{210}Pb, ^{137}Cs, and ^{40}K in 2006 are 806.9, 81.7 Bq m^{-2}, 257.5, and 7858.8 mBq m^{-2}, respectively. In Greece the annual ^{7}Be wet-deposition ranged from 457.9 to 1164.1 Bq m^{-2} in the years 1987-1992 [Ioannidou06]. The annual ^{7}Be depositions in Tsukuba in 2000 and 2001, and

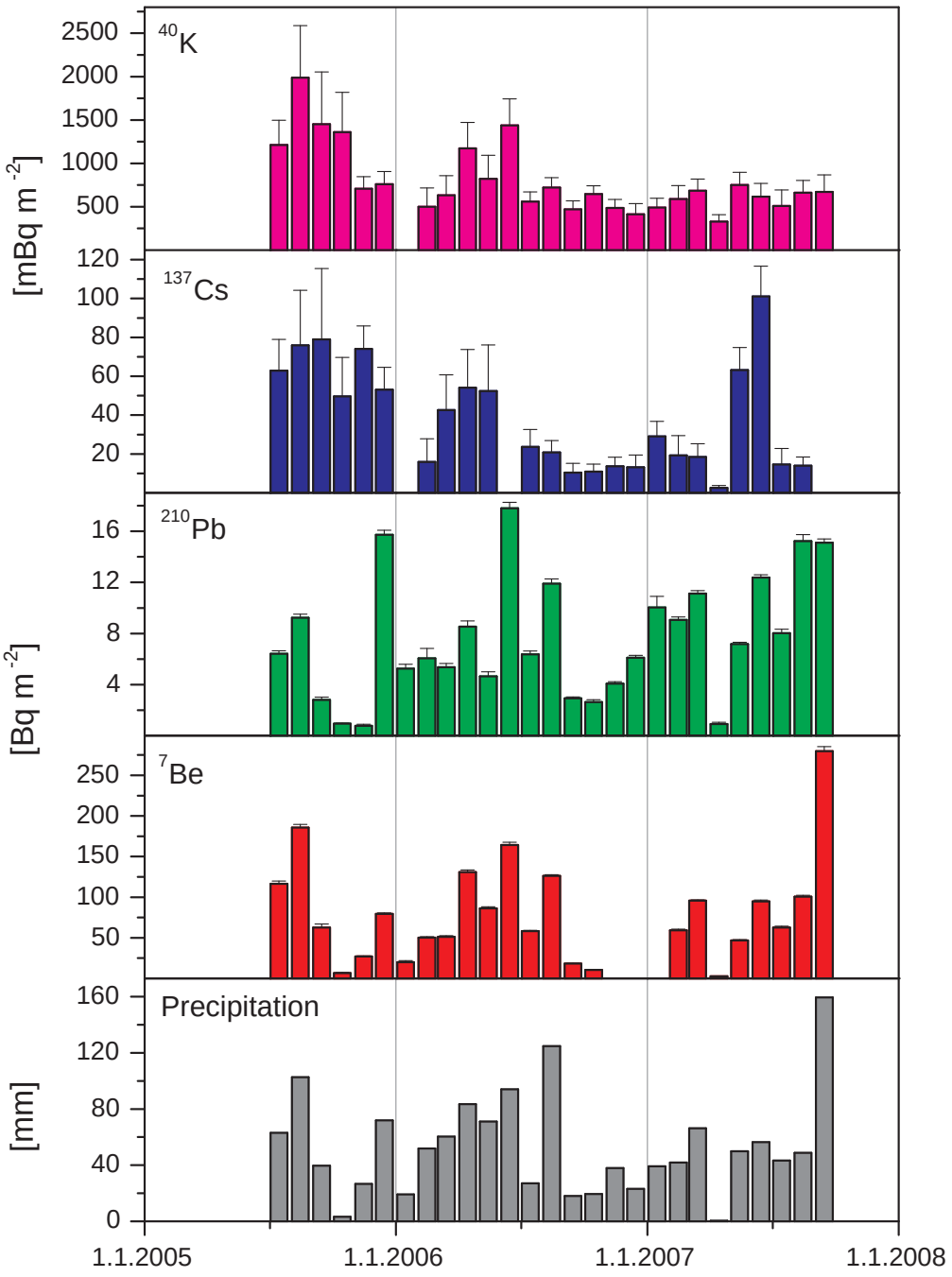

Figure 6.11: Monthly depositions of ^{7}Be, ^{210}Pb, ^{137}Cs, and ^{40}K and precipitation amount in Bratislava for the period July 2005 - September 2007.

Nagasaki in 2000 were 1324, 918, and 1474 Bq m^{-2}, respectively [Hirose04]. Ioannidou and Papastefanou measured ^{137}Cs in precipitations with the total annual

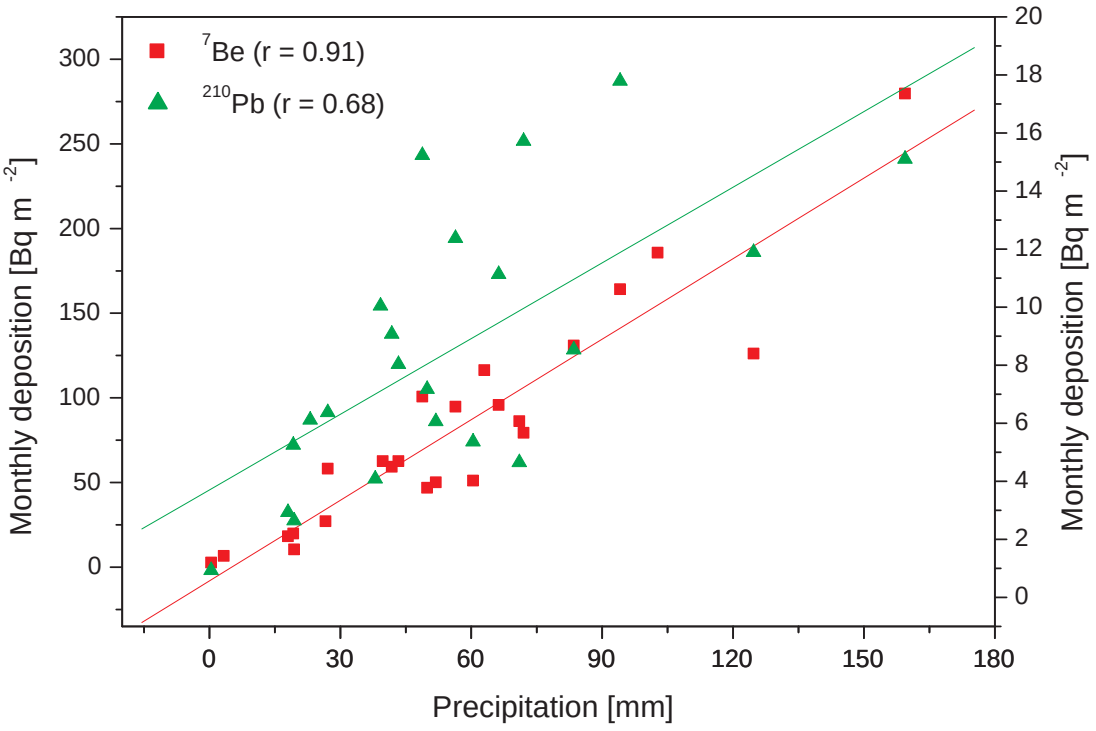

Figure 6.12: Positive correlation between monthly deposition of ^{7}Be and ^{210}Pb and monthly precipitation.

depositions ranging between 135.5 (1987) and 12.3 (1992) Bq m^{-2} [Ioannidou06]. Their data showed a significant decrease as expected for natural removal and radioactive decay and no new rerelease occurred for any reason. They estimated the removal half-life of ^{137}Cs to be 16 months. Therefore, the recent value of ^{137}Cs annual deposition is supposed to be at the level of few mBq m^{-2}, which corresponds to our result.

The estimated fractions of dry to total deposition of ^{7}Be indicate that the dry deposition is generally less than 10%. According Rosner *et al.* [Rosner96] the ratio of dry to total deposition of ^{7}Be ranged from 0.03 to 0.237 with the mean value of 0.114. Todd *et al.* [Todd89] reported a dry deposition of 8%, while Ioannidou and Papastefanou [Ioannidou06] less than 9.37%. Therefore we can assume that the dry deposition constitutes for approximately 10% of total deposition and the values of ^{7}Be annual total deposition for year 2006 is 888 Bq m^{-2}. This value is in the range of inter-annual variation of the annual ^{7}Be deposition in the mid-latitude region. If we consider similar deposition pattern of ^{210}Pb the corrected total (wet and dry) annual deposition for year 2006 is 89.9 Bq m^{-2}.

No pronounced seasonal variations of radionuclide depositions are observed

(Figure 6.11). It may be due to short monitoring period. But generally the highest values of depositions are coincident with the highest precipitation. Considering the low relation between ^{7}Be and ^{210}Pb activity concentrations in the atmosphere and in the monthly depositions (R = 0.28 and -0.12), it is evident that the amount of precipitation is the crucial factor controlling the deposition of radionuclides. Nevertheless, the concentrations of radionuclides in air were stated as significant factors dictating the amount removed by precipitation and deposited on to the Earth's surface [Ioannidou06], [Hirose04]. The discrepancy of our result among other observations, may be attributed to short investigation period.

6.3 Vertical concentration profile of ^{7}Be

The study of the mean vertical concentration profile and of the deposition of cosmogenic radionuclides provides information on the vertical transport in the stratosphere and troposphere and the processes of scavenging.

The one-dimensional model of the steady state vertical turbulent movement of the atmospheric air masses is applied. Vertical mixing in the troposphere and stratosphere, the radioactive decay, wet deposition as well as gravitational sedimentation are physical processes considered in the model. The U.S. standard average atmospheric model with the relative vertical distribution of air temperature, pressure, and density is used [USSA62]. Since the main part of the atmospheric mass (about 99%) is accumulated at an altitude of up to 30 km, the model is limited up to this height. Seasonal variations of the tropopause height during year are considered.

The parameters of the turbulent diffusion and washout are calculated using experimental data of the ^{7}Be monthly average activity concentrations in ground level air and the ^{7}Be depositional fluxes.

6.3.1 Diffusion of aerosol particles in the atmosphere

The equation that describes the vertical diffusion of the substance is a continuity equation:

$$\frac{\partial c}{\partial t} = -\vec{\nabla} \cdot \vec{j} + S - R \tag{6.2}$$

c is the substance concentration, $\vec{j}$ is the flux of the substance, S describes the generation, and R the removal of the substance. The total flux is the sum of laminar and turbulent component. Considering the laminar flow to be characterized by the flux $\vec{j_l} = \vec{u}c$ and turbulent $\vec{j_t} = K\vec{\nabla}c$ then Equation 6.2 transforms to

$$\frac{\partial c}{\partial t} = -\vec{\nabla} \cdot (\vec{j_l} + \vec{j_t}) + S - R = -\vec{\nabla} \cdot (\vec{u}c + K\vec{\nabla}c) + S - R \tag{6.3}$$

Assuming the transport in horizontal plane to be negligible ($\frac{\partial c}{\partial x} \approx \frac{\partial c}{\partial y} \ll \frac{\partial c}{\partial z}$), then Equation 6.3 is simplified to one-dimensional partial differential equation

$$\frac{\partial c}{\partial t} = -\frac{\partial u_z c}{\partial z} + \frac{\partial}{\partial z}\Big(K\frac{\partial c}{\partial z}\Big) + S - R \tag{6.4}$$

If density ρ of the carrier medium (in our case it is air) is changed with the altitude, then this fact has to be considered. The term of sedimentation (v is the gravitational sedimentation velocity) is not accounted, while in the process of sedimentation the carrier medium is not moving and only the substance is falling down.

Two processes of ^{7}Be removal are occurring, the radioactive decay and deposition by washout characterized by $-\lambda c$ and $-\sigma c$, respectively.

$$\frac{\partial c}{\partial t} = -\frac{c}{\rho}\frac{\partial u_z \rho}{\partial z} - \frac{\partial (u_z - v)c}{\partial z} + \frac{\partial}{\partial z}\Big(K\rho\frac{\partial (c/\rho)}{\partial z}\Big) - (\lambda + \sigma)c + S \tag{6.5}$$

In long-term time scale (month) one can assume the values of u, S, σ, v, K, and ρ to be stable and the solution of 6.5 goes in limitation close to stationary

$$0 = -\frac{c}{\rho}\frac{\partial u_z \rho}{\partial z} - \frac{\partial (u_z - v)c}{\partial z} + \frac{\partial}{\partial z}\Big(K\rho\frac{\partial (c/\rho)}{\partial z}\Big) - (\lambda + \sigma)c + S \tag{6.6}$$

In the monthly average can be the velocity $\vec{u}$ considered to be zero. Therefore the first term in 6.6 is eliminated

$$0 = \frac{\partial vc}{\partial z} + \frac{\partial}{\partial z}\Big(K\rho\frac{\partial (c/\rho)}{\partial z}\Big) - (\lambda + \sigma)c + S \tag{6.7}$$

Boundary conditions

Since the Equation 6.7 is the ordinary differential equation of the second order, two boundary conditions are required for the sole solution. The first boundary condition is the assumption that there is an equilibrium between formation and radioactive decay of ^{7}Be in high altitudes (z = 30 km).

$$-\lambda c(30) + q(30) = 0 \tag{6.8}$$

The second boundary condition is the assumption that the turbulent component of substance velocity at the ground level (z = 0)is zero

$$K(0)\rho(0)\frac{\partial (c/\rho)}{\partial z}\Big|_{z=0} = 0 \tag{6.9}$$

Parameterization of individual terms

The v stands for the gravitational sedimentation velocity or velocity of dry deposition. For very small spherical objects which are falling down in a continuous

viscous fluid under the assumption of ideal laminar flow from the Navier-Stokes equations follows the Stokes law

$$v = \frac{2}{9} r^2 g \frac{\rho_p - \rho_0}{\eta} \tag{6.10}$$

where r is the radius of the particle, g is the gravitational acceleration, ρ_p is the density of the particles, ρ_0 is the density of the fluid (in our case it is air), and η is the fluid (air) viscosity.

According the standard average atmospheric model is the air density exponentially decreasing with increasing altitude. By solving the simplified stationary Navier-Stokes equations can be the air density described with

$$\rho(z) = \rho_0 e^{-\frac{Mg}{kT} z} \tag{6.11}$$

where M is the weight of air molecules, g is the gravitational acceleration, k is the Boltzmann constant, and T is the average temperature. This equation is describing the ideal isothermal atmosphere but for our purpose is its accuracy sufficient.

Viscosity η is a function of the temperature, as can be seen in the following Equation:

$$\eta = \eta_0 \frac{T_0 + C}{T_z + C} \Big(\frac{T(z)}{T_0} \Big)^{\frac{3}{2}} \tag{6.12}$$

where $C = 120$ K is the air constant and $\eta_0 = 18.27 \times 10^{-6}$ Pa s is the reference viscosity at the reference temperature $T_0 = 291.25$ K. Therefore, it is necessary to know the vertical profile of the temperature for the sedimentation velocity determination.

Turbulent diffusion coefficient

Turbulent diffusion is not yet satisfactory described phenomenon. For its quantitative characterization is often the molecular diffusion analogy used where is the coefficient of molecular diffusion replaced by the macroscopic analogue. It indicates that K is a dynamical function of altitude. Taking into account the recent works [Jasiulionis05] and [Talpos97] we decided to characterize the coefficient of turbulent diffusion by following form

$$K = \begin{cases} K_0(\frac{9}{10} z + \frac{9}{10}), z \in \langle 0, 1) \\ K_0, z \in \langle 1, z_T) \\ \frac{K_0}{10}, z \geq z_T \end{cases} \tag{6.13}$$

The parameter z_T [km] stands for the tropopause height, which is varying with typical seasonal pattern. The tropopause level moves upward in summer season, and this upward movement introduces stratospheric air masses into the troposphere.

Since we can measure the ^{7}Be activity concentration at the ground level $c_{exp}(0)$ we are able to determine the value of turbulent diffusion coefficient K using a simple numerical method. The K is determined by the constant K_0. The coefficient K_0 is varied with particular step until is the calculated value $c_{cal}(0)$ corresponding with the experimentally determined value of $c_{exp}(0)$.

Scavenging coefficient

Scavenging of aerosols by precipitation is characterized by the quantity σ. Scavenging efficiency σ is a function of height. It was assumed to be constant and non-zero below the altitude z_P, what is the average height of the precipitation clouds and up to this altitude is the air intensively scavenged by rain. Above this height is σ equal to zero. The value of σ can be determined using the activity concentration of ^{7}Be in the precipitation according the following model.

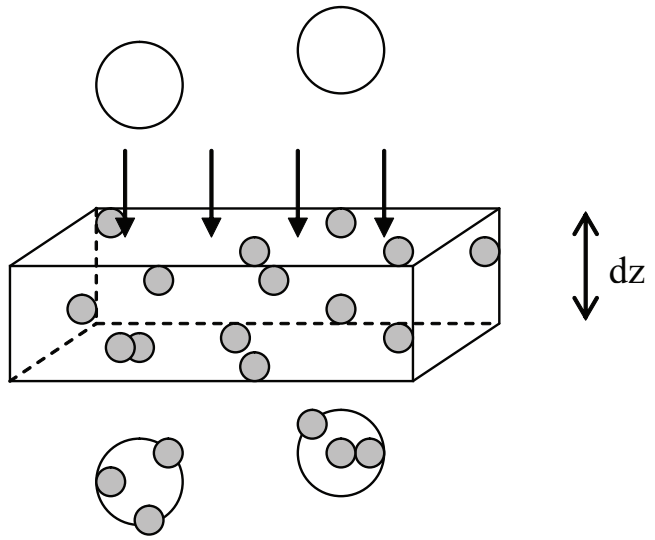

Figure 6.13: Scavenging of aerosol particles by raindrops.

We suppose that aerosol particles as well as raindrops are of spherical shape with the radius r_A and r_D, respectively. If $c_A(z)$ is concentration of aerosol particles in height z, then in the volume element of air with base S and width dz is present $c_A(z)Sdz$ of aerosol particles (Figure 6.13). The rain drops passing trough the volume element are scavenging the particles present with the efficiency . The raindrop-aerosol collision efficiency takes into account the contribution of the three removal mechanisms: Brownian diffusion, interception, and inertial impaction. We are using the parameterization according to Slinn [Slin83] which states the value of α approximately 10%.

The scavenging probability is a product of geometrical probability and efficiency α. The geometrical probability of collision of one single aerosol particle with a raindrop in the volume of thickness dz is equal to ratio of surfaces $\pi(r_D + r_A)^2$ and S. The number of collisions is proportional to aerosol concentration and the

number of raindrops. The volume of one raindrop is $V_0 = \frac{4}{3}\pi r_D^3$ and the volume of precipitation is V, hence the number of raindrops is ratio $\frac{V}{V_0}$. Thereafter it can be the number of aerosol particles attached to drop on the path dz calculated by

$$dN_A = \alpha \frac{\pi(r_D + r_A)^2}{S} c_A S dz \frac{3V}{4\pi r_D^3} = \alpha \frac{3V}{4} \frac{(r_D + r_A)^2}{r_D^3} c_A dz \tag{6.14}$$

If is in the volume element dV aerosol concentration c_A and ^{7}Be concentration c, then on one aerosol particle is $\frac{c}{c_A}$ atoms of ^{7}Be attached and the Equation 6.14 is transformed to

$$dN = dN_A \frac{c}{c_A} = \alpha \frac{3V}{4} \frac{(r_D + r_A)^2}{r_D^3} c dz \tag{6.15}$$

Assuming the constant radius of aerosol particles and raindrops within all altitudes, then number of ^{7}Be in precipitation will be

$$N = \alpha \frac{3V}{4} \frac{(r_D + r_A)^2}{r_D^3} \int_0^{z_p} c dz \tag{6.16}$$

Studying the temporal change of ^{7}Be activity concentration in air we can draw following equation

$$\frac{dc}{dt} = -\alpha \frac{3h}{4\tau} \frac{(r_D + r_A)^2}{r_D^3} c \tag{6.17}$$

where h is the precipitation height [mm]. The term

$$\sigma = \alpha \frac{3V}{4} \frac{(r_D + r_A)^2}{r_D^3} \tag{6.18}$$

in Equation 6.16 corresponds to the scavenging coefficient σ. This parameter represents the scavenging rate of particular precipitation event. Comparing Equations 6.16 and 6.18 we can calculate the scavenging coefficient σ according the following formula

$$\sigma = \frac{N}{\tau S \int_0^{z_p} c dz} \tag{6.19}$$

where N is the number of ^{7}Be atoms in the precipitation sample collected on surface S within time period τ, and z_P is the height of clouds.

For the calculation of the scavenging coefficient σ we use the recurrent method. We choose a value of σ and using Equation 6.7 we calculate coefficient K. The byproduct is the vertical profile $c(z)$. The value of σ and vertical profile $c(z)$ are used in Equation 6.19 and compared to experimentally determined deposition. The procedure is repeated until is the calculated deposition similar to the one measured.

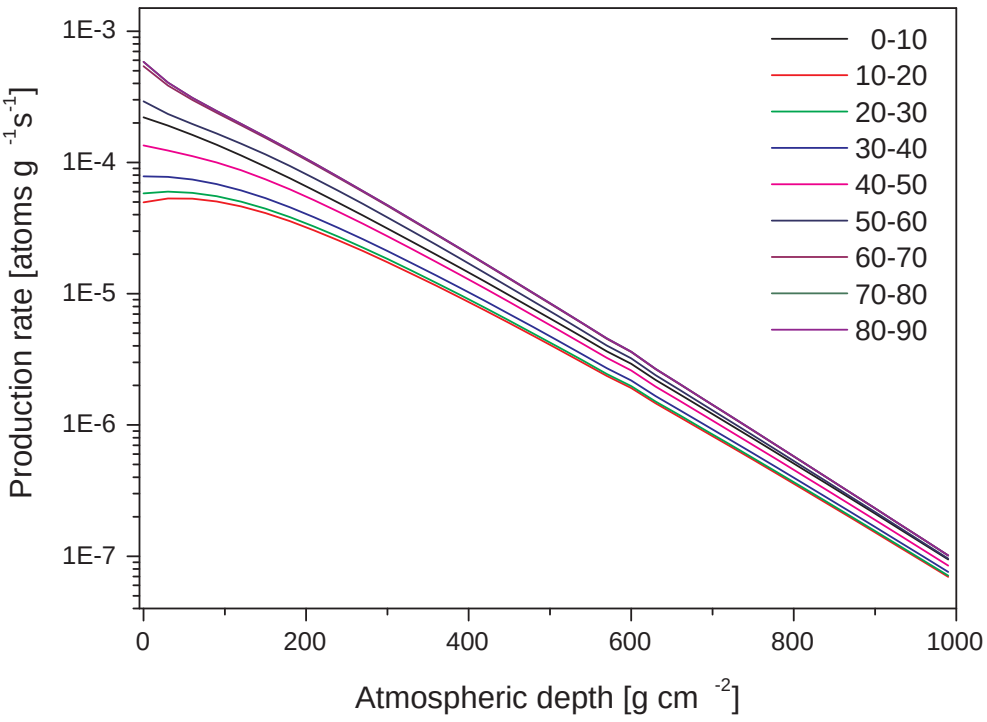

Figure 6.14: Depth dependent latitudinal production rates of ^{7}Be in the Earth's atmosphere. Each line represents a latitude interval of 10°. The production rate decreases with decreasing latitude for all depths in the atmosphere [Masarik99].

Numerical treatment

Numerical methods commonly used for the solving of the non-linear ordinary differential equations of the second grade can not be applied to our problem since they converge to the solution very slowly. We used the procedure that assumes the coefficients in Equation 6.7 to be constant within the division intervals. On this condition was Equation 6.7 solved analytically and integration constants of partial solutions were calculated in order to assure continuity of the solution as well as the continuity of its first derivative.

6.3.2 Results of turbulent diffusion and scavenging coefficients

The coefficients of turbulent diffusion K and washout σ were calculated from experimental data of ^{7}Be concentrations and depositions (Table 6.7). The differential equation system was applied. For calculations was the height of clouds z_P considered to be 4 km. According the literature we used the density of aerosol particles

ρ_P to be 1.5 g cm^{-3} [Kannosto06], and the size of aerosol particles r_A equal to 702 nm [Gründel04]. Since no measurements of precipitation rate are available, for the raindrop size r_D was constant value of 1 mm used. The data of tropopause height were supplied by the Slovak Hydrometeorological Institute. The ^{7}Be production rates for latitude interval 40-50° from Masarik and Beer [Masarik99] were used (Figure 6.14).

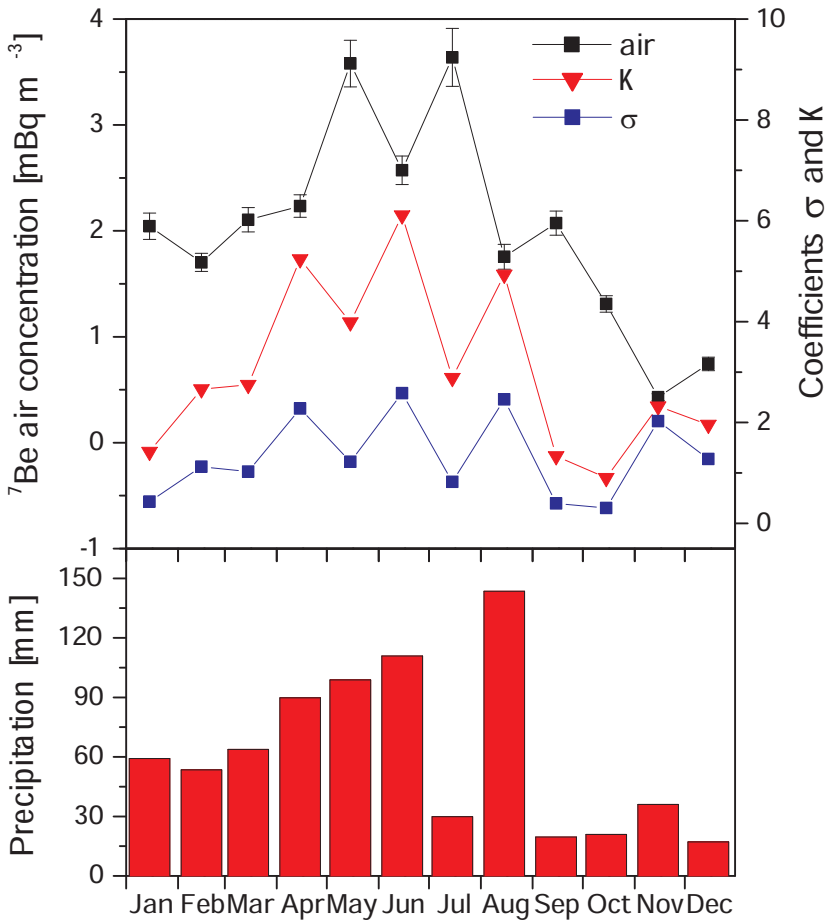

Figure 6.15: Temporal variations of ^{7}Be activity concentration measured in air, variations of monthly coefficient of the turbulent diffusion K and the washout coefficient σ determined by the model, and total monthly precipitation amounts in 2006.

The results are presented in Figure 6.15 and Table 6.8. Diffusion as well as the scavenging processes is affected by the seasonal variations of meteorological conditions. Our results are comparable to values of Jasiulionis and Wershofen [Jas05].

The low values of K are corresponding to relatively low atmospheric concentrations of ^{7}Be in months from September to March. The ^{7}Be activity concentration

Table 6.7: Monthly ^{7}Be activity concentration in ground level air and wet deposition, monthly average of tropopause height and total amount of precipitation in 2006

Month	Air conc. [mBq m^{-3}]	Deposition [Bq m^{-2}]	Tropopause [km]	Precipitation [mm]
January 2006	2.04	19.89	10.86	59.2
February 2006	1.70	50.15	9.83	53.5
March 2006	2.11	51.10	9.83	63.8
April 2006	2.23	130.88	10.34	89.8
May 2006	3.58	86.19	10.69	98.8
June 2006	2.57	164.17	10.98	110.9
July 2006	3.64	58.20	11.97	29.9
August 2006	1.76	126.12	10.78	143.5
September 2006	2.07	18.25	11.70	19.6
October 2006	1.31	10.47	11.87	20.9
November 2006	0.43	52.22	11.40	36.0
December 2006	0.74	39.29	11.44	17.1

Table 6.8: Monthly coefficients of the turbulent diffusion K and the washout σ.

Month	k_z $[m^2\ s^{-1}]$	σ $[\times 10^{-6}\ s^{-1}]$
January 2006	1.42	0.431
February 2006	2.66	1.125
March 2006	2.75	1.028
April 2006	5.24	2.278
May 2006	3.99	1.222
June 2006	6.11	2.583
July 2006	2.89	0.825
August 2006	4.94	2.458
September 2006	1.34	0.397
October 2006	0.90	0.306
November 2006	2.32	2.028
December 2006	1.96	1.278

in ground level air increases with increasing K, because the turbulent diffusion is more efficient, and with decreasing σ, because small values of scavenging efficiency determine a small number of aerosols scavenged by precipitation. A typical exam-

ple can by seen in August 2006, when high precipitation occurred. Although, the turbulent diffusion was very efficient, the precipitation scavenging reduced activity concentration by half. Unexpected, low value of K in July 2006 indicated the decrease of air concentrations, but low precipitation rate did not scavenged ^{7}Be out from the atmosphere and the activity concentration remained high.

6.3.3 Temporal variations of ^{7}Be vertical profile

The values of both the turbulent diffusion coefficient and the scavenging coefficient were used for the calculation of the ^{7}Be concentrations at different altitudes. In Figure 6.16 are ^{7}Be vertical profiles for each month of the year 2006 presented. The ^{7}Be activity concentrations were calculated in 10 m interval of altitude. As can be seen the activity concentrations are almost stable above the tropopause (9 - 12 km) in all seasons, but below this altitude are varying quite significantly.

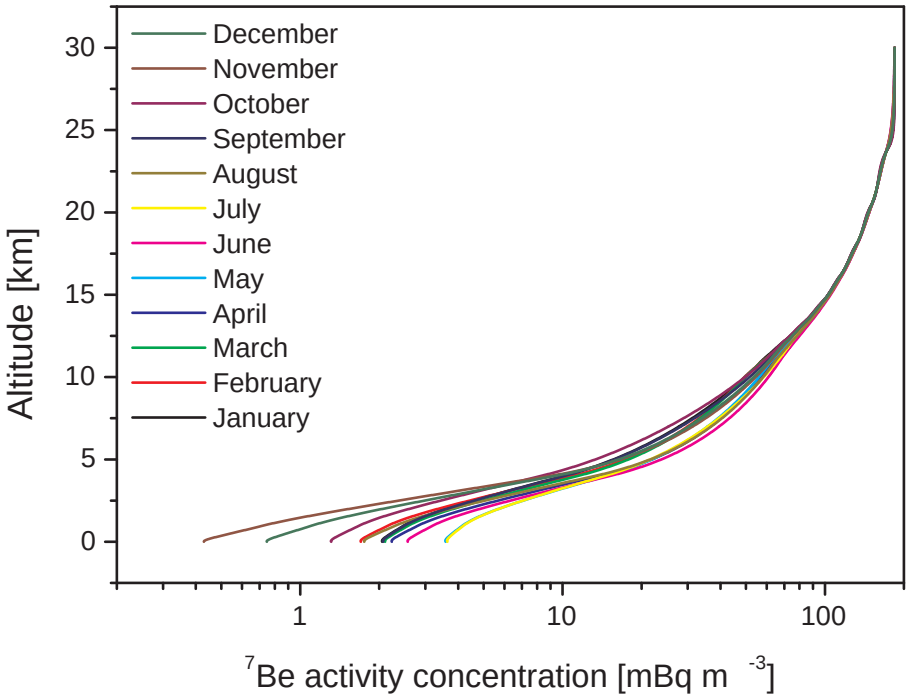

Figure 6.16: Vertical concentration profiles of ^{7}Be in the atmosphere up to 30 km of altitude for each month of year 2006.

The distribution of ^{7}Be activity concentrations evaluated using presented model are generally similar to the experimental results. Figure 6.17 presents the vertical concentration profiles of ^{7}Be up to the level of 15 km, measured by Kownacka [Kownacka01]. Between the modeled and measured values relatively good

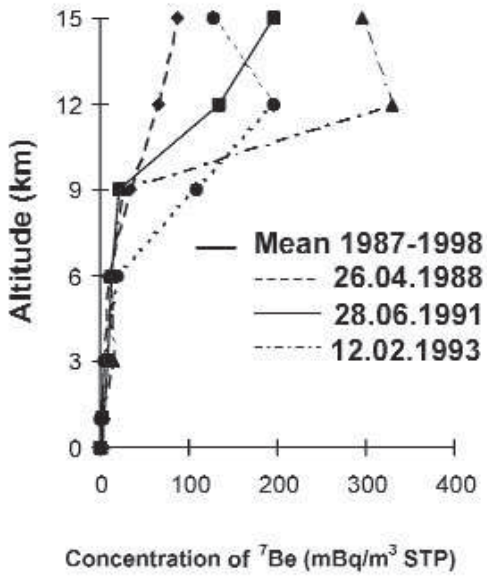

Figure 6.17: Vertical concentration profiles of ^{7}Be in the atmosphere [Kownacka01].

agreement is observed. The results obtained by the presented diffusion model are under preparation for journal publication.

6.4 Elemental content in atmospheric aerosols

In the year 2004 were 36 aerosol filter samples collected. From these we selected 16 samples for the INAA and AAS to evaluate the elemental contents in the atmospheric aerosols. A total of 30 elements were determined by the INAA at IBR-2 reactor in Dubna in total airborne particulate matter. Another six elements were determined using AAS (Cr was determined by both techniques) [Medveď98], [Medveď03]. These results were presented in following publications [Merešová06], [Merešová05-06], [Florek06], [Merešová07].

Observed data can be considered representative of the elemental concentrations in the atmospheric aerosol of Bratislava and are unique in Slovak Republic. For the first time such an extensive range of elements (Figure 6.18) were determined at a long-term scale. The results of descriptive statistics (min, max, median, average, standard deviation) applied to the experimental data are presented in Table 6.9. The complete data are presented in Appendix C.

Figure 6.19 shows the decreasing trend of air pollution by heavy metals in Bratislava since the year 1981. The emissions of Pb have decreased, reflecting the shift from leaded to unleaded gasoline. Since the 1^{st} of January 2001 it is mandatory to use unleaded gasoline with Pb concentration lower than 0.005 g l^{-1} [SR04]. The next reason of this decreasing trend is the decline of the industry production in the Slovak Republic after the year 1989, since the fuel burning processes in thermal

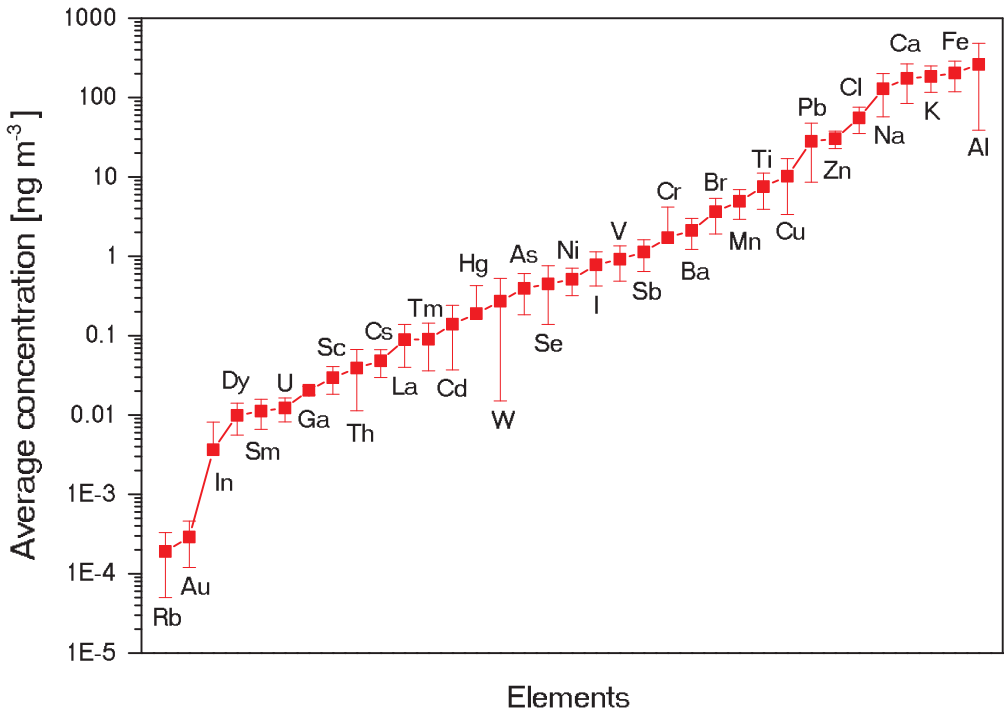

Figure 6.18: The range of average elemental concentrations in the Bratislava atmosphere in 2004. The error bars correspond to standard deviations of the measured data.

power plants and industrial activities are a major source of atmospheric pollution with heavy metals. Also the emissions of pollutants were reduced via application of stricter requirements in the environmental legislation, desulphurization of power plants, and introducing of more sophisticated technologies in smelters.

6.4.1 Crustal enrichment factors

The concept of enrichment factors (EF) was introduced by Rahn [Rahn71] to detect contributions of non-crustal sources on observed concentrations of elements. EF compares the ratio of the concentration of element $c(X)$ in question to that of a selected reference element $c(Al)$ in a sample, and the corresponding ratio in the average composition of the Earth's crust.

$$EF = \frac{(\frac{c(X)}{c(Al)})_{Sample}}{(\frac{c(X)}{c(Al)})_{Crust}} \tag{6.20}$$

Aluminum was used as a soils (crust) reference element. The average elemental concentrations in humus horizon of soil for Slovakia are used in the EF calculations [Čurlík99].

Table 6.9: Concentrations of elements [ng m^{-3}] in atmospheric aerosol

Element	Number of samples	Min	Max	Median	Average	Standard deviation
Na	16	59	308	104	129	72
Al	16	40	912	189	261	223
Cl	16	32	102	49	56	20
K	16	72	290	195	184	67
Ca	16	54	312	179	175	91
Sc	7	0.007	0.04	0.032	0.03	0.011
Ti	15	3.2	14.1	7.8	7.5	3.6
V	16	0.28	1.62	0.83	0.92	0.43
Cr	9	0.3	8.1	1.1	1.7	2.5
Mn	16	1.9	8.6	4.9	4.9	2
Fe	5	85	285	252	204	85
Ni	6	0.39	0.9	0.45	0.51	0.19
Cu	15	4	27	8	10	7
Zn	15	20	45	28	30	8
Ga	4	0.018	0.024	0.02	0.02	0.003
As	7	0.11	0.71	0.3	0.39	0.21
Se	7	0.13	1.01	0.42	0.45	0.31
Br	16	1.7	8.6	3.5	3.6	1.7
Rb	3	0.0001	0.0003	0.0001	0.0002	0.0001
Cd	14	0.02	0.4	0.11	0.14	0.1
In	14	0.0004	0.0149	0.001	0.0036	0.0045
Sb	7	0.5	1.9	1	1.1	0.5
I	16	0.28	1.65	0.66	0.78	0.36
Cs	6	0.03	0.072	0.045	0.048	0.018
Ba	15	0.7	3.8	2.1	2.1	0.9
La	6	0.038	0.166	0.085	0.089	0.049
Sm	7	0.002	0.016	0.012	0.011	0.005
Dy	14	0.002	0.016	0.01	0.01	0.004
Tm	6	0.025	0.144	0.098	0.09	0.054
W	7	0.05	0.82	0.22	0.27	0.26
Au	7	0.0001	0.0007	0.0002	0.0003	0.0002
Hg	6	0.01	0.56	0.06	0.19	0.24
Pb	15	10	81	22	28	20
Th	5	0.005	0.08	0.042	0.039	0.028
U	16	0.005	0.019	0.012	0.012	0.004

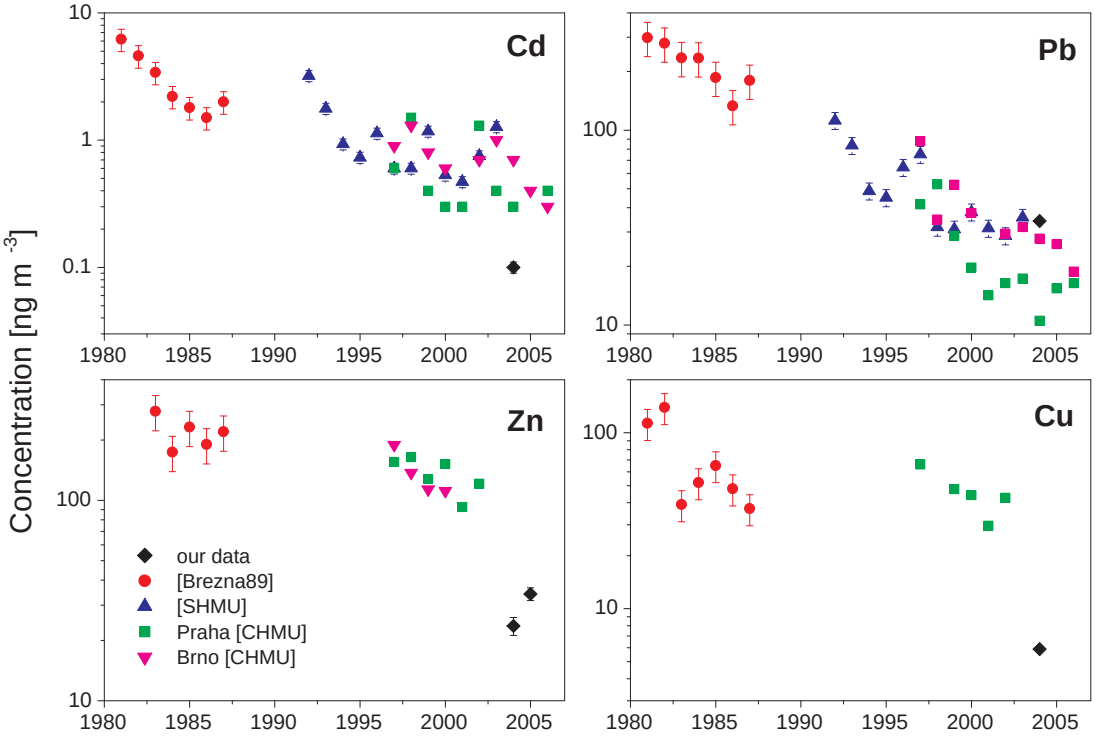

Figure 6.19: Temporal variation of atmospheric concentrations of Cd, Pb, Zn, and Cu in Bratislava, red - [Brežná89], blue - [SHMU], black - our data. For comparison are shown also elemental concentrations in Prague (green) and Brno (violet) [ČHMU].

Enrichment indicates natural votilization, marine sources and anthropogenic activities. Rahn [Rahn76] suggested classification criteria of EF: when EF < 7, then the air particulate is of crustal origin, and when EF > 10, it is of the anthropogenic one. Enrichment factors were calculated for 24 elements. The results are presented in Figure 6.20. The values of EF close to one indicate the soil origin of Ba, La, Th and U. Following Rahn's criteria, it can be concluded that Cu, Zn, As, Se, Cd, Sb, Hg, and Pb are of the anthropogenic origin.

Non-ferrous smelters are the sources of Cu, Zn, and Pb. Pb is emitted also in automotive exhausts. The largest source of airborne Cd in the environment, is the burning of fossil fuels such as coal or oil, and incineration of municipal waste materials. Cd may also be emitted into the air from zinc, lead, or copper smelters. The contamination by As is connected with the coal combustion, with nonferrous metal processing and pesticides utilization [Čurlík99]. The content of As in lignite mined in Handlova (the region of the Central Slovakia) is one of the highest in the world [Keegan06]. Se is a good tracer for coal combustion, mostly of brown coal or

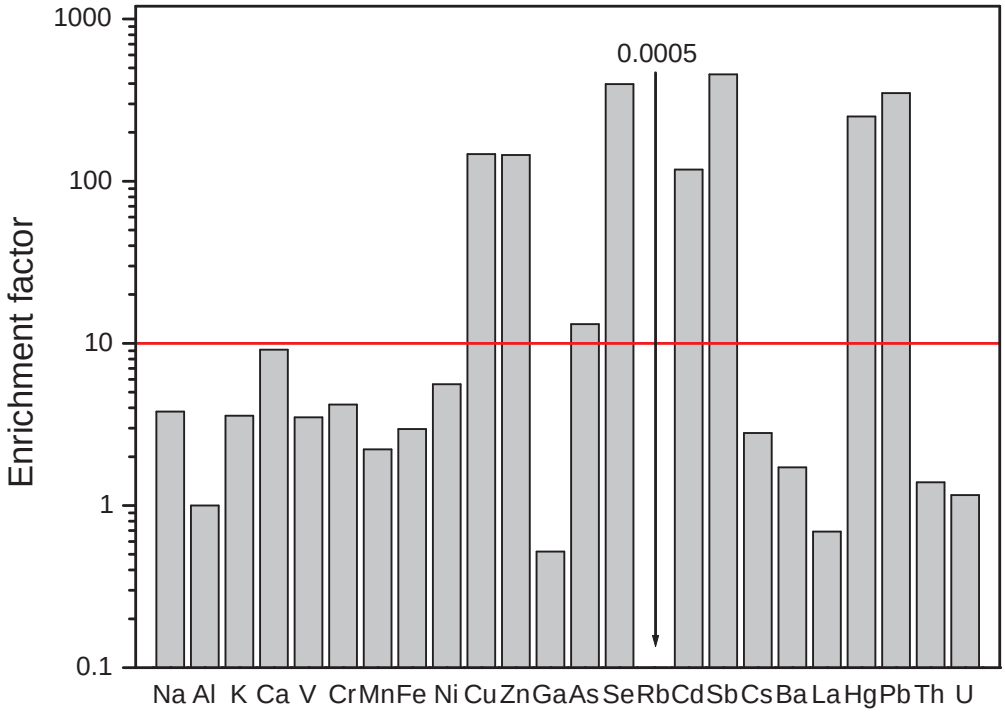

Figure 6.20: Enrichment factors for investigated elements, red line represents the Rahn's classification (EF = 10).

lignite. Ross estimated that more that 70% of the Se emissions from combustion of fossil fuels north of 30°N comes from coal [Ross85]. Se can be also accumulated in aerosols of marine origin [Čurlík99]. Other important sources of Se are non-ferrous smelters, refuse incineration and mining.

6.4.2 Seasonal variations

A seasonal variation in elemental concentration can be expected as a result of changes in emission rates of pollution sources, atmospheric transport processes and dispersion efficiency during the year. In order to study the seasonal elemental concentration variation, average concentration values were calculated for four periods: winter (December - February), spring (March - May), summer (June - August), and autumn (September - November).

Some of the elemental concentrations indicate seasonal variations over the year with elevated values in spring/summer season as shown in Figure 6.21. Most of these elements are soil derived (Al, Ca, Ti, Mn, Ba, U), although they may also be emitted as fly-ash from the combustion of coal, and as dust from other mineral-related activities. Only Cu was according to the EF classified as anthropogenic.

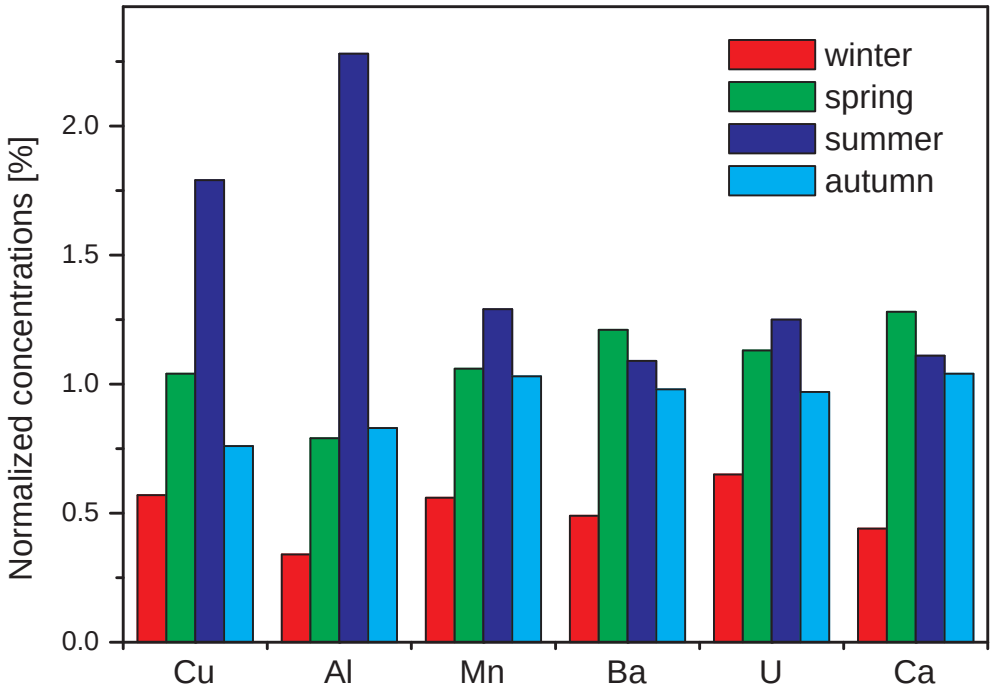

Figure 6.21: Seasonal average elemental concentrations of Cu, Al, Mn, Ba, U, and Ca in atmospheric aerosol in Bratislava during the year of 2004 normalized to the average concentration.

From these we can conclude that the temporal variations of these elements are not significantly influenced by human activities.

A correlation analysis with the meteorological parameters was performed (Table 6.10) in order to evaluate the influences. The concentrations of soil derived elements are correlated with the air temperature what indicates the relation to atmospheric circulation phenomenon. The rise of concentrations might be caused by intensive vertical mixing within the troposphere typical for hot season, and consequently results in stronger resuspension of soil dust from the Earth's surface. Generally it can be concluded that the air temperature is the main factor influencing temporal variations of soil derived elements in the low-level atmosphere.

The correlations with other meteorological parameters are seldom observed, nevertheless their influence is also important and very complex. It has to be noted that the one-week sampling period is quite long compared with the typical time scale of variations of meteorological parameters so that the correlation might be underestimated.

On the contrary elements like As, Se, V, and Cd show the lowest values in summer (Figure 6.22). This corresponds to higher emission rates during cold

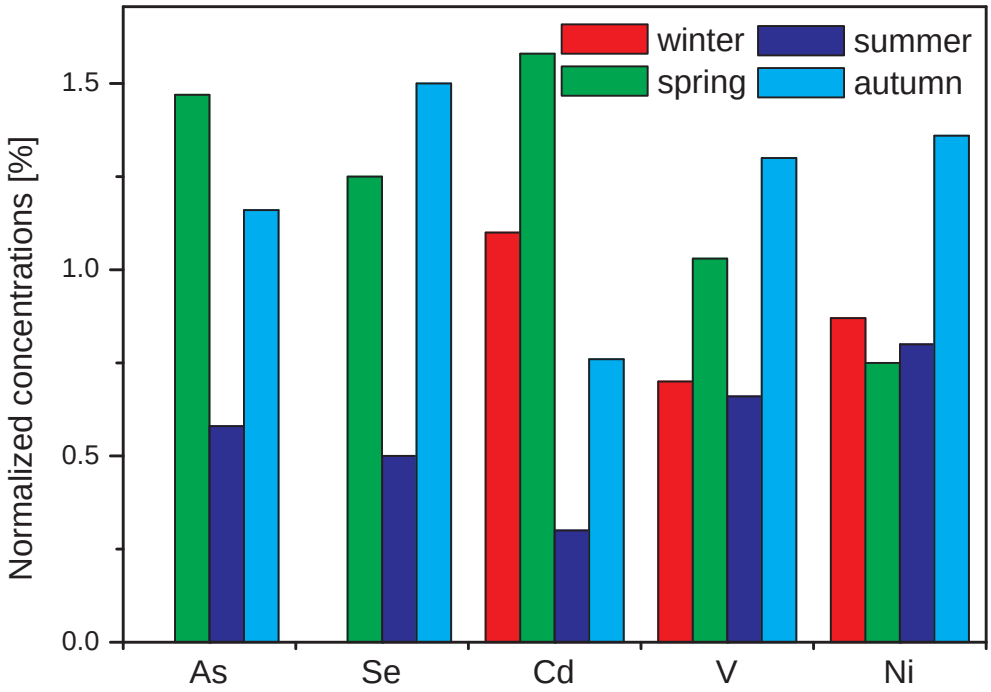

Figure 6.22: Seasonal average elemental concentrations of As, Se, Cd, V, and Ni in atmospheric aerosol in Bratislava during the year of 2004 normalized to the average concentration.

months, since these elements are usually connected to coal combustion.

For other elements (Cl, K, Zn, Br) are the atmospheric concentrations relatively stable over the investigated period, or the data set is not complete (Fe, Ga, Rb, Th) for evaluation of temporal variations. In general, the measurements over more than one year would be needed to sufficiently prove the trend of seasonal variations.

6.4.3 Comparison with other locations

The results of the present study were compared to six other European cities (Table 6.11). The concentrations of almost all elements are lower in Bratislava compared to other localities or comparable to Italian sites of Ponzone and Ispra, which are typical low pollution areas.

First of all the objectives of compared studies has to be taken into account. Ponzone is a small town where the major part of wool industries is settled and Ispra is a residential settlement in north Italy. The city of Milan is the industrial center of northern Italy, thus concentrations of almost all elements are obviously the highest in relevant aerosols. Only concentrations of K, Ca, Ti are higher in Colchester;

Table 6.10: Linear correlation coefficients between elemental concentrations and some meteorological parameters

Element	Pressure	Humidity	Precipitation	Temperature	Wind
Na	-0.05	-0.13	-0.05	0.43	-0.32
Al	-0.25	-0.32	-0.32	0.65	-0.29
Cl	-0.23	-0.29	-0.20	0.70	-0.33
K	0.08	0.48	-0.31	0.09	-0.63
Ca	-0.14	-0.35	-0.20	0.63	-0.41
Ti	0.01	-0.29	-0.20	0.55	-0.42
V	0.14	0.52	-0.17	-0.12	-0.23
Mn	-0.07	-0.12	-0.40	0.59	-0.44
Cu	-0.14	-0.34	-0.25	0.45	-0.06
Zn	0.25	0.19	-0.33	0.06	-0.58
Br	0.61	0.57	-0.43	-0.39	-0.46
Cd	0.49	0.30	-0.05	-0.35	-0.30
In	0.02	0.04	0.25	0.01	-0.02
In	0.09	0.44	0.11	-0.68	0.01
Ba	-0.18	-0.31	-0.04	0.60	-0.32
Dy	-0.04	0.02	-0.15	0.33	-0.65
Pb	-0.06	-0.27	0.15	0.30	-0.33
U	-0.15	-0.13	-0.23	0.59	-0.51

Na, Al, Cl in Budapest and Ga in Krakow are higher. Colchester is a relatively small town and with the exception of motor vehicle traffic it is not expected to contribute high aerosol emissions to the surrounding area. Other aerosol inputs to this area may result from the London Metropolitan area and the North Sea. The main goal of the Krakow research study was to determine the contribution of traffic to the particulate air pollution, and to characterize transport of aerosols in urban area that are close to the vicinity (5 m) of a main road. Location of Szena Square in Budapest has a more closed downtown character, and is affected by heavy traffic.

The low-level atmospheric pollution in Bratislava may be caused by the small number of sources of pollution, and in particular typical of this location is the high number of windy days per year. This statement is supported by the negative correlation found between the wind velocity and the elemental concentrations in our samples. The small contents of V, Ni, and As may be attributed to weaker frequency of oil and coal combustion in the Bratislava, compared to other locations. Oil combustion is practically the only source of V, while Ni can also be emitted from high quality steel production plants and Ni smelters [Swietlicky96].

Table 6.11: Contents of stable elements [ng m^{-3}] in atmosphere for seven European locations

Location	Bratislava (Slovakia)	Colchester[1] (UK)	Krakow[2] (Poland)	Budapest[3] (Hungary)	Ponzone[4]	Ispra[5] (Italy)	Milan[6]
Method	INAA, AAS	PIXE	PIXE	INAA, PIXE	INAA, ET-AAS		
Na	104		172	349			
Al	189		369	857			
Cl	49		179	249			
K	195	1590	247	353	493	413	1217
Ca	179	4332	1181	2002			
Sc	0.032				0.25	1.1	0.4
Ti	7.8	322	45.3	100	41	19	147
V	0.83	4	2.19	4.2	12.1	3.5	13.9
Cr	1.1	8		3.4	7	6.5	38.6
Mn	4.9	44	17	27	23	14	98
Fe	252	2653	788	1969	807	511	5800
Ni	0.45			2.9	20.5	12.2	25.1
Cu	8	13	18.7	32.7	21.4	10.5	185
Zn	28		60.5	147	98	119	392
Ga	0.02		0.87	0.13			
As	0.3			1.62	0.77	0.99	2.3
Se	0.42		0.77	0.48	0.6	0.037	1.8
Br	3.5			8.4	4.9	11	250
Rb	0.0001				1	0.76	5.2
Cd	0.11				0.75	0.51	3.42
In	0.001						
Sb	1				4.9	4.5	68.3
I	0.66						
Cs	0.045				0.05	0.24	0.22
Ba	2.1		11.9	33.4	8	19.9	103
La	0.085				1.05	0.31	1.41
Sm	0.012						
Dy	0.01						
Tm	0.1						
W	0.22				0.07	0.2	2.3
Au	0.0002						
Hg	0.064						
Pb	22		45.9	29	36	98	475
Th	0.042				0.22	0.05	0.5
U	0.012						

[1][Eleftheriadis01] [2][Wróbel00] [3][Salma02] [4][Rizzio01] [5][Rizzio99] [6][Gallorini99]

Chapter 7

Conclusions

Ground level air concentrations of natural radionuclides ^{7}Be, ^{210}Pb, and ^{40}K, and anthropogenic radionuclide ^{137}Cs were measured. In the time period from March 2001 to September 2007, 245 sets of aerosol filters were sampled. The concentration of radionuclides in the surface atmosphere is a result of the interplay between three processes: production, transport, and deposition.

- The activity concentrations of ^{7}Be ranged from 0.2 to 5.1 mBq m^{-3}, with the average value of 2.5 mBq m^{-3}. The range of ^{210}Pb activity concentrations for this period was 0.1 to 3.1 mBq m^{-3}, with the average of 0.77 mBq m^{-3}.

- The activity concentrations of ^{7}Be and ^{210}Pb exhibit the pattern of seasonal variations. ^{7}Be concentrations are higher in spring comparing to autumn and winter season. It is connected to the air-mass exchange processes between the stratosphere and the troposphere enhanced by the heating of the Earth's surface, since the stratosphere and the lower troposphere are reservoirs of the cosmogenic radionuclides. In cold months these exchange processes are reduced. On the contrary, the concentrations of ^{210}Pb, the daughter product of ^{222}Rn exhaled from soil surfaces, reach high values in autumn and winter. That is attributed to frequent inversion conditions of the surface air layers and the decline in spring and summer is the result of intensive air mixing.

- The correlation study has been carried out between atmospheric concentrations of radionuclides ^{7}Be and ^{210}Pb and meteorological conditions. The only significant correlation was found between the ^{7}Be concentration and air temperature, indicating the significance of exchange processes to the actual atmospheric concentration of the radionuclide.

- Since the activity concentrations of ^{137}Cs and ^{40}K in air are very low, the cumulated monthly samples were used for the activity determination. Values of ^{137}Cs and ^{40}K reached the level of 0.52 and 5.2 Bq m^{-3}, respectively.

Since the year 2004 the technique of precipitation sampling has been developed. Activity concentrations in precipitation and depositional fluxes of ^{7}Be, ^{210}Pb, ^{137}Cs, and ^{40}K have been determined since the July 2005.

- Average ^{7}Be and ^{210}Pb concentrations in rainwater were 1.66 and 0.27 kBq m^{-3}, respectively. Concentrations of ^{137}Cs and ^{40}K reached lower values 1.64 and 61.5 Bq m^{-3}, respectively. No significant correlation between activity concentrations and amount of precipitation was found. High correlation was found among the activity concentrations of individual radionuclides. This observation suggests similar behavior of aerosol particles carrying the radionuclides.

- Average monthly depositions of ^{7}Be and ^{210}Pb were 79.4 and 7.92 Bq m^{-2}, respectively. Simultaneously ^{137}Cs and ^{40}K depositions in precipitation were 38.1 and 794 mBq m^{-2}, respectively. Monthly depositions of ^{7}Be and ^{210}Pb radionuclides are relatively highly correlated with total monthly precipitation, meanwhile the depositions of ^{137}Cs and ^{40}K have a lower dependency on the rainwater amount.

- Assuming that the dry deposition of ^{7}Be and ^{210}Pb constitutes for approximately 10% of total deposition, the values of ^{7}Be and ^{210}Pb annual total depositions for year 2006 were 888 and 89.9 Bq m^{-2}, respectively.

Theoretical model for vertical profile of ^{7}Be activity concentration up to 30 km has been developed and used for calculations of turbulent diffusion coefficient and scavenging coefficient. The study of the mean vertical concentration profile and of the deposition of cosmogenic radionuclides provides information on the vertical transport in the stratosphere and troposphere and processes of scavenging.

- The one-dimensional model of the steady state vertical turbulent movement of atmospheric air masses is applied. Vertical mixing in the troposphere and stratosphere, the radioactive decay, wet deposition as well as gravitational sedimentation are physical processes considered in the model. Parameters of the turbulent diffusion and washout are calculated using measured data of the ^{7}Be monthly average activity concentrations in ground level air and the ^{7}Be monthly depositions.

- The ^{7}Be ground level activity concentration is increasing with the increasing turbulent diffusion coefficient, because the turbulent diffusion is more efficient. The ^{7}Be concentration increases also with the decreasing scavenging coefficient, because small values of scavenging efficiency determine a small number of aerosols scavenged by precipitation.

- The values of both the turbulent diffusion coefficient and the scavenging coefficient were used for the calculation of ^{7}Be concentrations at different altitudes. Vertical profiles for each month of the year 2006 are presented. As can be seen, the activity concentrations are almost stable above the tropopause (9 - 12 km) in all seasons, but below this altitude they are varying quite significantly.

16 samples from the year 2004 were selected for the analysis to evaluate the elemental content in the atmospheric aerosols. The total of 30 elements were determined by the instrumental neutron activation analysis at IBR-2 reactor in Dubna, Russia. Other six elements were determined using atomic absorption spectrometry (Cr was determined by both techniques).

- The decreasing trend of air pollution by heavy metals in Bratislava since the year 1981 has been observed. It results mainly from the decline of industry production in the Slovak Republic after the year 1989 and nowadays via application of stricter requirements in the environmental legislation, desulphurization of power plants, and introducing of more sophisticated technologies in smelters.

- The concept of crustal enrichment factors was applied to the data. When the enrichment factor is lower than 7, the air particulate is of crustal origin, and when the factor is higher than 7, it is of the anthropogenic one. The values close to 1 indicate the soil origin of Ba, La, Th, and U. Following these criteria, it can be concluded that Zn, As, Se, Cd, Sb, Hg, and Pb are of the anthropogenic origin.

- Some of the elemental concentrations indicate seasonal variations over the year with elevated values in summer. Most of these elements are soil derived (Ca, Ti, Mn, Ba, U). Concentrations of these elements are correlated with the air temperature what indicates the relation to atmospheric circulation phenomenon. The rise of concentrations might be caused by intensive vertical mixing and consequently results in stronger resuspension of soil dust from the Earth's surface. Generally it can be concluded that the air temperature is the main factor influencing temporal variations of elemental content in the low-level atmosphere. Measurements over more than one year would be needed to really prove the trend of seasonal variations.

- On the contrary elements like As, Se, V, and Cd show the lowest values in summer. This corresponds to higher emission rates during cold months, since these elements are usually connected to coal combustion.

- Elemental contents in atmospheric aerosol particles were compared to other six European cities. The concentrations of almost all elements are lower in Bratislava compared to other localities or comparable to typical low pollution areas (Ponzone and Ispra in Italy). The low level of atmospheric pollution in Bratislava may be caused by the small number of sources of pollution, and in particular the high number of windy days per year, which is typical of this location. This statement is supported by the negative correlation found between the wind velocity and the elemental concentrations in our samples.

This thesis presents complex results of the study of natural and artificial radioactivity of atmospheric aerosols and their elemental composition. The detail

investigation of experimental techniques used for sampling, measurement, and evaluation was performed. The obtained data were analyzed in order to obtain valuable information about the processes taking place in the atmosphere and about its level of pollution. Since we believe this topic has its potential and perspective and further study can bring new interesting outcomes, we will continue in this research in the future.

Zhrnutie

V predkladanej práci sú prezentované výsledky meraní koncentrácie prírodných rádionuklidov ^{7}Be, ^{210}Pb a ^{40}K a antropogénneho rádionuklidu ^{137}Cs v prízemnej vrstve atmosféry. V období od marca 2001 do septembra 2007 bolo odobratých 245 sád vzoriek aerosólových filtrov.

- Koncentrácie aktivity ^{7}Be boli namerané v rámci hodnôt od 0.2 do 5.1 mBq m^{-3}, pričom priemerná hodnota bola 2.5 mBq m^{-3}. Rozpätie objemových aktivít ^{210}Pb sa pohybovalo od 0.1 do 3.1 mBq m^{-3}, s priemerom 0.77 mBq m^{-3}.

- Objemové aktivity ^{7}Be a ^{210}Pb vykazujú sezónne variácie, pričom koncentrácie ^{7}Be sú vyššie v jarnom a letnom období. Je to výsledok výmeny vzdušných más medzi stratosférou a troposférou v tomto období, pričom stratosféra a vyššia troposféra sú rezervoármi kozmogénnych rádionuklidov. Práve na jar a v lete sú tieto procesy provokované vzdušnými prúdmi, ktoré stúpajú od zohriateho zemského povrchu. V zime sú tieto výmenné procesy potlačené. Naopak, koncentrácie ^{210}Pb dosahujú vyššie hodnoty na jeseň a v zime. Tento jav je spojený s najmä s inverziou, ktorá je pomerne častým javom v týchto obdobiach roka.

- Korelačná analýza medzi koncentráciami rádionuklidov v atmosfére a základnými meteorologickými parametrami poukázala na teplotu vzduchu ako jediný faktor významnejšie vplývajúci na úroveň ^{7}Be v prízemnom vzduchu.

- Objemové aktivity ^{137}Cs a ^{40}K vo vzduchu sa pohybujú na veľmi nízkych hodnotách. Preto bolo potrebné pri ich stanovovaní spájať dokopy niekoľko týždňových vzoriek. Priemerné hodnoty ^{137}Cs a ^{40}K za sledované obdobie boli stanovené na 0.52 a 5.2 Bq m^{-3}.

Od roku 2004 bola vyvýjaná metodika odberu atmosférických zrážok. Objemové koncentrácie v zrážkach a mesačné depozície rádionuklidov ^{7}Be, ^{210}Pb, ^{137}Cs a ^{40}K boli stanovované od júla 2005.

- Priemerné koncentrácie ^{7}Be a ^{210}Pb v dažďovej vode boli počas sledovaného obdobia 1.66 a 0.29 kBq m^{-3}. Koncentrácie ^{137}Cs a ^{40}K dosahovali nižšie hodnoty 1.64 a 61.5 Bq m^{-3}. Medzi objemovými koncentráciami rádionuklidov a úhrnom zrážok nebola pozorovaná signifikantná korelácia. Vysoká

korelácia však bola nájdená medzi jednotlivými objemovými aktivitami rádionuklidov, čo naznačuje podobné procesy vymývania aerosólov charakteristických pre jednotlivé rádionuklidy.

- Priemerné mesačné depozície ^{7}Be a ^{210}Pb boli 79.4 a 8.47 Bq m^{-2}. Súčasne boli stanovené depozície ^{137}Cs a ^{40}K rovné 38.1 a 794 mBq m^{-2}. Na rozdiel od objemových koncentrácií depozície rádionuklidov ^{7}Be a ^{210}Pb sú relatívne vysoko korelované s mesačným úhrnom zrážok. Depozície ^{137}Cs a ^{40}K majú tieto korelačné koeficienty nižšie, čo naznačuje menšiu závislosť procesov depozície na množstve zrážok.

- Za predpokadu, že suchá depozícia aerosólov nesúcich rádionuklidy ^{7}Be a ^{210}Pb predstavuje 10% z celkovej depozície, možno celkovú depozíciu za rok 2006 ohodnotiť na 888 a 89.9 Bq m^{-2}.

Bol vytvorený teoretický model vertikálneho profilu koncenrácie ^{7}Be v atmosfére do výšky 30 km a bol použitý na výpočet koeficientov turbulentnej difúzie a vymývania aerosólov. Štúdium takéhoto modelu poskutuje informácie o vertikálnom transporte v nižšej stratosfére a v troposfére, ako aj o procesoch vymývania aerosólov zrážkami.

- Bol aplikovaný statický jedno-rozmerný model vertikálneho turbulentného pohybu atmosféry. Tento model zahŕňa vertikálne premiešavanie v rámci troposféry a stratosféry, rádioaktívnu premenu nuklidov, depozíciu zrážkami ako aj gravitačnú sedimentáciu aerosólov. Koeficienty turbulentnej difúzie a vymývania aerosólov sú vypočítané pomocou experimentálnych hodnôt objemovej aktivity ^{7}Be v prízemnej atmosfére a mesačných depozícií ^{7}Be.

- Koncentrácia ^{7}Be v prízemnej atmosfére vzrastá s rastúcim koeficientom turbulentnej difúzie a s klesajúcim koeficientom vymývania.

- Koeficienty turbulentnej difúzie a vymývania aerosólov boli použité na stanovenie koncentrácií ^{7}Be v rôznych nadmorských výškach. Sú prezentované vertiálne profily do nadmorskej výšky 30 km. Nad úrovňou tropopauzy (9-12 km) sú koncentrácie viacmenej stabilné v priebehu roka. Pod tropopauzou sú variácie ^{7}Be výrazné.

Z celkového počtu 36 vzoriek aerosólových filtrov z roku 2004 bolo 16 vybraných na prvkovú analýzu. Pomocou neutrónovej aktivačnej analýzy na reaktore IBR-2 v Dubne (Ruská federácia) boli stanovené koncentrácie 30 prvkov. Dodatočne bolo atómovou absorpčnou analýzou stanovených ďalších 6 prvkov (Cr bol stanovený oboma metódami).

- Od roku 1981 sa v Bratislave pozoruje klesajúci trend znečistenia atmosféry ťažkými kovmi. Je to jednak dôsledkom poklesu priemyselných aktivít na Slovensku po roku 1989 a v súčasnosti je tiež tento trend výsledkom prísnejších legislatívnych opatrení.

- Na výsledné hodnoty bol aplikovaný koncept faktorov pôdneho obohatenia. Ak je faktor obohatenia nižší ako 7, potom možno daný prvok zaradiť do skupiny prvkov pôdneho pôvodu. Ak je faktor väčší ako 10, potom ho možno považovať za antropogénny. Hodnoty faktorov pre prvky Ba, La, Th a U blízke jednotke indikujú ich pôdny pôvod. Prvky Zn, As, Se, Cd, Sb, Hg a Pb vzhľadom na tieto kritéria považujeme za antropogénne.

- Koncentrácie niektorých prvkov vykazujú sezónne variácie s hodnotami vyššími v letných mesiacoch. Väčšina týchto prvkov je pôdneho pôvodu (Ca, Ti, Mn, Ba, U). Ich atmosférické koncentrácie sú korelované s teplotou vzduchu, čo naznačuje súvis s cirkuláciou atmosféry. Nárast koncentrácií niektorých prvkov môže byť následkom intenzívnej resuspenzie zo zemského povrchu. Vo všeobecnosti možno tvrdiť, že teplota vzduchu je hlavným faktorom ovplyvňujúcim variácie niektorých prvkov v prízemnej atmosfére. Avšak na potvrdenie týchto pozorovaní by bolo potrebné sledovať úroveň koncentrácie prvkov po dobu dlhšiu ako jeden rok.

- Naopak, prvky ako As, Se, V a Cd vykazujú v letnom období najnižšie hodnoty. Toto pozorovanie korešponduje s faktom, že v chladných mesiacoch sú emisie týchto prvkov vyššie vzhľadom na vyššiu spotrebu uhlia v tomto období.

- Výsledky atmosférických koncentrácií prvkov v Bratislave boli porovnávané so šiestimi európskymi mestami. Koncentrácie väčšiny prvkov sú najnižšie v Bratislave alebo porovnateľné s úrovňami v málo znečistených oblastiach ako sú Ponzone a Ispra v Taliansku. Nízke hodnoty znečistenia ovzdušia v Bratislave sú výsledkom relatívne malého počtu zdrojov polutantov. Treba tiež podotknúť, že Bratislava sa vyznačuje veterným podnebím. Antikorelácia koncentrácií prvkov s rýchlosťou vetra, indikuje čistiaci efekt vetra.

Táto dizertačná práca prezentuje výsledky komplexnej štúdie prírodnej a antropogénnej rádioaktivity atmosférických aerosólov a ich prvkového zloženia. Bola vykonaná detailná analýza experimentálnych postupov použitých pri odbere vzoriek, ich meraní a hodnotení. Získané dáta boli analyzované s cieľom získania cenných informácií o procesoch prebiehajúcich v atmosfére a o úrovni jej znečistenia. Do budúcnosti plánujeme pokračovať v tomto výskume, pretože veríme že môže priniesť ešte mnoho zaujímavých a cenných výsledkov.

Appendix A

Activity concentrations in air

Table A.1: Activity concentrations of ^{7}Be and ^{210}Pb in Bratislava ground level air from March 2001 to September 2007 (The 2σ uncertainties are used)

Sampling date	**^{7}Be [mBq m^{-3}]**	**^{210}Pb [mBq m^{-3}]**
26.3.-30.3.01	1.35 ± 0.06	0.65 ± 0.03
30.3.-3.4.01	1.35 ± 0.08	0.74 ± 0.05
3.4.-6.4.01	3.63 ± 0.12	0.57 ± 0.02
6.4.-9.4.01	1.91 ± 0.07	0.30 ± 0.02
9.4.-11.4.01	1.74 ± 0.07	0.31 ± 0.02
20.4.-23.4.01	0.59 ± 0.04	0.26 ± 0.02
25.4.-30.4.01	0.94 ± 0.04	0.34 ± 0.02
30.4.-3.5.01	3.48 ± 0.16	0.81 ± 0.04
4.5.-7.5.01	3.86 ± 0.12	0.79 ± 0.03
18.5.-23.5.01	2.69 ± 0.11	0.41 ± 0.03
23.5.-28.5.01	4.62 ± 0.17	0.64 ± 0.03
28.5.-31.5.01	3.27 ± 0.12	0.48 ± 0.02
5.6.-7.6.01	2.57 ± 0.13	0.42 ± 0.03
8.6.-12.6.01	1.95 ± 0.09	0.43 ± 0.02
12.6.-14.6.01	2.54 ± 0.18	0.43 ± 0.03
15.6.-20.6.01	2.09 ± 0.13	0.38 ± 0.05
22.6.-25.6.01	2.43 ± 0.16	0.37 ± 0.07
25.6.-27.6.01	4.29 ± 0.26	0.62 ± 0.04
13.7.-15.7.01	3.38 ± 0.14	1.05 ± 0.06
16.7.-19.7.01	1.23 ± 0.06	0.28 ± 0.02
23.7.-26.7.01	3.01 ± 0.11	0.54 ± 0.03
31.7.-2.8.01	4.11 ± 0.18	0.78 ± 0.03
14.8.-22.8.01	2.73 ± 0.09	1.13 ± 0.05
28.8.-31.8.01	1.72 ± 0.06	0.25 ± 0.01
6.9.-10.9.01	1.33 ± 0.07	0.25 ± 0.02

continued ...

continued ...

Sampling date	**^{7}Be [mBq m^{-3}]**	**^{210}Pb [mBq m^{-3}]**
11.9.-17.9.01	1.79 ± 0.07	0.41 ± 0.02
17.9.-21.9.01	1.48 ± 0.10	0.52 ± 0.03
21.9.-26.9.01	1.22 ± 0.05	0.73 ± 0.03
28.9.-3.10.01	1.43 ± 0.10	1.12 ± 0.04
12.10.-18.10.01	1.77 ± 0.09	0.94 ± 0.04
9.11.-11.11.01	1.19 ± 0.16	0.55 ± 0.06
12.11.-14.11.01	1.09 ± 0.09	0.56 ± 0.05
26.11.-30.11.01	1.10 ± 0.10	0.54 ± 0.04
13.12.-18.12.01	1.72 ± 0.11	3.07 ± 0.09
4.1.-7.1.02 *	3.58 ± 0.15	1.67 ± 0.07
7.1.-10.1.02 *	2.08 ± 0.11	1.33 ± 0.04
10.1.-12.1.02 *	2.34 ± 0.14	2.16 ± 0.05
14.1.-17.1.02 *	1.55 ± 0.05	1.53 ± 0.04
18.1.-21.1.02	1.80 ± 0.09	1.47 ± 0.06
22.1.-25.1.02	2.60 ± 0.11	1.81 ± 0.07
29.1.-1.2.02	3.80 ± 0.19	1.16 ± 0.05
1.2.-5.2.02	3.77 ± 0.23	2.03 ± 0.12
9.2.-12.2.02	1.85 ± 0.10	0.53 ± 0.04
14.2.-18.2.02	3.30 ± 0.18	0.89 ± 0.06
11.3.-15.3.02	3.17 ± 0.15	0.77 ± 0.04
8.4.-12.4.02	3.07 ± 0.10	1.28 ± 0.05
18.4.-22.4.02	1.51 ± 0.06	0.95 ± 0.04
26.4.-30.4.02	3.83 ± 0.14	0.47 ± 0.02
9.5.-13.5.02	3.54 ± 0.12	0.96 ± 0.04
24.5.-29.5.02	1.13 ± 0.04	0.49 ± 0.02
6.6.-13.6.02	2.03 ± 0.08	0.50 ± 0.03
27.6.-2.7.02	3.26 ± 0.13	0.53 ± 0.03
13.9.-18.9.02	2.36 ± 0.11	0.64 ± 0.05
21.10.-25.10.02 *	1.37 ± 0.06	0.57 ± 0.03
25.10.-30.10.02 *	1.55 ± 0.07	0.28 ± 0.02
8.11.-25.11.02 *	1.59 ± 0.05	0.64 ± 0.02
25.11.-2.12.02 *	1.29 ± 0.08	1.33 ± 0.04
5.12.-16.12.02	2.07 ± 0.09	1.78 ± 0.07
23.12.02-7.1.03	2.95 ± 0.13	1.73 ± 0.07
24.1.-4.2.03	1.13 ± 0.06	0.51 ± 0.03
5.2.-17.2.03	1.69 ± 0.06	1.14 ± 0.04
17.2.-28.2.03	1.86 ± 0.09	1.03 ± 0.04
28.2.-6.3.03	3.83 ± 0.20	0.61 ± 0.04
6.3.-14.3.03	2.65 ± 0.12	1.12 ± 0.04
14.3.-24.3.03	2.07 ± 0.13	0.78 ± 0.04
24.3.-4.4.03	3.43 ± 0.12	1.15 ± 0.05

continued ...

continued ...

Sampling date	**^{7}Be [mBq m^{-3}]**	**^{210}Pb [mBq m^{-3}]**
4.4.-14.4.03	2.48 ± 0.15	0.56 ± 0.03
16.5.-30.5.03	2.43 ± 0.12	0.76 ± 0.03
9.10.-10.11.03 *	1.21 ± 0.04	0.71 ± 0.02
10.11.-25.11.03 *	1.38 ± 0.05	1.53 ± 0.05
25.11.-9.12.03 *	1.05 ± 0.08	1.26 ± 0.06
12.12.-23.12.03	1.21 ± 0.07	0.67 ± 0.03
23.12.03-7.1.04	1.64 ± 0.09	0.71 ± 0.04
7.1.-19.1.04	1.21 ± 0.05	0.45 ± 0.02
19.1.-2.2.04	1.19 ± 0.06	0.57 ± 0.03
2.2.-12.2.04	1.62 ± 0.08	0.29 ± 0.03
16.2.-1.3.04	1.55 ± 0.07	0.41 ± 0.03
2.3.-16.3.04	1.33 ± 0.06	0.53 ± 0.03
20.3.-5.4.04	3.18 ± 0.13	0.62 ± 0.03
6.4.-20.4.04	2.84 ± 0.11	0.52 ± 0.03
26.4.-10.5.04	2.95 ± 0.10	0.70 ± 0.03
12.5.-25.5.04	4.17 ± 0.12	0.49 ± 0.03
27.5.-1.6.04	3.08 ± 0.11	0.47 ± 0.03
3.6.-10.6.04	3.30 ± 0.10	0.48 ± 0.02
14.6.-21.6.04	3.15 ± 0.10	0.42 ± 0.03
21.6.-25.6.04	4.79 ± 0.17	0.57 ± 0.04
25.6.-2.7.04	4.30 ± 0.18	0.50 ± 0.04
2.7.-9.7.04	4.04 ± 0.20	0.54 ± 0.03
9.7.-15.7.04	2.51 ± 0.10	0.28 ± 0.02
15.7.-22.7.04	3.67 ± 0.16	1.05 ± 0.04
22.7.-26.7.04	3.41 ± 0.23	0.92 ± 0.09
27.7.-3.8.04	3.65 ± 0.16	0.52 ± 0.03
4.8.-11.8.04	4.52 ± 0.18	0.88 ± 0.05
13.8.-20.8.04	3.74 ± 0.16	0.76 ± 0.05
20.8.-27.8.04	3.00 ± 0.11	0.45 ± 0.03
27.8.-3.9.04	4.06 ± 0.16	0.71 ± 0.04
13.9.-17.9.04	3.28 ± 0.14	0.65 ± 0.03
21.9.-27.9.04	2.75 ± 0.14	0.29 ± 0.02
30.9.-6.10.04	3.37 ± 0.18	0.96 ± 0.03
6.10.-15.10.04	3.19 ± 0.10	1.05 ± 0.03
15.10.-25.10.04	1.98 ± 0.24	0.89 ± 0.03
26.10.-3.11.04	2.99 ± 0.14	1.41 ± 0.04
3.11.-10.11.04	1.72 ± 0.07	0.65 ± 0.02
10.11.-16.11.04	1.53 ± 0.14	0.72 ± 0.04
16.11.-24.11.04	1.81 ± 0.09	0.29 ± 0.01
25.11.-1.12.04	2.62 ± 0.09	1.15 ± 0.04
1.12.-8.12.04	1.93 ± 0.16	1.39 ± 0.04

continued ...

continued ...

Sampling date	**^{7}Be [mBq m^{-3}]**	**^{210}Pb [mBq m^{-3}]**
9.12.-16.12.04	3.30 ± 0.18	1.36 ± 0.05
16.12-22.12.04	2.42 ± 0.14	0.84 ± 0.04
22.12.04-3.1.05	1.19 ± 0.06	0.73 ± 0.04
4.1.-12.1.05	1.65 ± 0.08	0.94 ± 0.04
13.1.-18.1.05	1.03 ± 0.03	0.28 ± 0.01
19.1.-26.1.05	0.91 ± 0.04	0.33 ± 0.02
26.1.-2.2.05	0.86 ± 0.05	0.65 ± 0.03
2.2.-9.2.05	1.52 ± 0.08	1.32 ± 0.06
9.2.-14.2.05	3.27 ± 0.18	1.31 ± 0.07
23.2.-2.3.05	0.68 ± 0.04	1.11 ± 0.04
4.3.-16.3.05	1.20 ± 0.06	0.52 ± 0.03
16.3.-23.3.05	1.50 ± 0.07	0.42 ± 0.03
23.3.-30.3.05	1.09 ± 0.06	0.58 ± 0.04
30.3.-6.4.05	3.94 ± 0.16	1.15 ± 0.06
6.4.-13.4.05	3.32 ± 0.16	0.61 ± 0.04
20.4.-27.4.05	3.24 ± 0.18	0.77 ± 0.04
27.4.-4.5.05	3.38 ± 0.18	0.68 ± 0.03
4.5.-11.5.05	2.59 ± 0.48	0.28 ± 0.01
11.5.-19.5.05	2.16 ± 0.13	0.45 ± 0.03
19.5.-25.5.05	4.41 ± 0.24	0.50 ± 0.03
25.5.-1.6.05	4.30 ± 0.22	0.93 ± 0.07
1.6.-6.6.05	4.01 ± 0.21	0.55 ± 0.04
15.6.-22.6.05	2.93 ± 0.16	0.53 ± 0.03
22.6.-29.6.05	3.74 ± 0.20	1.23 ± 0.06
29.6.-6.7.05	3.21 ± 0.17	0.57 ± 0.04
6.7.-13.7.05	2.23 ± 0.13	0.43 ± 0.03
13.7.-21.7.05	2.48 ± 0.13	0.78 ± 0.05
21.7.-27.7.05	2.59 ± 0.16	0.52 ± 0.03
27.7.-3.8.05	4.51 ± 0.25	1.41 ± 0.07
3.8.-10.8.05	1.71 ± 0.11	0.32 ± 0.02
10.8.-17.8.05	2.46 ± 0.14	0.53 ± 0.03
18.8.-24.8.05	3.00 ± 0.27	0.86 ± 0.05
24.8.-31.8.05	4.14 ± 0.23	1.16 ± 0.06
31.8.-7.9.05	3.75 ± 0.34	1.16 ± 0.06
7.9-14.9.05	3.22 ± 0.20	1.30 ± 0.06
14.9.-21.9.05	2.40 ± 0.13	0.49 ± 0.03
21.9.-28.9.05	2.96 ± 0.18	1.47 ± 0.07
28.9.-5.10.05	1.84 ± 0.10	1.28 ± 0.06
5.10.-12.10.05	4.04 ± 0.22	1.81 ± 0.08
12.10.-19.10.05	2.37 ± 0.17	1.60 ± 0.07
19.10.-26.10.05	1.84 ± 0.11	1.29 ± 0.08

continued ...

continued ...

Sampling date	**^{7}Be [mBq m^{-3}]**	**^{210}Pb [mBq m^{-3}]**
26.10.-2.11.05	2.19 ± 0.12	1.06 ± 0.06
2.11.-9.11.05	1.10 ± 0.07	1.44 ± 0.07
9.11.-16.11.05	2.03 ± 0.28	2.07 ± 0.10
16.11.-21.11.05	1.32 ± 0.12	0.63 ± 0.05
7.12.-14.12.05	2.27 ± 0.15	0.84 ± 0.05
14.12.-21.12.05	1.59 ± 0.06	0.31 ± 0.02
21.12.-29.12.05	1.75 ± 0.13	0.53 ± 0.03
29.12.-4.1.06	0.77 ± 0.05	0.82 ± 0.05
4.1.-11.1.06	2.68 ± 0.16	1.27 ± 0.07
11.1.-18.1.06	1.82 ± 0.11	1.56 ± 0.07
18.1.-25.1.06	1.94 ± 0.12	2.11 ± 0.10
25.1.-1.2.06	3.01 ± 0.18	2.37 ± 0.11
1.2.-8.2.06	1.77 ± 0.11	1.73 ± 0.08
8.2.-15.2.06	1.90 ± 0.09	0.61 ± 0.04
15.2.-22.2.06	1.63 ± 0.06	0.63 ± 0.04
22.2.-1.3.06	1.51 ± 0.08	0.66 ± 0.03
1.3.-8.3.06	1.83 ± 0.11	1.04 ± 0.05
8.3.-15.3.06	1.70 ± 0.08	0.58 ± 0.03
15.3.-22.3.06	1.93 ± 0.11	1.34 ± 0.06
22.3.-30.3.06	2.96 ± 0.16	0.60 ± 0.04
30.3.-5.4.06	2.50 ± 0.10	0.43 ± 0.02
5.4.-12.4.06	2.97 ± 0.17	0.93 ± 0.06
12.4.-19.4.06	2.25 ± 0.10	0.32 ± 0.04
19.4.-26.4.06	1.30 ± 0.07	1.59 ± 0.08
26.4.-3.5.06	2.15 ± 0.09	0.52 ± 0.05
3.5.-10.5.06	5.09 ± 0.28	0.99 ± 0.06
10.5.-17.5.06	3.43 ± 0.20	0.72 ± 0.04
17.5.-24.5.06	2.92 ± 0.20	0.42 ± 0.03
24.5.-31.5.06	2.88 ± 0.20	0.22 ± 0.02
31.5.-7.6.06	1.65 ± 0.07	0.30 ± 0.03
7.6.-14.6.06	3.09 ± 0.16	1.08 ± 0.05
14.6.-21.6.06	2.83 ± 0.15	0.49 ± 0.03
21.6.-28.6.06	2.72 ± 0.16	0.63 ± 0.03
28.6.-6.7.06	4.36 ± 0.23	0.68 ± 0.04
6.7.-13.7.06	3.65 ± 0.32	0.60 ± 0.05
13.7.-19.7.06	3.02 ± 0.24	0.41 ± 0.04
19.7.-26.7.06	3.90 ± 0.33	0.85 ± 0.05
26.7.-2.8.06	3.26 ± 0.25	0.78 ± 0.04
2.8.-9.8.06	1.52 ± 0.11	0.28 ± 0.02
9.8.-16.8.06	1.37 ± 0.10	0.28 ± 0.02
16.8.-24.8.06	2.26 ± 0.14	0.49 ± 0.03

continued ...

continued ...

Sampling date	**^{7}Be [mBq m^{-3}]**	**^{210}Pb [mBq m^{-3}]**
24.8.-30.8.06	1.87 ± 0.12	0.31 ± 0.02
30.8.-6.9.06	1.77 ± 0.10	0.34 ± 0.03
6.9.-13.9.06	1.99 ± 0.12	0.55 ± 0.03
22.9.-27.9.06	2.46 ± 0.12	0.94 ± 0.05
27.9.-4.10.06	1.70 ± 0.09	1.59 ± 0.07
4.10.-11.10.06	1.45 ± 0.06	0.57 ± 0.03
11.10.-18.10.06	1.51 ± 0.11	0.72 ± 0.03
18.10.-25.10.06	1.39 ± 0.09	0.62 ± 0.03
25.10.-31.10.06	0.50 ± 0.04	0.18 ± 0.02
31.10.-8.11.06	0.62 ± 0.05	0.13 ± 0.01
8.11.-15.11.06	0.54 ± 0.04	0.14 ± 0.01
15.11.-22.11.06	0.33 ± 0.02	0.38 ± 0.03
22.11.-29.11.06	0.23 ± 0.02	0.26 ± 0.02
29.11.-6.12.06	0.91 ± 0.07	1.00 ± 0.06
6.12.-13.12.06	0.47 ± 0.04	0.28 ± 0.02
13.12.-20.12.06	0.55 ± 0.05	0.47 ± 0.03
20.12.-27.12.06	0.60 ± 0.04	0.24 ± 0.02
27.12.-3.1.07	1.19 ± 0.12	1.34 ± 0.08
3.1.-10.1.07	1.43 ± 0.13	0.74 ± 0.06
10.1.-17.1.07	2.75 ± 0.22	0.69 ± 0.04
17.1.-24.1.07	2.51 ± 0.14	0.76 ± 0.04
24.1.-31.1.07	1.68 ± 0.09	0.31 ± 0.02
31.1.-7.2.07	1.52 ± 0.08	0.40 ± 0.03
7.2.-14.2.07	1.48 ± 0.11	0.52 ± 0.03
14.2.-21.2.07	1.66 ± 0.13	0.82 ± 0.03
21.2.-28.2.07	1.99 ± 0.10	1.27 ± 0.04
28.2.-7.3.07	2.21 ± 0.10	0.39 ± 0.02
7.3.-14.3.07	2.78 ± 0.13	0.56 ± 0.02
14.3.-21.3.07	2.11 ± 0.10	0.42 ± 0.02
21.3.-28.3.07	2.42 ± 0.10	0.54 ± 0.03
28.3.-4.4.07	3.60 ± 0.13	0.89 ± 0.03
4.4.-11.4.07	2.40 ± 0.15	0.32 ± 0.01
11.4.-18.4.07	3.81 ± 0.22	0.40 ± 0.02
18.4.-25.4.07	4.48 ± 0.23	0.51 ± 0.02
25.4.-2.5.07	3.85 ± 0.15	0.59 ± 0.02
2.5.-9.5.07	3.04 ± 0.17	0.61 ± 0.02
9.5.-16.5.07	2.40 ± 0.11	0.61 ± 0.02
16.5.-23.5.07	3.10 ± 0.13	0.62 ± 0.02
23.5.-30.5.07	3.21 ± 0.11	0.79 ± 0.02
30.5.-6.6.07	2.08 ± 0.08	0.48 ± 0.02
6.6.-13.6.07	5.01 ± 0.17	0.84 ± 0.03

continued ...

continued ...

Sampling date	**^{7}Be [mBq m^{-3}]**	**^{210}Pb [mBq m^{-3}]**
13.6.-20.6.07	3.57 ± 0.18	0.69 ± 0.02
20.6.-27.6.07	2.90 ± 0.17	0.50 ± 0.02
27.6.-4.7.07	2.74 ± 0.12	0.50 ± 0.02
4.7.-11.7.07	2.13 ± 0.09	0.28 ± 0.01
11.7.-18.7.07	2.67 ± 0.11	0.76 ± 0.02
18.7.-25.7.07	3.39 ± 0.14	0.91 ± 0.03
25.7.-1.8.07	2.80 ± 0.12	0.46 ± 0.02
1.8.-9.8.07	3.14 ± 0.14	0.75 ± 0.03
9.8.-15.8.07	2.03 ± 0.09	0.72 ± 0.02
15.8.-22.8.07	3.16 ± 0.14	0.79 ± 0.03
22.8.-30.8.07	3.09 ± 0.15	0.78 ± 0.04
30.8.-5.9.07	2.88 ± 0.30	0.49 ± 0.02
5.9.-12.9.07	1.43 ± 0.07	0.24 ± 0.01
13.9.-19.9.07	3.64 ± 0.33	0.88 ± 0.04
19.9.-26.9.07	4.21 ± 0.34	0.80 ± 0.04

* Samples were collected at the Slovak Institute of Metrology

Table A.2: Monthly average activity concentrations of ^{7}Be and ^{210}Pb in Bratislava ground level air from October 2003 to September 2007 (The 2σ uncertainties are used)

Month/Year	**^{7}Be [mBq m^{-3}]**	**^{210}Pb [mBq m^{-3}]**
October 2003	1.21 ± 0.04	0.72 ± 0.02
November 2003	1.38 ± 0.05	1.53 ± 0.05
December 2003	1.30 ± 0.08	0.88 ± 0.04
January 2004	1.20 ± 0.06	0.51 ± 0.03
February 2004	1.59 ± 0.08	0.35 ± 0.03
March 2004	2.26 ± 0.10	0.58 ± 0.03
April 2004	2.84 ± 0.11	0.52 ± 0.03
May 2004	3.40 ± 0.11	0.55 ± 0.03
June 2004	3.89 ± 0.14	0.49 ± 0.03
July 2004	3.46 ± 0.17	0.66 ± 0.04
August 2004	3.83 ± 0.15	0.70 ± 0.04
September 2004	3.02 ± 0.14	0.47 ± 0.03
October 2004	2.88 ± 0.17	1.08 ± 0.03
November 2004	1.92 ± 0.10	0.70 ± 0.03
December 2004	2.55 ± 0.16	1.20 ± 0.04
January 2005	1.13 ± 0.05	0.59 ± 0.03
February 2005	1.82 ± 0.10	1.25 ± 0.06
March 2005	1.26 ± 0.06	0.51 ± 0.03
April 2005	3.47 ± 0.17	0.80 ± 0.04
May 2005	3.37 ± 0.27	0.54 ± 0.04
June 2005	3.56 ± 0.19	0.77 ± 0.04
July 2005	3.00 ± 0.17	0.74 ± 0.04
August 2005	2.83 ± 0.19	0.72 ± 0.04
September 2005	3.08 ± 0.21	1.11 ± 0.06
October 2005	2.23 ± 0.13	1.41 ± 0.07
November 2005	1.48 ± 0.16	1.38 ± 0.07
December 2005	1.87 ± 0.11	0.56 ± 0.03
January 2006	2.04 ± 0.12	1.63 ± 0.08
February 2006	1.70 ± 0.09	0.91 ± 0.05
March 2006	2.11 ± 0.12	0.89 ± 0.05
April 2006	2.23 ± 0.11	0.76 ± 0.05
May 2006	3.58 ± 0.22	0.59 ± 0.04
June 2006	2.57 ± 0.14	0.63 ± 0.04
July 2006	3.64 ± 0.27	0.66 ± 0.04
August 2006	1.76 ± 0.12	0.34 ± 0.02
September 2006	2.07 ± 0.11	0.61 ± 0.04
October 2006	1.31 ± 0.08	0.74 ± 0.04

continued ...

continued ...

Month/Year	**^{7}Be [mBq m^{-3}]**	**^{210}Pb [mBq m^{-3}]**
November 2006	0.43 ± 0.03	0.23 ± 0.02
December 2006	0.74 ± 0.06	0.67 ± 0.04
January 2007	2.09 ± 0.15	0.63 ± 0.04
February 2007	1.66 ± 0.11	0.75 ± 0.03
March 2007	2.62 ± 0.11	0.56 ± 0.02
April 2007	3.64 ± 0.19	0.46 ± 0.02
May 2007	2.94 ± 0.13	0.66 ± 0.02
June 2007	3.26 ± 0.14	0.60 ± 0.02
July 2007	2.75 ± 0.12	0.60 ± 0.02
August 2007	2.86 ± 0.13	0.76 ± 0.03
September 2007	3.04 ± 0.26	0.60 ± 0.03

Table A.3: Activity concentrations of ^{137}Cs and ^{40}K in Bratislava ground level air from October 2003 to April 2007 (The 2σ uncertainties are used)

Sampling date	**^{137}Cs [μBq m^{-3}]**	**^{40}K [μBq m^{-3}]**
9.10.-9.12.2003	0.52 ± 0.10	6.06 ± 0.82
12.12.-19.1.2004	< 0.41	3.21 ± 0.66
19.1.-1.3.2004	0.42 ± 0.08	4.35 ± 0.72
2.3.-20.4.2004	0.49 ± 0.12	6.68 ± 1.40
26.4.-1.6.2004	1.01 ± 0.20	7.44 ± 1.28
3.6.-25.6.2004	< 0.37	4.14 ± 0.86
25.6.-15.7.2004	< 0.29	1.20 ± 0.18
15.7.-11.8.2004	0.63 ± 0.12	5.00 ± 0.92
13.8.-3.9.2004	< 0.29	4.39 ± 0.60
13.9.-27.7.2004	< 0.37	1.55 ± 0.36
30.9.-15.10.2004	< 0.27	5.04 ± 0.84
15.10.-3.11.2004	0.51 ± 0.14	7.63 ± 1.54
3.11.-16.11.2004	0.76 ± 0.16	5.10 ± 0.96
16.11.-1.12.2004	0.72 ± 0.12	4.91 ± 0.62
1.12.-16.12.2004	0.59 ± 0.12	4.96 ± 0.76
16.12.2004-3.1.2005	1.05 ± 0.14	7.35 ± 0.94
19.1.-2.2.2005	0.54 ± 0.10	5.59 ± 0.80
2.2.-14.2.2005	1.10 ± 0.22	10.30 ± 1.60
23.2.-16.3.2005	0.54 ± 0.12	8.67 ± 1.24
16.3.-30.3.2005	0.40 ± 0.08	5.87 ± 0.88
30.3.-13.4.2005	0.79 ± 0.16	4.12 ± 0.94
20.4.-4.5.2005	< 0.25	< 0.24
4.5.-19.5.2005	< 0.23	2.74 ± 0.42
19.5.-1.6.2005	< 0.36	4.41 ± 0.74
1.6.-22.6.2005	< 0.47	8.27 ± 1.76
22.6.-6.7.2005	0.36 ± 0.10	2.33 ± 0.48
6.7.-21.7.2005	< 0.31	1.64 ± 0.38
21.7.-3.8.2005	0.69 ± 0.22	8.39 ± 1.72
3.8.-17.8.2005	0.47 ± 0.12	3.88 ± 0.78
18.8.-31.8.2005	< 0.41	< 0.47
31.8.-28.9.2005	0.36 ± 0.10	6.20 ± 1.06
28.9.-12.10.2005	0.61 ± 0.14	12.97 ± 1.74
5.10.-2.11.2005	0.69 ± 0.14	11.82 ± 1.64
2.11.-21.11.2005	0.54 ± 0.14	10.51 ± 2.02
7.12.-29.12.2005	0.89 ± 0.18	7.22 ± 1.50
4.1.-1.2.2006	1.25 ± 0.16	10.75 ± 1.44
1.2.-1.3.2006	0.91 ± 0.16	7.94 ± 1.44
1.3.-30.3.2006	0.82 ± 0.18	5.47 ± 1.22

continued ...

continued ...

Sampling date	^{137}**Cs** [μ**Bq m**$^{-3}$]	^{40}**K** [μ**Bq m**$^{-3}$]
30.3.-26.4.2006	0.26 ± 0.08	4.97 ± 0.98
3.5.-31.5.2006	0.59 ± 0.12	3.87 ± 0.94
31.5.-28.6.2006	0.21 ± 0.06	1.48 ± 0.32
28.6.-2.8.2006	0.12 ± 0.04	2.09 ± 0.44
2.8.-30.8.2006	$<$ 0.12	2.10 ± 0.48
30.8.-4.10.2006	0.10 ± 0.02	2.60 ± 0.46
4.10.-31.10.2006	0.11 ± 0.02	2.91 ± 0.40
31.10.-29.11.2006	$<$ 0.09	1.62 ± 0.50
29.11.2006-3.1.2007	0.18 ± 0.04	4.45 ± 0.70
3.1.-31.1.2007	0.49 ± 0.06	4.01 ± 0.54
31.1.-28.2.2007	0.38 ± 0.06	4.61 ± 0.74
28.2.-28.3.2007	0.24 ± 0.04	3.41 ± 0.56
28.3.-18.4.2007	0.37 ± 0.06	5.51 ± 0.82
18.4.-2.5.2007	0.30 ± 0.10	7.62 ± 1.54
30.5.-27.6.07	0.20 ± 0.02	3.81 ± 0.25
37.6.-1.8.07	0.20 ± 0.02	2.77 ± 0.19
1.8.-30.8.07	0.22 ± 0.02	3.18 ± 0.16
30.8.-26.9.07	0.20 ± 0.02	2.29 ± 0.20

Appendix B

Activity concentrations in precipitation and depositions

Table B.1: Activity concentration and monthly deposition of ^{7}Be in Bratislava from July 2005 to March 2007 (The 2σ uncertainties are used)

Month	**Concentration [kBq m^{-3}]**	**Deposition [Bq m^{-2}]**
July 2005	1.85 ± 0.06	116.41 ± 3.56
August 2005	1.84 ± 0.06	185.72 ± 3.98
September 2005	1.58 ± 0.11	62.58 ± 4.37
October 2005	2.03 ± 0.22	6.60 ± 0.70
November 2005	1.02 ± 0.04	27.10 ± 0.58
December 2005	1.10 ± 0.02	79.40 ± 1.19
January 2006	0.79 ± 0.10	19.89 ± 1.98
February 2006	0.97 ± 0.06	50.15 ± 1.38
March 2006	0.85 ± 0.02	51.10 ± 1.49
April 2006	1.57 ± 0.03	130.87 ± 2.70
May 2006	1.21 ± 0.03	86.19 ± 2.12
June 2006	1.74 ± 0.04	164.17 ± 3.43
July 2006	2.14 ± 0.04	58.20 ± 1.00
August 2006	1.01 ± 0.01	126.12 ± 1.50
September 2006	1.01 ± 0.04	18.25 ± 0.60
October 2006	0.54 ± 0.02	10.47 ± 0.33
November 2006	1.38 ± 0.02	52.22 ± 0.73
December 2006	1.70 ± 0.01	39.29 ± 0.20
January 2007	2.96 ± 0.03	116.06 ± 1.11
February 2007	1.42 ± 0.03	59.30 ± 1.40
March 2007	1.44 ± 0.02	95.77 ± 1.07
April 2007	6.72 ± 0.40	2.75 ± 0.16
May 2007	0.94 ± 0.02	46.88 ± 0.91

continued ...

continued ...

Month	Concentration [kBq m^{-3}]	Deposition [Bq m^{-2}]
June 2007	1.68 ± 0.03	94.82 ± 1.73
July 2007	1.44 ± 0.04	62.63 ± 1.72
August 2007	2.06 ± 0.03	100.70 ± 1.56
September 2007	1.76 ± 0.03	279.76 ± 5.53

Table B.2: Activity concentration and monthly deposition of ^{210}Pb in Bratislava from July 2005 to March 2007 (The 2σ uncertainties are used)

Month	Concentration [kBq m^{-3}]	Deposition [Bq m^{-2}]
July 2005	0.10 ± 0.01	6.41 ± 0.24
August 2005	0.09 ± 0.01	9.24 ± 0.28
September 2005	0.11 ± 0.01	2.81 ± 0.22
October 2005	0.39 ± 0.08	0.96 ± 0.04
November 2005	0.30 ± 0.01	7.89 ± 0.11
December 2005	0.22 ± 0.01	15.72 ± 0.36
January 2006	0.26 ± 0.03	5.25 ± 0.34
February 2006	0.24 ± 0.03	6.06 ± 0.78
March 2006	0.19 ± 0.01	5.36 ± 0.30
April 2006	0.20 ± 0.01	8.53 ± 0.46
May 2006	0.13 ± 0.01	4.65 ± 0.36
June 2006	0.19 ± 0.01	17.79 ± 0.47
July 2006	0.23 ± 0.01	6.37 ± 0.27
August 2006	0.10 ± 0.00	11.89 ± 0.38
September 2006	0.16 ± 0.01	2.93 ± 0.12
October 2006	0.14 ± 0.01	2.64 ± 0.18
November 2006	0.11 ± 0.00	4.08 ± 0.16
December 2006	0.26 ± 0.01	6.11 ± 0.18
January 2007	0.26 ± 0.02	10.04 ± 0.86
February 2007	0.22 ± 0.01	9.07 ± 0.22
March 2007	0.17 ± 0.00	11.13 ± 0.23
April 2007	2.27 ± 5.53	0.93 ± 0.13
May 2007	0.14 ± 0.00	7.17 ± 0.14
June 2007	0.22 ± 0.00	12.37 ± 0.23
July 2007	0.19 ± 0.01	8.03 ± 0.30
August 2007	0.31 ± 0.01	15.23 ± 0.51
September 2007	0.09 ± 0.01	15.10 ± 0.30

Table B.3: Activity concentration and monthly deposition of ^{137}Cs in Bratislava from July 2005 to March 2007 (The 2σ uncertainties are used)

Month	**Concentration [Bq m^{-3}]**	**Deposition [mBq m^{-2}]**
July 2005	1.00 ± 0.26	62.83 ± 16.16
August 2005	0.75 ± 0.28	75.87 ± 28.36
September 2005	1.99 ± 0.92	78.91 ± 36.47
October 2005	15.21 ± 6.16	49.57 ± 20.10
November 2005	2.79 ± 0.45	74.04 ± 11.89
December 2005	0.74 ± 0.16	53.09 ± 11.48
January 2006	NA	NA
February 2006	0.31 ± 0.23	15.93 ± 11.91
March 2006	0.72 ± 0.30	42.55 ± 18.14
April 2006	0.65 ± 0.24	54.13 ± 19.64
May 2006	0.75 ± 0.34	52.35 ± 23.71
June 2006	NA	NA
July 2006	0.87 ± 0.33	23.63 ± 8.93
August 2006	0.17 ± 0.05	20.82 ± 6.05
September 2006	0.58 ± 0.27	10.38 ± 4.81
October 2006	0.56 ± 0.20	10.91 ± 3.88
November 2006	0.36 ± 0.13	13.62 ± 4.77
December 2006	0.57 ± 0.27	13.20 ± 6.23
January 2007	0.74 ± 0.20	29.07 ± 7.70
February 2007	0.46 ± 0.24	19.29 ± 10.16
March 2007	0.28 ± 0.10	18.46 ± 6.81
April 2007	6.21 ± 2.99	2.54 ± 1.23
May 2007	1.27 ± 0.23	63.20 ± 11.60
June 2007	1.79 ± 0.28	101.02 ± 15.65
July 2007	0.34 ± 0.19	14.59 ± 8.21
August 2007	0.29 ± 0.09	13.96 ± 4.47
September 2007	NA	NA

NA: Not measured

Table B.4: Activity concentration and monthly deposition of ^{40}K in Bratislava from July 2005 to March 2007 (The 2σ uncertainties are used)

Month	**Concentration [Bq m^{-3}]**	**Deposition [mBq m^{-2}]**
July 2005	19.24 ± 4.54	1211.81 ± 285.87
August 2005	19.66 ± 5.94	1987.38 ± 600.19
September 2005	36.62 ± 15.20	1452.18 ± 602.72
October 2005	417.44 ± 140.72	1360.85 ± 458.76
November 2005	26.66 ± 5.30	706.58 ± 140.58
December 2005	10.56 ± 2.04	759.67 ± 146.58
January 2006	NA	NA
February 2006	9.67 ± 4.18	500.13 ± 216.28
March 2006	10.59 ± 3.81	631.64 ± 227.41
April 2006	14.06 ± 3.57	1173.93 ± 298.32
May 2006	11.70 ± 3.85	822.12 ± 270.59
June 2006	15.29 ± 3.24	1438.39 ± 304.87
July 2006	20.56 ± 4.17	557.97 ± 113.25
August 2006	5.78 ± 0.93	720.20 ± 115.96
September 2006	26.17 ± 5.46	471.05 ± 98.24
October 2006	33.22 ± 5.00	645.42 ± 97.06
November 2006	12.78 ± 2.61	485.10 ± 99.14
December 2006	17.85 ± 5.38	412.83 ± 124.55
January 2007	12.48 ± 2.74	489.53 ± 107.34
February 2007	14.05 ± 3.74	588.00 ± 156.37
March 2007	10.34 ± 2.00	685.32 ± 132.84
April 2007	798.88 ± 199.18	327.54 ± 81.67
May 2007	15.08 ± 2.92	751.58 ± 145.65
June 2007	10.93 ± 2.70	616.74 ± 152.23
July 2007	11.75 ± 4.25	509.11 ± 184.15
August 2007	13.56 ± 2.87	662.42 ± 140.11
September 2007	4.22 ± 1.23	672.00 ± 195.63

NA: Not measured

Appendix C

Concentrations of elements in air

Table C.1: Elemental concentrations of Na, Al, and Cl in Bratislava ground level air in 2004 [ng m^{-3}] (The 1σ uncertainties are used)

Sampling date	**Na [ng m^{-3}]**	**Al [ng m^{-3}]**	**Cl [ng m^{-3}]**
7.1.-19.1.04	73.0 ± 6.9	39.7 ± 3.3	42.0 ± 3.2
2.2.-12.2.04	68.0 ± 7.8	53.9 ± 2.6	37.3 ± 14.9
2.3.-16.3.04	94.6 ± 10.0	68.5 ± 3.4	40.2 ± 15.4
6.4.-20.4.04	127.1 ± 12.7	206.0 ± 9.8	36.6 ± 14.9
12.5.-25.5.04	99.3 ± 9.4	130.0 ± 14.4	48.8 ± 3.8
27.5.-1.6.04	120.6 ± 12.1	425.6 ± 20.1	72.6 ± 20.2
14.6.-21.6.04	218.9 ± 20.4	912.4 ± 43.0	85.6 ± 22.2
9.7.-15.7.04	58.5 ± 7.0	372.1 ± 17.6	40.2 ± 15.4
13.8.-20.8.04	108.1 ± 11.2	507.5 ± 23.9	65.1 ± 19.1
13.9.-17.9.04	261.9 ± 23.8	311.4 ± 14.7	58.6 ± 18.1
13.9.-29.9.04	307.9 ± 27.6	123.3 ± 5.9	76.5 ± 20.7
6.10.-15.10.04	78.1 ± 7.4	319.8 ± 35.3	63.4 ± 4.9
14.10.-28.10.04	97.2 ± 10.3	135.8 ± 6.5	48.3 ± 16.6
3.11.-10.11.04	141.8 ± 13.9	289.4 ± 13.7	102.1 ± 24.7
16.11.-24.11.04	117.1 ± 11.8	115.6 ± 5.5	39.5 ± 15.2
9.12.-16.12.04	92.9 ± 9.8	172.2 ± 8.2	31.7 ± 14.2

Table C.2: Elemental concentrations of K, Ca, and Sc in Bratislava ground level air in 2004 [ng m^{-3}] (The 1σ uncertainties are used)

Sampling date	**K [ng m^{-3}]**	**Ca [ng m^{-3}]**	**Sc [ng m^{-3}]**
7.1.-19.1.04	140.1 ± 32.2	54.3 ± 12.6	NA
2.2.-12.2.04	71.6 ± 14.0	59.3 ± 8.9	NA
2.3.-16.3.04	133.3 ± 24.5	91.3 ± 12.2	NA
6.4.-20.4.04	218.5 ± 33.3	307.5 ± 25.5	0.0321 ± 0.0070
12.5.-25.5.04	95.1 ± 24.8	185.2 ± 41.0	NA
27.5.-1.6.04	203.8 ± 31.2	311.9 ± 33.1	0.0400 ± 0.0086
14.6.-21.6.04	262.6 ± 63.1	249.4 ± 24.0	0.0309 ± 0.0071
9.7.-15.7.04	109.0 ± 26.8	72.8 ± 10.8	0.0074 ± 0.0026
13.8.-20.8.04	165.2 ± 47.1	262.0 ± 25.4	0.0320 ± 0.0097
13.9.-17.9.04	207.4 ± 28.9	243.9 ± 24.6	NA
13.9.-29.9.04	185.3 ± 29.9	173.4 ± 18.9	0.0400 ± 0.0131
6.10.-15.10.04	221.7 ± 54.8	261.0 ± 57.9	NA
14.10.-28.10.04	244.4 ± 42.8	134.3 ± 15.5	0.0242 ± 0.0141
3.11.-10.11.04	290.1 ± 42.6	202.9 ± 20.1	NA
16.11.-24.11.04	118.7 ± 19.7	73.2 ± 9.1	NA
9.12.-16.12.04	273.1 ± 26.9	117.4 ± 14.3	NA

Table C.3: Elemental concentrations of Ti, V, and Cr in Bratislava ground level air in 2004 [ng m^{-3}] (The 1σ uncertainties are used)

Sampling date	**Ti [ng m^{-3}]**	**V [ng m^{-3}]**	**Cr [ng m^{-3}]**
7.1.-19.1.04	3.80 ± 1.07	0.69 ± 0.03	0.26 ± 0.03
2.2.-12.2.04	4.37 ± 0.90	0.28 ± 0.06	NA
2.3.-16.3.04	3.24 ± 1.29	1.42 ± 0.28	NA
6.4.-20.4.04	10.54 ± 2.96	1.13 ± 0.23	1.15 ± 0.31
12.5.-25.5.04	7.78 ± 1.89	0.57 ± 0.03	0.40 ± 0.01
27.5.-1.6.04	13.48 ± 3.30	0.65 ± 0.13	1.38 ± 0.39
14.6.-21.6.04	< 2.70	0.59 ± 0.17	1.48 ± 0.32
9.7.-15.7.04	5.81 ± 2.97	0.39 ± 0.09	0.56 ± 0.23
13.8.-20.8.04	8.07 ± 4.26	0.85 ± 0.18	< 0.10
13.9.-17.9.04	14.07 ± 3.53	1.12 ± 0.23	NA
13.9.-29.9.04	8.10 ± 2.16	0.82 ± 0.16	1.39 ± 0.97
6.10.-15.10.04	12.03 ± 2.74	1.61 ± 0.08	0.68 ± 0.02
14.10.-28.10.04	4.57 ± 2.34	1.62 ± 0.32	8.15 ± 2.34
3.11.-10.11.04	8.38 ± 4.11	1.46 ± 0.29	NA
16.11.-24.11.04	3.40 ± 1.13	0.53 ± 0.11	NA
9.12.-16.12.04	5.38 ± 1.50	0.97 ± 0.19	NA

Table C.4: Elemental concentrations of Mn, Fe and Ni in Bratislava ground level air in 2004 [ng m^{-3}] (The 1σ uncertainties are used)

Sampling date	**Mn [ng m^{-3}]**	**Fe [ng m^{-3}]**	**Ni [ng m^{-3}]**
7.1.-19.1.04	1.87 ± 0.16	NA	0.491 ± 0.040
2.2.-12.2.04	1.96 ± 0.08	NA	< 0.230
2.3.-16.3.04	4.06 ± 0.17	NA	< 0.232
6.4.-20.4.04	5.79 ± 0.23	251.7 ± 38.5	< 0.245
12.5.-25.5.04	3.86 ± 0.33	NA	0.385 ± 0.028
27.5.-1.6.04	7.23 ± 0.28	285.2 ± 40.8	< 0.240
14.6.-21.6.04	8.56 ± 0.36	143.7 ± 33.9	< 0.244
9.7.-15.7.04	3.80 ± 0.16	85.4 ± 21.2	< 0.176
13.8.-20.8.04	6.71 ± 0.28	252.0 ± 88.7	0.410 ± 0.153
13.9.-17.9.04	5.97 ± 0.24	NA	< 0.204
13.9.-29.9.04	3.52 ± 0.15	< 60.0	< 0.230
6.10.-15.10.04	7.52 ± 0.64	NA	0.896 ± 0.026
14.10.-28.10.04	5.25 ± 0.22	< 60.0	< 0.270
3.11.-10.11.04	5.80 ± 0.24	NA	NA
16.11.-24.11.04	2.56 ± 0.11	NA	0.499 ± 0.079
9.12.-16.12.04	4.46 ± 0.18	NA	0.399 ± 0.133

Table C.5: Elemental concentrations of Cu, Zn and Ga in Bratislava ground level air in 2004 [ng m^{-3}] (The 1σ uncertainties are used)

Sampling date	**Cu [ng m^{-3}]**	**Zn [ng m^{-3}]**	**Ga [ng m^{-3}]**
7.1.-19.1.04	4.28 ± 0.10	26.2 ± 2.7	NA
2.2.-12.2.04	8.04 ± 0.06	24.9 ± 0.1	NA
2.3.-16.3.04	9.12 ± 0.05	30.1 ± 0.1	NA
6.4.-20.4.04	5.36 ± 0.03	28.5 ± 0.2	0.0177 ± 0.0023
12.5.-25.5.04	5.11 ± 0.12	24.7 ± 2.5	NA
27.5.-1.6.04	22.74 ± 0.07	43.7 ± 0.1	0.0194 ± 0.0023
14.6.-21.6.04	27.24 ± 0.09	44.9 ± 0.2	0.0237 ± 0.0036
9.7.-15.7.04	13.68 ± 0.06	26.6 ± 0.1	< 0.0070
13.8.-20.8.04	13.87 ± 0.05	30.5 ± 0.1	0.0210 ± 0.0036
13.9.-17.9.04	5.70 ± 0.02	28.6 ± 0.2	NA
13.9.-29.9.04	5.61 ± 0.03	26.1 ± 0.1	< 0.0070
6.10.-15.10.04	8.32 ± 0.17	19.9 ± 2.0	NA
14.10.-28.10.04	6.16 ± 0.03	30.9 ± 0.2	< 0.0070
3.11.-10.11.04	NA	NA	NA
16.11.-24.11.04	12.79 ± 0.06	25.6 ± 0.0	NA
9.12.-16.12.04	5.16 ± 0.05	42.9 ± 0.1	NA

Table C.6: Elemental concentrations of As, Se and Br in Bratislava ground level air in 2004 [ng m^{-3}] (The 1σ uncertainties are used)

Sampling date	**As [ng m^{-3}]**	**Se [ng m^{-3}]**	**Br [ng m^{-3}]**
7.1.-19.1.04	NA	NA	2.11 ± 0.22
2.2.-12.2.04	NA	NA	1.85 ± 0.26
2.3.-16.3.04	NA	NA	4.04 ± 0.55
6.4.-20.4.04	0.712 ± 0.022	0.477 ± 0.175	4.26 ± 0.59
12.5.-25.5.04	NA	NA	2.05 ± 0.22
27.5.-1.6.04	0.445 ± 0.016	0.642 ± 0.215	3.86 ± 0.54
14.6.-21.6.04	0.279 ± 0.014	0.422 ± 0.181	3.65 ± 0.52
9.7.-15.7.04	0.108 ± 0.007	0.131 ± 0.068	1.68 ± 0.24
13.8.-20.8.04	0.304 ± 0.015	0.125 ± 0.152	2.80 ± 0.40
13.9.-17.9.04	NA	NA	3.61 ± 0.50
13.9.-29.9.04	0.295 ± 0.018	0.333 ± 0.203	3.14 ± 0.44
6.10.-15.10.04	NA	NA	3.38 ± 0.36
14.10.-28.10.04	0.621 ± 0.023	1.014 ± 0.611	4.16 ± 0.57
3.11.-10.11.04	NA	NA	6.03 ± 0.82
16.11.-24.11.04	NA	NA	3.01 ± 0.41
9.12.-16.12.04	NA	NA	8.65 ± 1.16

Table C.7: Elemental concentrations of Rb, Cd and In in Bratislava ground level air in 2004 [ng m^{-3}] (The 1σ uncertainties are used)

Sampling date	**Rb [ng m^{-3}]**	**Cd [ng m^{-3}]**	**In [ng m^{-3}]**
7.1.-19.1.04	NA	0.120 ± 0.016	4.40E-03 ± 6.24E-04
2.2.-12.2.04	NA	0.092 ± 0.051	< 8.00E-04
2.3.-16.3.04	NA	0.255 ± 0.058	4.76E-03 ± 3.64E-04
6.4.-20.4.04	3.40E-04 ± 1.56E-04	0.160 ± 0.026	2.23E-03 ± 2.53E-04
12.5.-25.5.04	NA	0.067 ± 0.005	7.68E-03 ± 1.09E-03
27.5.-1.6.04	1.47E-04 ± 8.28E-05	0.397 ± 0.027	1.05E-03 ± 2.25E-04
14.6.-21.6.04	6.76E-05 ± 5.14E-05	< 0.019	7.07E-04 ± 3.34E-04
9.7.-15.7.04	< 1.50E-04	0.018 ± 0.012	< 8.00E-04
13.8.-20.8.04	< 1.50E-04	0.065 ± 0.041	9.46E-04 ± 3.21E-04
13.9.-17.9.04	NA	0.031 ± 0.010	5.23E-04 ± 1.88E-04
13.9.-29.9.04	< 1.50E-04	0.161 ± 0.016	1.49E-02 ± 8.65E-04
6.10.-15.10.04	NA	0.108 ± 0.011	1.08E-02 ± 1.53E-03
14.10.-28.10.04	< 1.50E-04	0.135 ± 0.027	4.10E-04 ± 2.17E-04
3.11.-10.11.04	NA	NA	7.73E-04 ± 2.84E-04
16.11.-24.11.04	NA	0.092 ± 0.012	9.00E-04 ± 1.66E-04
9.12.-16.12.04	NA	0.250 ± 0.020	8.68E-04 ± 1.71E-04

Table C.8: Elemental concentrations of Sb, I and Cs in Bratislava ground level air in 2004 [ng m^{-3}] (The 1σ uncertainties are used)

Sampling date	**Sb [ng m^{-3}]**	**I [ng m^{-3}]**	**Cs [ng m^{-3}]**
7.1.-19.1.04	NA	1.65 ± 0.22	NA
2.2.-12.2.04	NA	0.65 ± 0.03	NA
2.3.-16.3.04	NA	1.19 ± 0.06	NA
6.4.-20.4.04	1.058 ± 0.531	0.90 ± 0.05	0.0663 ± 0.0393
12.5.-25.5.04	NA	0.79 ± 0.11	NA
27.5.-1.6.04	1.923 ± 0.965	0.65 ± 0.04	0.0720 ± 0.0436
14.6.-21.6.04	1.623 ± 0.815	0.39 ± 0.03	0.0305 ± 0.0211
9.7.-15.7.04	1.025 ± 0.549	0.28 ± 0.02	0.0367 ± 0.0236
13.8.-20.8.04	0.997 ± 0.501	0.46 ± 0.03	0.0300 ± 0.0212
13.9.-17.9.04	NA	0.61 ± 0.03	NA
13.9.-29.9.04	0.476 ± 0.240	0.52 ± 0.03	$<$ 0.0300
6.10.-15.10.04	NA	1.30 ± 0.17	NA
14.10.-28.10.04	0.822 ± 0.414	0.68 ± 0.04	0.0534 ± 0.0347
3.11.-10.11.04	NA	0.92 ± 0.05	NA
16.11.-24.11.04	NA	0.59 ± 0.03	NA
9.12.-16.12.04	NA	0.92 ± 0.05	NA

Table C.9: Elemental concentrations of Ba, La and Sm in Bratislava ground level air in 2004 [ng m^{-3}] (The 1σ uncertainties are used)

Sampling date	**Ba [ng m^{-3}]**	**La [ng m^{-3}]**	**Sm [ng m^{-3}]**
7.1.-19.1.04	1.17 ± 0.46	NA	NA
2.2.-12.2.04	0.91 ± 0.40	NA	NA
2.3.-16.3.04	1.62 ± 0.71	NA	NA
6.4.-20.4.04	2.68 ± 1.08	0.121 ± 0.036	1.38E-02 ± 3.69E-03
12.5.-25.5.04	2.65 ± 0.97	NA	NA
27.5.-1.6.04	3.32 ± 1.28	0.042 ± 0.021	1.47E-02 ± 3.86E-03
14.6.-21.6.04	2.34 ± 1.03	0.038 ± 0.019	1.58E-02 ± 4.58E-03
9.7.-15.7.04	2.56 ± 1.28	$<$ 0.057	2.10E-03 ± 1.82E-03
13.8.-20.8.04	2.03 ± 1.07	0.070 ± 0.041	9.02E-03 ± 3.26E-03
13.9.-17.9.04	2.91 ± 1.13	NA	NA
13.9.-29.9.04	1.61 ± 0.72	0.099 ± 0.078	1.12E-02 ± 3.99E-03
6.10.-15.10.04	3.79 ± 1.50	NA	NA
14.10.-28.10.04	1.27 ± 0.71	0.166 ± 0.079	1.19E-02 ± 5.02E-03
3.11.-10.11.04	2.11 ± 1.01	NA	NA
16.11.-24.11.04	0.74 ± 0.38	NA	NA
9.12.-16.12.04	$<$ 1.52	NA	NA

Table C.10: Elemental concentrations of Dy, Tm and W in Bratislava ground level air in 2004 [ng m^{-3}] (The 1σ uncertainties are used)

Sampling date	**Dy [ng m^{-3}]**	**Tm [ng m^{-3}]**	**W [ng m^{-3}]**
7.1.-19.1.04	< 3.00E-03	NA	NA
2.2.-12.2.04	2.64E-03 ± 1.00E-03	NA	NA
2.3.-16.3.04	5.31E-03 ± 2.66E-03	NA	NA
6.4.-20.4.04	1.34E-02 ± 4.24E-03	0.034 ± 0.025	0.0949 ± 0.0541
12.5.-25.5.04	1.02E-02 ± 2.10E-03	NA	NA
27.5.-1.6.04	1.56E-02 ± 4.09E-03	0.127 ± 0.082	0.1897 ± 0.0990
14.6.-21.6.04	7.40E-03 ± 4.41E-03	< 0.030	0.2275 ± 0.1190
9.7.-15.7.04	< 3.00E-03	0.025 ± 0.019	0.2935 ± 0.1523
13.8.-20.8.04	1.36E-02 ± 4.83E-03	0.139 ± 0.113	0.8226 ± 0.4368
13.9.-17.9.04	1.07E-02 ± 3.14E-03	NA	NA
13.9.-29.9.04	9.75E-03 ± 3.70E-03	0.144 ± 0.130	0.0508 ± 0.0513
6.10.-15.10.04	1.43E-02 ± 4.16E-03	NA	NA
14.10.-28.10.04	7.58E-03 ± 4.45E-03	0.070 ± 0.061	0.2225 ± 0.1239
3.11.-10.11.04	1.19E-02 ± 4.82E-06	NA	NA
16.11.-24.11.04	2.33E-03 ± 1.08E-03	NA	NA
9.12.-16.12.04	1.34E-02 ± 8.04E-03	NA	NA

Table C.11: Elemental concentrations of Au, Hg and Pb in Bratislava ground level air in 2004 [ng m^{-3}] (The 1σ uncertainties are used)

Sampling date	**Au [ng m^{-3}]**	**Hg [ng m^{-3}]**	**Pb [ng m^{-3}]**
7.1.-19.1.04	NA	NA	24.9 ± 0.9
2.2.-12.2.04	NA	NA	18.1 ± 0.2
2.3.-16.3.04	NA	NA	32.8 ± 0.2
6.4.-20.4.04	2.35E-04 ± 8.54E-05	0.0344 ± 0.0247	29.7 ± 0.1
12.5.-25.5.04	NA	NA	55.2 ± 1.3
27.5.-1.6.04	2.13E-04 ± 8.22E-05	0.0114 ± 0.0076	80.7 ± 0.4
14.6.-21.6.04	6.60E-04 ± 2.12E-04	< 0.0100	39.3 ± 0.4
9.7.-15.7.04	2.12E-04 ± 7.49E-05	0.0184 ± 0.0140	39.9 ± 0.1
13.8.-20.8.04	2.57E-04 ± 1.61E-04	0.5613 ± 0.2745	21.0 ± 0.3
13.9.-17.9.04	NA	NA	13.2 ± 0.2
13.9.-29.9.04	3.26E-04 ± 1.64E-04	0.4164 ± 0.3015	11.8 ± 0.1
6.10.-15.10.04	NA	NA	22.5 ± 0.6
14.10.-28.10.04	1.23E-04 ± 1.08E-04	0.0945 ± 0.0601	12.3 ± 0.2
3.11.-10.11.04	NA	NA	NA
16.11.-24.11.04	NA	NA	10.0 ± 0.1
9.12.-16.12.04	NA	NA	10.8 ± 0.1

Table C.12: Elemental concentrations of Th, and U in Bratislava ground level air in 2004 [ng m^{-3}] (The 1σ uncertainties are used)

Sampling date	**Th [ng m^{-3}]**	**U [ng m^{-3}]**
7.1.-19.1.04	NA	0.0090 ± 0.0024
2.2.-12.2.04	NA	0.0045 ± 0.0012
2.3.-16.3.04	NA	0.0122 ± 0.0024
6.4.-20.4.04	0.0421 ± 0.0129	0.0126 ± 0.0027
12.5.-25.5.04	NA	0.0160 ± 0.0042
27.5.-1.6.04	0.0446 ± 0.0118	0.0145 ± 0.0033
14.6.-21.6.04	0.0242 ± 0.0066	0.0188 ± 0.0065
9.7.-15.7.04	0.0048 ± 0.0038	0.0100 ± 0.0032
13.8.-20.8.04	0.0796 ± 0.0299	0.0171 ± 0.0082
13.9.-17.9.04	NA	0.0125 ± 0.0029
13.9.-29.9.04	$<$ 0.0120	0.0125 ± 0.0028
6.10.-15.10.04	NA	0.0181 ± 0.0050
14.10.-28.10.04	$<$ 0.0120	0.0119 ± 0.0028
3.11.-10.11.04	NA	0.0113 ± 0.0034
16.11.-24.11.04	NA	0.0049 ± 0.0014
9.12.-16.12.04	NA	0.0105 ± 0.0020

NA: Concentration of the particular element was not determined

Bibliography

[Azahra03] M. Azahra, A. Camacho-García, C. González-Gómez, J.J. López-Peñalver, T. El Bardouni (2003) Seasonal ^{7}Be Concentrations in Near-Surface Air of Granada (Spain) in the Period 1993-2001. *Applied Radiation and Isotopes* **59**, 159-164.

[Bailey02] R.A. Bailey, H.M. Clark, J.P. Ferris, S. Krause, R.L. Strong (2002) Chemistry of the environment, Elsevier, Academic Press, ISBN: 978-0-12-073461-0.

[Baskaran01] M. Baskaran, G.E. Shaw (2001) Residence time of artic haze aerosols using the concentrations and activity ratios of ^{210}Po, ^{210}Pb and ^{7}Be. *Aerosol Science* **32**, 443-452.

[Baust67] E. Baust (1967) Die Anlagerung von radioaktiven Atomen und Ionen na Aerosolteilchen. *Zeitschrift für Rhysik* **199**, 187-206.

[Bem03] H. Bem, M. Galorini, E. Rizzio, M. Krzemińska (2003) Comparative studies on the concentrations of some elements in the urban air particulate matter in Lodz City of Poland and in Milan, Italy. *Environment International* **29**, 123-128.

[Berdowski97] J.J.M. Berdowski, J. Baas, J.P.J. Bloos, A.J.H. Visschedijk, P.Y.J. Zandveld (1997) The European emission inventory of heavy metals and persistent organic pollutants for 1990. Apeldoorn, TNO Institute of Environmental Sciences, Energy Research and Process Innovation (UBA-FB Report 104 02 672/03).

[Bhandari66] N. Bhandari, D. Lal, Rama (1966) Stratospheric Circulation Studies Based on Natural and Artificial Radioactive Tracer Elements. *Tellus* **XVIII**, 391-406.

[Blake99] W.H. Blake, D.E. Walling, Q. He (1999) Fallout beryllium-7 as a tracer in soil erosion investigations. *Applied Radiation and Isotopes* **51**, 599-605.

[Bleichrodt63] J.F. Bleichrodt and E.R. van Abkoude (1963) On the Deposition of Cosmic-Ray-Produced Beryllium 7. *Journal of Geophysical Research* **68**, 5283-5288.

[Bleichrodt63a] J.F. Bleichrodt and E.R. van Abkoude (1963) Artificial Beryllium 7 in the Lower Stratosphere. *Journal of Geophysical Research* **68**, 4629-4631.

[Bleichrodt78] J.F. Bleichrodt (1978) Mean Tropospheric Residence Time of Cosmic-Ray-Produced Beryllium 7 at North Temperate Latitudes. *Journal of Geophysical Research* **83**, 3058-3062.

[Bode96] P. Bode (1996) Instrumental and organizational aspects of a neutron activation analysis laboratory, CIP-DATA Koninklijkw bibliotheek, Den Haag.

[Bondietti84] E.A. Bondietti, F.O. Hoffman and I.L. Larsen (1984) Air-to-vegetation transfer rates of submicron aerosols. *Journal of Environmental Radioactivity* **1**, 5-27.

[Bondietti88] E.A. Bondietti, J.N. Brantley, C. Rangarajan (1988) Size Distributions and Growth of Natural and Chernobyl-derived Submicron Aerosols in Tennessee. *Journal of Environmental Radioactivity* **6**, 99-120.

[Brežná89] M. Brežná, D. Závodský (1989) Heavy Metals in Atmospheric Aerosols in the Region of Slovakia. (in Slovak) *Air Protection* **6**, 144-148.

[Brown89] L. Brown, G. J. Stensland, J. Klein, R. Middleton (1989) Atmospheric Deposition of ^{7}Be and ^{10}Be. *Geochimica et Cosmochimica Acta* **53**, 135-142.

[Brun87] B. Brun *et al.* (1987) GEANT3 User's Guide, Rep. DD/EE/84-1.

[Cabáneková98] H. Cabáneková, M. Vladár (1998) The Monitoring of Air Contamination in the Territory of Slovak Republic. *Journal of Radiology* **6**, 13-18.

[Cannizzaro04] F. Cannizzaro, G. Greco, M. Raneli, M.C. Spitale, E. Tomarchio (2004) Concentration measurements of Be-7 at ground level air at Palermo, Italy - comparison with solar activity over a period of 21 years. *Journal of Environmental Radioactivity* **72**, 259-271.

[Cao02] L. Cao, W. Tian, B. Ni, Y. Zhang, P. Wang (2002) Preliminary study of airborne particulate matter in a Beijing sampling station by instrumental neutron activation analysis. *Atmospheric Environment* **36**, 1951-1956.

[Cheng00] M.T. Cheng and Y.I. Tsai (2000) Characterization of visibility and atmospheric aerosols in urban, suburban, and remote areas. *The Science of The Total Environment* **263**, 101-114.

[ČHMU] ČHMU (1997-2006) Air quality. Reports of Czech Hydrometeorological Institute for years 1997 - 2006. http://www.chmi.cz/

[Ciffroy03] P. Ciffroy, J.-L. Reyss, F. Siclet (2003) Determination of the residence time of suspended particles in the turbidity maximum of the Loire estuary by ^{7}Be analysis. *Estuarine, Coastal and Shelf Science* **57**, 553-568.

[Čurlík99] J. Čurlík, P. Šefčík (1999) Geochemical atlas of the Slovak Republic. Soil. Ministry of the Environment of Slovak Republic, ISBN: 80-88833-14-0.

[Danielson42] G.C. Danielson, C. Lanczos (1942) Some improvements in practical Fourier analysis and their application to X-ray scattering from liquids. *Journal of the Franklin Institute* **233**, 365-380.

[Dockery93] D.W. Dockery, C.A. Pope, X. Xu, J.D. Spengler, J.H. Ware, M.E. Fay, B.G. Ferris, F.E. Speizer (1993) An association between air pollution and mortality in six U.S. cities. *New England Journal of Medicines* **329**, 1753-1759.

[Donaldson98] K. Donaldson, X. Y. Li, W. MacNee (1998) Ultrafine (nanometre) particle mediated lung injury. *Journal of Aerosol Science* **29**, 553-560.

[Dueñas90] C. Dueñas, M.C. Fernández, and M Senciales (1990) Usefulness of Rn, decay products of Rn, and Th B to study diffusion in the lower atmosphere. *Atmospheric Environment* **24A**, 1255-1261.

[Dueñas99] C. Dueñas, M.C. Fernández, E. Liger, J. Carretero (1999) Gross alpha, gross beta activities and ^{7}Be concentrations in surface air: analysis of their variations and prediction model. *Atmospheric Environment* **33**, 3705-3715.

[Dueñas03] C. Dueñas, M.C. Fernández, J. Carretero, E. Liger, S. Canete (2003) ^{7}Be and ^{210}Pb concentrations in air in Málaga (Spain). *Journal of Radioanalytical and Nuclear Chemistry* **257**, 249-253.

[Dueñas04] C. Dueñas, M.C. Fernández, J. Carretero, E. Liger, S. Canete (2004) Long-term variation of the concentrations of long-lived Rn descendants and cosmogenic ^{7}Be and determination of the MRT of aerosols. *Atmospheric Environment* **38**, 1291-1301.

[Ďurana96] L. Ďurana, M. Chudý, J. Masarik (1996) Investigation of ^{7}Be in the Bratislava atmosphere. *Journal of Radioanalytical and Nuclear Chemistry* **207**, 345-356.

[Dutkiewitz85] V.A. Dutkiewitz and L. Husain (1985) Stratospheric and tropospheric components of ^{7}Be in surface air. *Journal of Geophysical Research* **90**, 5783-5788.

[EC166/2000] http://ec.europa.eu/environment/air

[Eisenbud97] M. Eisenbud and T. Gesell (1997) Environmental Radioactivity: From Natural, Industrial, and Military Sources 4^{th} edition, San Diego, CA: Academic.

[El-Daoushy88] F. El-Daoushy (1988) A Summary on the Lead-210 Cycle in Nature and Related Applications in Scandinavia. *Environment International* **14**, 305-319.

[Eleftheriadis01] K. Eleftheriadis, I. Colbeck (2001) Coarse atmospheric aerosol: size distributions of trace elements. *Atmospheric Environment* **35**, 5321-5330.

[El-Hussein01] A. El-Hussein, A. Mohamemed, M. Abd EL-Hady, A.A. Ahmed, A.E. Ali, A. Barakat (2001) Diurnal and seasonal variation of short-lived radon progeny concentration and atmospheric temporal variations of ^{210}Pb and ^{7}Be in Egypt. *Atmospheric Environment* **35**, 4305-4313.

[Ewa01] I.O.B. Ewa, D. Bodizs, Sz. Cifrus, Zs. Molnar (2001) Monte Carlo determination of full energy peak efficiency for a HPGe detector. *Applied Radiation and Isotopes* **55**, 103-108.

[Feely60] H.W. Feely (1960) Strontium-90 content of the stratosphere. *Science* **131**, 645-649.

[Feely89] H.W. Feely, R.J. Larsen, C.G. Sanderson (1989) Factors that Cause Seasonal Variations in Beryllium-7 Concentrations in Surface Air. *Journal of Environmental Radioactivity* **9**, 223-249.

[Florek06] M. Florek, K. Holý, J. Merešová, I. Sýkora, M. V. Frontasyeva, E. E. Ermakova, S. S. Pavlov (2006) Application of NAA and AAS in Environmental Research in Slovakia. Conference proceedings of Environmental Physics Conference, 18-22 February 2006, Alexandria, Egypt (in press).

[Frontasyeva97] M.V. Frontasyeva, E. Steinnes (1997) Epithermal neutron activation analysis for studying the environment. Proc. Int. Symposium on Harmonization of Health Related Environmental Measurements Using Nuclear and Isotopic Techniques (Hyderabad, India, 4-7 November, 1996), IAEA 1997, 302-311.

[Frontasyeva00a] M.V. Frontasyeva, S.S. Pavlov (2000) Analytical investigation at the IBR-2 reactor in Dubna. Proceedings of the VII International Seminar on Interaction of Neutrons with Nuclei. Dubna. May 17-20. 2000. E3-2000-192. 219-227. JINR (Also JINR Preprint. E14-2000-177. Dubna. 2000).

[Frontasyeva00b] M.V. Frontasyeva, A.B. Ramadan, T.Ye. Galinskaya (2000) Weekly cycles of element pollutants in air of the Greater Cario Area (Egypt) studied by neutron activation analysis. Book of abstracts, International Aerosol Conference, 26-30 June 2000, Moscow, Russia.

[Frontasyeva06] M.V. Frontasyeva (2006) Neutron activation analysis at the IBR-2 reactor in Dubna for life sciences. *Ecological Chemistry and Engineering* **13**, 1-9.

[Gäggeler95] H.W. Gäggeler (1995) Radioactivity in the Atmosphere. *Radiochimica Acta* **70/71**, 345-353.

[Gallorini99] M. Gallorini, E. Rizzio, C. Birattari, M. Bonardi, F. Croppi (1999) Content of trace elements in the respirable fractions of the air particulate of urban and rural areas monitored by neutron activation analysis. *Biological Trace Element Research* **71**, 209-222.

[Garabík97] R. Garabík (1997) Modelovanie účinnosti HPGe detektora pre veľkoobjemové vzorky životného prostredia, Diploma Thesis, Comenius University, Bratislava.

[Gerasopoulos01] E. Gerasopoulos, P. Zanis, A. Stohl, C.S. Zerefos, C. Papastefanou, W. Ringer, L. Tobler, S. Hubener, H.W. Gäggeler, H.J. Kanter, L. Tositti, S. Sandrini (2001) A climatology of ^{7}Be at four high-altitude stations at the Alps and the northern Appennines. *Atmospheric Environment* **35**, 6347-6360.

[Graustein83] W.C. Graustein, K.K. Turekian (1983) ^{210}Pb as a tracer of the deposition of sub-micrometer aerosols. *Precipitation Scavenging, Dry Deposition, and Resuspension*, 1315-1324.

[Graustein90] W.C. Graustein, K.K. Turekian (1983) Radon fluxes from soils to the atmosphere measured by ^{210}Pb - ^{210}Ra disequilibrium in soils. *Geophysical Research Letters* **17**, 841-844.

[Graustein96] W.C. Graustein, K.K. Turekian (1996) ^{7}Be and ^{210}Pb indicate an upper troposphere source for elevated ozon in the summertime subtropical free troposphere of the eastern North Atlantic. *Geophysical Research Letters* **23**, 539-542.

[Gründel04] M. Gründel, J. Porstendörfer (2004) Differences between the activity size distributions of the different radionuclide aerosols in outdoor air. *Atmospheric Environment* **38**, 3723-3728.

[Guyodo96] Y. Guyodo and J.-P. Valet (1996) Relative variations in geomagnetic intensity from sedimentary records: The past 200,000 years. *Earth and Planetary Science Letters* **143**, 23-36.

[Heinrich07] P. Heinrich, O. Coindeau, X. Blanchard, P. Gross (2007) Simulation of the atmospheric concebtrations of ^{210}Pb and ^{7}Be and comparison with daily observations at theree surface sites. *Atmospheric Environment* **41**, 6610-6621.

[Hinds82] W.C. Hinds (1982) Aerosol Technology: Properties, Behavior, and Measurement of Airborne Particles. Wiley, New York.

[Hirose04] K. Hirose, T. Honda, S. Yagishita, Y. Igarashi, M. Aoyama (2004) Deposition behaviors of ^{210}Pb, ^{7}Be and thorium isotopes observed in Tsukuba and Nagasaki, Japan. *Atmospheric Environment* **38**, 6601-6608.

[Holý098] K. Holý, R. Böhm, I. Bosá, A. Polášková, O. Holá (1998) ^{222}Rn concentration in the outdoor atmosphere and its relation to the atmospheric stability. Conference Proceedings of the 21^{st} RHD. Jasna pod Chopkom, Slovakia. 213-216.

[Holý01] K. Holý, I. Bosá, A. Polášková, R. Böhm, O. Holá, D. Ondo-Eštok, M. Bulko (2003) Ten years of continual monitoring of ^{222}Rn concentration in Bratislava atmosphere. IRPA Regional Congress on Radiation Protection in Central europe, Bratislava, Slovakia, September 22-26, 2003, ISBN: 80-88806-43-7.

[Hötzl87] H. Hötzl and R. Winkler (1987) Activity concentrations of ^{226}Ra, ^{228}Ra, ^{210}Pb, ^{40}K and ^{7}Be and their temporal variations in surface air. *Journal of Environmental Radioactivity* **5**, 445-458.

[ICRP66] International Commision on Radiological Protection (1993) "Human Respiratory Tract Model for Radiological Protection", ICRP Publ. No. 66, Ann. of the ICRP, Vol. 24(1-3). Pergamon, Oxford.

[IPCC07] Intergovernmental Panel on Climate Change (2007) Summary for Policymakers. In: Climate change 2007: The Physical Science Basis. Contribution of working Group I to the Fourth Assessment Report of the IPCC. Cambridge University press, Cambridge, United Kingdom and New York, Ny, USA.

[Igarashi96] Y. Igarashi, M. Otsuji-Hatori and K. Hirose (1996) Recent deposition of ^{90}Sr and ^{137}Cs observed in Tsukuba. *Journal of Environmental Radioactivity*, **31**, 157-169.

[Ioannidou06] A. Ioannidou and C. Papastefanou (2006) Precipitation scavenging of ^{7}Be and^{137}Cs radionuclides in air. *Journal of Environmental Radioactivity* **85**, 121-136.

[Jasiulionis05] R. Jasiulionis, H. Wershofen (2005) A study of the vertical diffustion of the cosmogenic radionuclides, ^{7}Be and ^{22}Na in the atmosphere. *Journal of Environmental Radioactivity*, **79**, 157-169.

[Kannosto06] J. Kannosto, J. Ristimäki, A. Virtanen, J. Keskinen, P.P. Aalto, M. Kulmala (2006) Density analysis of boreal forest aerosols. *Chemical Engineering Transactions* **10**, 95-99.

[Keegan06] T.J. Keegan, M.E Farago, I. Thornton, Bing Hong, R.N. Colvile, B. Pesch, P. Jakubis and M.J. Nieuwenhuijsen (2006) Dispersion of As and selected heavy metals around a coal-burning power station in central Slovakia. *Science of the Total Environment* **358**, 61-71.

[Knies94] D.L. Knies, D. Elmore, P. Sharma, S. Vogt, R. Li, M.E. Lipschutz, G. Petty, J. Farrell, M.C. Monaghan, S. Fritz, E. Agee (1994) ^{7}Be, ^{10}Be, and

^{36}Cl in precipitation. *Nuclear Instruments and Methods in Physics Research* **B 92**, 340-344.

[Koch96] D.M. Koch and M.E. Mann (1996) Spatial and temporal variability of ^{7}Be surface concentrations. *Tellus* **48B**, 378-396.

[Koch96a] D.M. Koch, D.J. Jacob, W.C. Graustein (1996) Vertical transport of tropospheric aerosols as indicated by ^{7}Be and ^{210}Pb in a chemical tracer model. *Journal of Geophysical Research* **101**, 18,651-18,666.

[Koch98] D. Koch (1998) Beryllium 10/beryllium 7 as a tracer of stratospheric transport. *Journal of Geophysical Research* **103**, 3907-3917.

[Korčák06] D. Korčák (2006) Rádioaktivita atmosféry a jej variácie. Doctorate Thesis, Comenius University, Bratislava, Slovakia.

[Kownacka01] L. Kownacka (2001) Natural and artificial radionuclides in the tropospheric and lower stratospheric air over Poland. *Nukleonika* **46**, 175-177.

[Kozak97] K. Kozak, M. Jasinska, J.W. Mietelski (1997) Low-activity Gamma-emitters in the ground-level Air at Kraków. *Journal of Radioecology* **5**, 3-6.

[Kuča03] P. Kuča, L. Novák, P. Rulík, J. Tecl (2003) Radiation Monitoring Network of the Czech Republic. Proceedings of the IRPA Regional Congress on Radiation Protection in Central Europe, Bratislava, Slovakia, September 22-26, 2003.

[Kulan06] A. Kulan (2006) Seasonal ^{7}Be and ^{137}Cs activities in surface air before and after the Chernobyl event. *Journal of Environmental Radioactivity* **90**, 140-150.

[Lal67] D. Lal and B. Peters (1967) Cosmic ray produced radioactivity on the Earth, 551-612. Encyclopedia of physics. V. 46/2. Springer.

[Lamborg00] C.H. Lamborg, W.F. Fitzgerald, W.C. Graustein, K.K. Turekian (2000) An examination of the atmospheric chemistry of mercury using ^{210}Pb and ^{7}Be. *Journal of Atmospheric Chemistry* **36**, 325-338.

[Lamborg02] C.H. Lamborg, W.F. Fitzgerald, J. O'Donnell, T. Torgersen (2002) A non-steady-state compartmental model of global-scale mercury biogeochemistry with interhemispheric atmospheric gradients. *Geochimica et Cosmochimica Acta* **66**, 1105-1118.

[Lassen60] L. Lassen and G. Rau (1960) Die Anlagerung radioaktiver Atome an Aerosole (Schwebstoffe). *Zeitschriff für Physik* **160**, 504-519.

[Lee02] S.-H. Lee, M.K. Pham, P.P. Povinec (2002) Radionuclide variations in the air over Monaco. *Journal of Radioanalyt. and Nucl. Chemistry* **254**, 445-453.

[Likuku06] A.S. Likuku (2006) Factors influencing ambient concentrations of ^{210}Pb and ^{7}Be over the city of Edinburgh (55.9°N, 03.2°W). *Journal of Environmental Radioactivity* **87**, 289-304.

[Makarewicz05] M. Makarewicz (2005) Estimation of the uncertainty components associated with the measurement of radionuclides in air filters using γ-ray spectrometry. *Accreditation and Quality Assurance* **10**, 269-276.

[Mahover83] E.M. Mahover (1983) Climatology of tropopause. St. Petersbourgh: Gidrometeoizdat.

[Masarik99] J. Masarik and J. Beer (1999) Simulation of Particle Fluxes and Cosmogenic nuclide production in the Earth's atmosphere. *Journal of Geophysical Research* **104**, 12099-12111.

[Mason82] B. Mason (1982) "Principles of Geochemistry", 4th Ed. Wiley, New York.

[McMurray82] P.H. McMurray and J.C. Wilson (1982) Growth Laws For the Formation of Secondary Ambient Aerosols: Implications for Chemical Conversion Mechanisms. *Atmospheric Environment* **16**, 121-134.

[McNeary03] D. McNeary, M. Baskaran (2003) Depositional characteristics of ^{7}Be and ^{210}Pb in Southeastern Michigan. *Journal of Geophysical Research* **108**, 4210-4218.

[Medveď98] J. Medveď, V. Streško, J. Kubová, J. Polakovičová (1998) Efficiency of decomposition procedures for the determination of some elements in soils by atomic spectroscopic methods. *Fresenius Journal of Analytical Chemistry* **360**, 219-224.

[Medveď03] J. Medveď, V. Streško, J. Kubová, E. Chmielewská (2003) Evaluation of Atomic Spectroscopy Methods for Determination of Some Heavy Metals in Soils, Soil Extracts, Plants and Biota. *Chemical Papers* **57**, 169-171.

[Merešová02] J. Merešová (2002) Štúdium rádioaktivity aerosólovej zložky atmosféry. Diploma Thesis, Comenius University, Bratislava, Slovakia.

[Merešová04] J. Merešová, I. Sýkora, K. Holý, M. Chudý (2004) ^{210}Pb a ^{7}Be v aerosólovej zložke atmosféry v Bratislave. Conference proceedings of conference 6^{th} Banskoštiavnické dni 2004, 6-8 November 2004, Banská Štiavnica, Slovakia, 32-35.

[Merešová04a] J. Merešová, K. Holý, I. Sýkora, M. Chudý (2004) The Comparison of Radionuclides ^{222}Rn and ^{210}Pb Concentrations in the Atmosphere of Bratislava. Book of extended synopses of 26^{th} Days of Radiation Protection, Luhačovice, Czech Republic, 1-5 November 2004, 198-201

[Merešová06] J. Merešová, M. Florek, K. Holý, I. Sýkora, M. V. Frontasyeva, S.S. Pavlov (2006) Assesment of Elemental and Radionuclide Content through Analysis of Aerosol Filters from Bratislava, Slovakia. Conference proceedings of International Seminar on Interaction of Neutrons with Nuclei ISINN 13th, Dubna, Russia, 25-28 May 2005, ISBN: 5-9530-0102-9, 263-268.

[Merešová05-06] J. Merešová, M. Florek, K. Holý, I. Sýkora, M.V. Frontasyeva, S.S. Pavlov (2005-06) Concentration of Elements in Atmospheric Aerosol in Bratislava. *Acta Physica Universitatis Comenianae*, **XLVI-XLVII**, 73-82.

[Merešová05-06a] J. Merešová, I. Sýkora, K. Holý, M. Chudý (2005-06) Temporal Variations of ^{7}Be Activity Concentrations in Slovakia. *Acta Physica Universitatis Comenianae*, **XLVI-XLVII**, 83-90.

[Merešová07] J. Merešová, M. Florek, M. V. Frontasyeva, S. S. Pavlov, K. Holý, I. Sýkora (2007) Temporal Variations of Elemental Content in Atmospheric Aerosol in Bratislava, Slovakia. Conference proceedings of 15^{th} ISINN, Dubna, Russia, 16-19 May 2007 (in press).

[Moore73] H.E. Moore, S.E. Poet, E.A. Martell (1973) ^{222}Rn, ^{210}Pb, ^{210}Bi, and ^{210}Po profiles and aerosol residence times versus altitude. *Journal of Geophysical Research* **78**, 7065-7075.

[Nagai00] H. Nagai, W. Tada, T. Kobayashi (2000) Production rates of ^{7}Be and ^{10}Be in the atmosphere. *Nuclear Instruments and Methods in Physics Research* **B 172**, 796-801.

[Noone01] K. Noone (2001) The indirect radiative effect of aerosols. *IGACtivities Newsletter* **23**, 16-17.

[NRC79] NRC, National Research Council (1979) Airborne Particles. University Park Press, Baltimore, USA.

[NCRP87] National Council on Radiation Protection and Measurements (1987) Exposure of the population of the United States and Canada from natural background radiation. Report 94, Bethesda, Maryland.

[NGDC] National Geophysical Data Center, http://www.ngdc.noaa.gov/stp/ SOLAR/ftpsunspotnumber.html

[Ostrovnaya93] T.M. Ostrovnaya, L.S. Nefedyeva, V.M. Nazarov, S.V. Borzakov, L.P. Strelkova (1195) Software for INAA on the basis of relative and absolute methods using nuclear data base. In Proceedings "Activation Analysis in Environment Protection", D14-93-325, JINR, Dubna, 1993, p. 319-325.

[Papastefanou95] C. Papastefanou and A. Ioannidou (1995) Aerodynamic size association of Be-7 in ambient aerosols. *Journal of Environmental Radioactivity* **26**, 273-282.

[Papastefanou96] C. Papastefanou, M. Manolopoulou, S. Stoulos, A. Ioannidou (1996) Behavior of ^{137}Cs in the Environment one Decade after Chernobyl. *Journal of Radioecology* **4**, 9-14.

[Papastefanou06] C. Papastefanou (2006) Residence time of tropospheric aerosols in association with radioactive nuclides. *Applied Radiation and Isotopes* **64**, 93-100.

[Peresedov96] V.F. Peresedov, A.D. Rogov (1996) Simulation and analysis of neutron energy spectra from irradiation channels of the IBR-2 reactor. *J. Radioanal. And Nucl. Chem. Letters* **214(4)**, 277-283.

[Petterssen68] S. Petterssen (1968) "Introduction to Meteorology", 3rd Ed. McGraw-Hill, New York.

[Poet72] S.E. Poet, H.E/ Moore, E.A. Martell (1972) ^{210}Pb, ^{210}Bi, and ^{210}Po in the Atmosphere: Accurate measurements and application to aerosol residence time determination. *Journal of Geophysical Research* **77**, 6515-6527.

[Pope95] C.A. Pope, D.W. Dockery, J. Schwartz (1995) Review of epidemiological evidence of health effects of particulate air pollution. *Inhalation Toxicology* **7**, 1-18.

[Povinec88] P. Povinec, M. Chudý, I. Sýkora, J. Szarka, M. Pikna, K. Holý (1988) Aerosol radioactivity monitoring in Bratislava following the Chernobyl accident, *Journal of Radioanalytical and Nuclear Chemistry*, **126** 467-478.

[Rahn71] K.A. Rahn (1971) Sources of trace elements in aerosols - an approach to clean air. Ph.D. thesis, University of Michegan, Ann Arbor.

[Rahn76] K.A. Rahn (1976) The chemical composition of the atmospheric aerosols. Technical report, Graduate School of Oceanography, University of Rhode Island.

[Rahn81] K.A. Rahn (1981) Relative importances of North America and Eurasia as sources of arctic aerosol. *Atmospheric Environment* **15**, 1447-1455.

[Raisbeck81] G.M. Raisbeck, F. Yiou (1981) Cosmogenic ^{10}Be/^{7}Be as a Probe of Atmospheric Transport Processes. *Geophysical Research Letters* **8**, 1015-1018.

[Rangarajan86] C. Rangarajan, R. Madhavan and Smt.S. Gopalakrishnan (1986) Spatial and Temporal Distribution of Lead-210 in the Surface Layers of the Atmosphere. *Journal of Environmental Radioactivity* **3**, 23-33.

[Reiter74] E.R. Reiter (1974) The Role of the General Circulation of the Atmosphere in Radioactive Debris Transport. Report COO-1340-38. U.S. Atomic Energy Commission, Washington, D.C.

[Rehfeld95] S. Rehfeld and M. Heimann (1995) Three dimensional atmospheric transport simulation of the radioactive tracers ^{210}Pb, ^{7}Be, ^{10}Be, and ^{90}Sr

[Rizzio99] E. Rizzio, G. Giaveri, D. Arginelli, L. Gini, A. Profumo and M. Gallorini (1999) Trace elements total content and particle sizes distribution in the air particulate matter of a rural-residential area in north Italy investigated by instrumental neutron activation analysis. *The Science of The Total Environment* **226**, 47-56.

[Rizzio01] E. Rizzio, L. Bergamaschi, M.G. Valcuvia, A. Profumo, M. Gallorini (2001) Trace elements determination in lichens and in the airborne particulate matter for the evaluation of the atmospheric pollution in a region of northern Italy. *Environment International* **26**, 543-549.

[Roed87] J. Roed and R. J. Cannel (1987) Relationship between Indoor and Outdoor Aerosol Concentration Following the Chernobyl Accident. *Radiation Protection Dosimetry* **21**, 107-110.

[Rosner96] G. Rosner, H. Hötzl, and R. Winkler (1996) Continuous Wet-only and Dry-only Deposition Measurements of ^{137}Cs and ^{7}Be: an Indicator of their Origin. *Applied Radiation and Isotopes* **47**, 1135-1139.

[Ross85] H.B. Ross (1985) An atmospheric selenium budget for the region 30°N to 90°N. *Tellus* **37B**, 78-90.

[Salma02] I. Salma, W. Maenhaut, G. Záray (2002) Comparative study of elemental mass size distributions in urban atmospheric aerosol. *Aerosol Science* **33**, 339-356.

[Shea83] M.A. Shea and D.F. Smart (1983) World grid of calculated cosmic ray vertical cutoff rigidities for 1980.0. *Conf. Pap.. Int. Cosmic Ray Conf. 18th* **5**, 514-517.

[SHMU] SHMU (1992-2003) Air pollution in the Slovak Republic. Reports of Slovak Hydrometeorological Institute for years 1992 - 2003.

[Sima] O. Sima (1996) Applications of Monte Carlo Calculations to Gamma-spectrometric Measurements of Environmental Samples. *Applied Radiation Isotopes* **47**, 919-923.

[Simpson83] J.A. Simpson (1983) Elemental and Isotopic Composition of the Galactic Cosmic Rays. *Ann. Rev. Nuclear and Particle Science* **33**, 323-381.

[Simpson00] J.A. Simpson (2000) The cosmic ray nucleonic component: the invention and scientific uses of the neutron monitor. *Space Science Review* **93**, 11-32.

[SR04] Regulation of Ministry of environment of Slovak Republic 53/2004. Požiadavky na kvalitu palív a vedenie evidencie o palivách.

[Stoffregen63] W. Stoffregen, H. Derblom and B. Ånger (1963) Lithium emission in twilight at Uppsala during November 1962. *Nature* **197**, 783-785.

[Suchara07] I. Suchara, M. Florek, B. Godzik, B. Maňkovská, G. Rabnecz, J. Sucharová, Z. Tuba, P. Kapusta (2007) Mapping of main sources of pollutants and their transport in the Visegrad space, Part I: Eight toxic metals. Expert group on bio-monitoring the atmospheric deposition loads in the Visegrad countries, Pruhonice, KLEMO Zvolen, ISBN: 978-80-85116-53-3.

[Sullivan62] H.M. Sullivan and D.M. Hunten (1962) Lithium twilight at Saskatoon, 1960-1961. *Nature* **193**, 1064-1065.

[Swietlicky96] E. Swietlicky, R. Krejči (1996) Source characterization of the Central European atmospheric aerosol using multivariate statistical methods. *Nuclear Instruments and Methods in Physics Research* **B 109/110**, 519-525.

[Sýkora92] I. Sýkora, M. Ďurčík, J. Staníček, P. Povinec (1992) Rare Nuclear Processes, P. Povinec, Ed, World Scientific, Singapore, 321.

[Sýkora03] I. Sýkora, J. Merešová, M. Chudý, K. Holá (2003) The Study of Aerosol Component of Atmosphere in Bratislava. Proceedings on CD of the IRPA Regional Congress on Radiation Protection in Central Europe, Bratislava, Slovakia, 22-26 September 2003.

[Sýkora07] I. Sýkora, J. Merešová, M. Ješkovský, K. Holý (2007) Variation of Bratislava Atmosphere Aerosols Radioactivity. Conference proceedings of International Conference on Environmental Radioactivity: From Measurements and Assessments to Regulation IAEA-CN-145, 23-27 April 2007, Vienna, Austria (in press).

[Talpos97] S. Talpos, V. Cuculeanu (1997) A Study of the Vertical Diffusion of ^{7}Be in the Atmosphere. *Journal of Environmental Radioactivity* **36**, 93-106.

[Tanaka95] N. Tanaka and K.K. Turekian (1995) The determination of the dry deposition flux of SO_2 using cosmogenic ^{35}S and ^{7}Be measurements. *Journal of Geophysical Research* **100**, 2841-2848.

[Todd89] J.F Todd, G.T.F Wong, C.R. Olsen, I.L. Larsen (1989) Atmospheric depositional characteristics of beryllium-7 and lead-210 along the southeastern Virginia coast. *Journal of Geophysical Research* **94**, 11106-11116.

[Todorovic97] D. Todorovic (1997) The Effect of Tropopause Height on the Content of Radioactive Debris in Surface Atmosphere. *Environment International* **23**, 815-818.

[Todorovic99] D. Todorovic, D. Popovic, G. Djuric (1999) Concentration measurements of ^{7}Be and ^{137}Cs in ground level air in the Belgrade city area. *Environment International* **25**, 59-66.

[Todorovic00] D. Todorovic, D. Popovic, G. Djuric, M. Radenkovic (2000) ^{210}Pb in ground-level air in Belgrade city area. *Atmospheric Environment* **34** , 3245-3248.

[Todorovic05] D. Todorovic, D. Popovic, G. Djuric, M. Radenkovic (2005) Be-7 to Pb-210 concentration ratio in ground level air in Belgrade area. *Journal of Environmental Radioactivity* **79**, 297-307.

[Turekian89] K.K. Turekian, W.C. Graustein J.K. Cochran (1989) Lead-210 in the SEAREX program: an aerosol tracer across the Pacific. *Chemical Oceanography* **10**, 51-81.

[Twomey74] S. Twomey (1974) Pollution and the planetary albedo. *Atmospheric Environment* **8**, 1251-1256.

[Ueno03] T. Ueno, S. Nagano, H. Yamazawa (2003) Atmospheric deposition of ^{7}Be, ^{40}K, ^{137}Cs and ^{210}Pb during 1993-2001 at Tokai-mura, Japan. *Journal of Radioanalytical and Nuclear Chemistry* **255**, 335-339.

[UNSCEAR88] UNSCEAR (1988) Sources, Effects and Risks of Ionizing Radiation. Scientific Committee on the Effects of Atomic Radiation, UN, New York.

[UNSCEAR00] UNSCEAR (2000) Report Vol. I, Sources and Effects of Ionizing Radiation. Scientific Committee on the Effects of Atomic Radiation, UN, New York.

[USSA62] U.S. Standard Atmosphere (1962) U.S. Government Printing Office, Washington, D.C.

[Utsunomiya04] S. Utsunomiya, K.A. Jensen, G.J. Keeler, R.C. Ewing (2004) Direct Identification of Trace Metals in Fine and Ultrafine Particles in the Detroit Urban Atmosphere. *Environmental Science and Technology* **38**, 2289-2297.

[Vecchi05] R. Vecchi, G. Marcazzan, G. Valli (2005) Seasonal variation of ^{210}Pb activity concentration in outdoor air of Milan (Italy). *Journal of Environmental Radioactivity* **82**, 251-266.

[Viezee80] W. Viezee and H.B. Singh (1980) The distribution of Beryllium-7 in the troposphere: implications on stratospheric/tropospheric air exchange. *Geophysical Research Letters* **7** 805-808.

[Vogt90] S. Vogt, G.F. Herzog, and R.C. Reedy (1990) Cosmogenic nuclides in extraterrestrial materials. *Review of Geophysics* **28** 253-275.

[Warneck88] P. Warneck (1988) Chemistry of the natural atmosphere, Max-Planck Institut fur Chemie, Academic Press, INC., 375-391.

[Wilson03] C.G. Wilson, G. Matisoff, P.J. Whiting (2003) Short-term erosion rates from a ^{7}Be inventory balance. *Earth Surface Processes and Landforms* **28**, 967-977.

[Winkler98] R. Winkler, F. Dietl, G. Frank, J. Tschiersch (1998) Temporal Variation of ^{7}Be and ^{210}Pb Size Distributions in Ambient Aerosol. *Atmospheric Environment* **32**, 983-991.

[Wróbel00] A. Wróbel, E. Rokita, W. Maenhaut (2000) Transport of traffic-related aerosols in urban areas. *Science of the Total Environment* **257**, 199-211.

[Young80] J.A. Young and W.B. Silker (1980) Aerosol deposition velocity on the Pacific and Atlantic oceans calculated from Be-7 measurements. *Earth Planetary Science Letters* **50**, 92-104.

[Yu02] K.N. Yu, L.Y.L. Lee (2002) Measurements of Atmospheric ^{7}Be Properties Using High-Efficiency Gamma Spectroscopy. *Applied Radiation and Isotopes* **57**, 941-946.

[Závodský01] D. Závodský, M. Medveď, F. Ďurec (2001) Chémia atmosféry a modelovanie znečistenia ovzdušia, Univerzita Mateja Bela, Banská Bystrica.

[Zhang93] X.Q. Zhang, P.H. McMurry (1993) Evaporative losses of fine particulate nitrates during sampling. *Atmospheric Environment* **26A**, 3305-3312.